2D core ion temperature and impurity density measurements with CICERS at Wendelstein 7-X

R. Lopez-Cansino[1], V. Perseo[2], E. Viezzer[1], O.P. Ford[2], M. Kriete[3], T. Romba[2], J. Rueda-Rueda[1], P.Zs. Poloskei[2], F. Reimold[2] and the W7-X team

[1]Dept. Of Atomic, Molecular and Nuclear physics, University of Sevilla, Spain
[2]Max-Planck-Institute für Plasmaphysik, Greifswald Germany
[3]Auburn University, Auburn, AL, United States of America

25th Topical Conference on High Temperature Plasma Diagnostics 2024, Asheville

Charge eXchange Recombination Spectroscopy

- **CXRS**[1] → Standard technique to infer $\boldsymbol{T_i}$, $\boldsymbol{v_Z}$, $\boldsymbol{n_Z}$:
  - Spectral analysis of **CX radiation** upon **NBI injection** via spectrometers.

$$H^0 + A^{Z+} \rightarrow H^+ + A^{(Z-1)+*}$$

$$A^{(Z-1)+*} \rightarrow A^{(Z-1)+} + \gamma$$

  - **Limited LOS** # and **spatial resolution.**

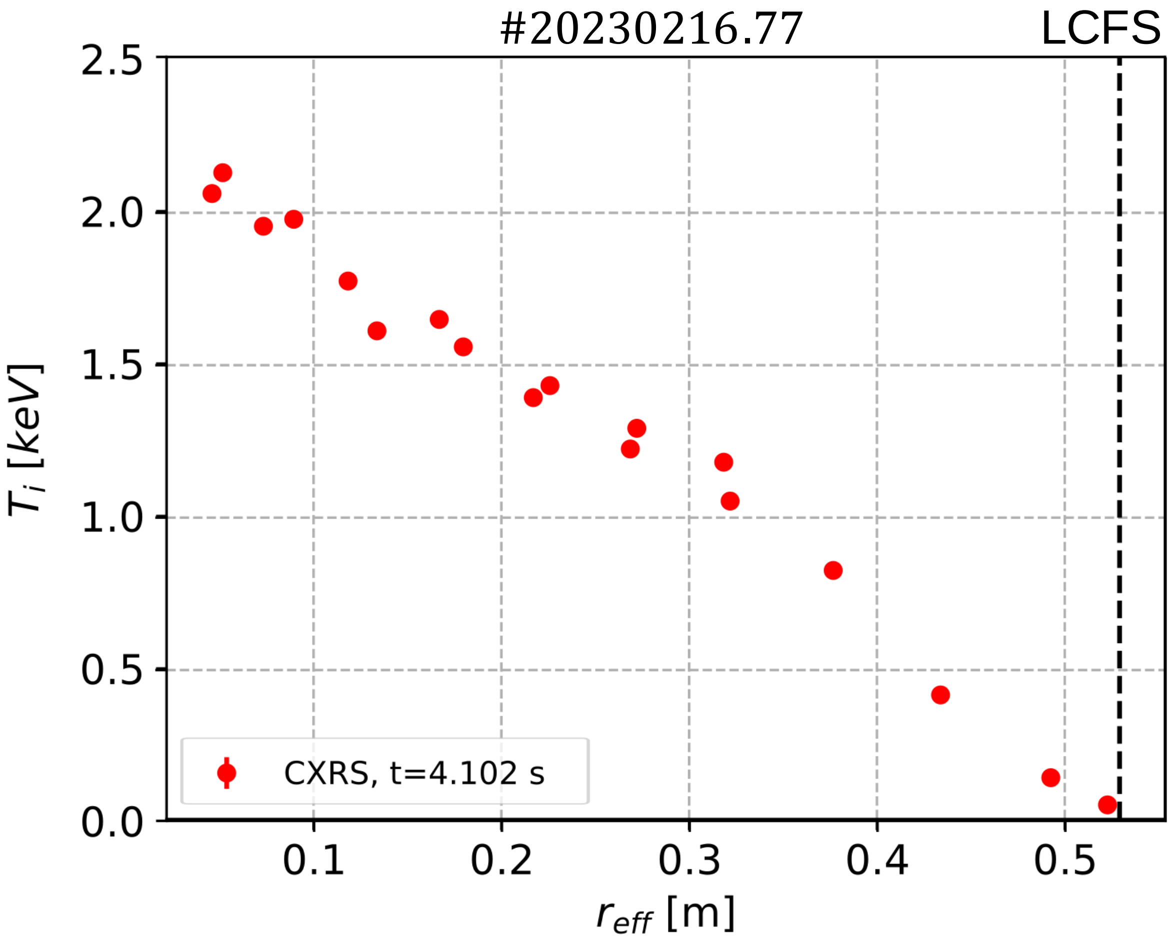

[1] O.P. Ford et al., RSI 2020

Coherence Imaging Spectroscopy

- **Coherence Imaging Spectroscopy (CIS)**[2]
  → **2D maps** of relevant plasma parameters via **polarization interferometry**
- Existing **CIS at W7-X**[3] → **Impurity flows** in the **Scrape-Off Layer** (SOL).
- **Multi-Delay CIS** for T_i in **SOL**
  → M. Kriete et al., this conference, **1.3.2**

Scrape-Off Layer (SOL) CIS

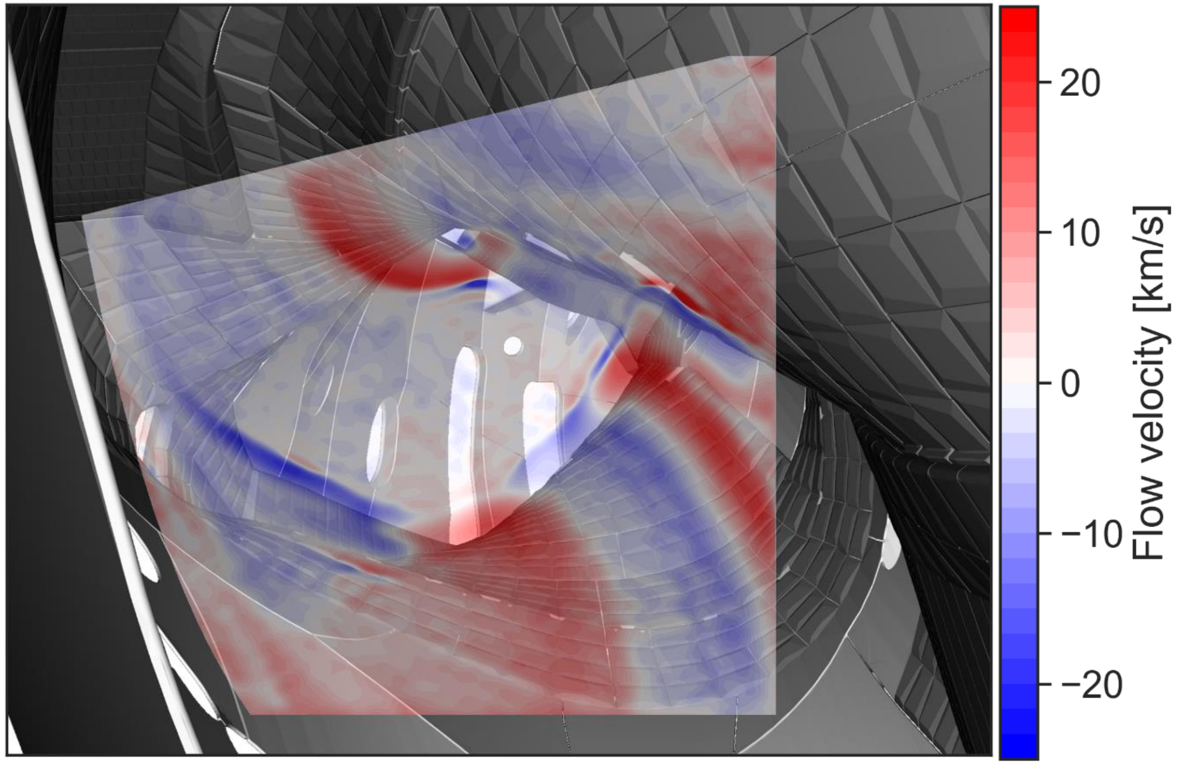

[Courtesy of V. Perseo, M. Kriete]

[2] J. Howard, J.Phys.B, 2010
[3] V. Perseo et al., RSI 2020

Coherence Imaging Charge Exchange Recombination Spectroscopy

- **CICERS** → Analysis of CX radiation with CIS:

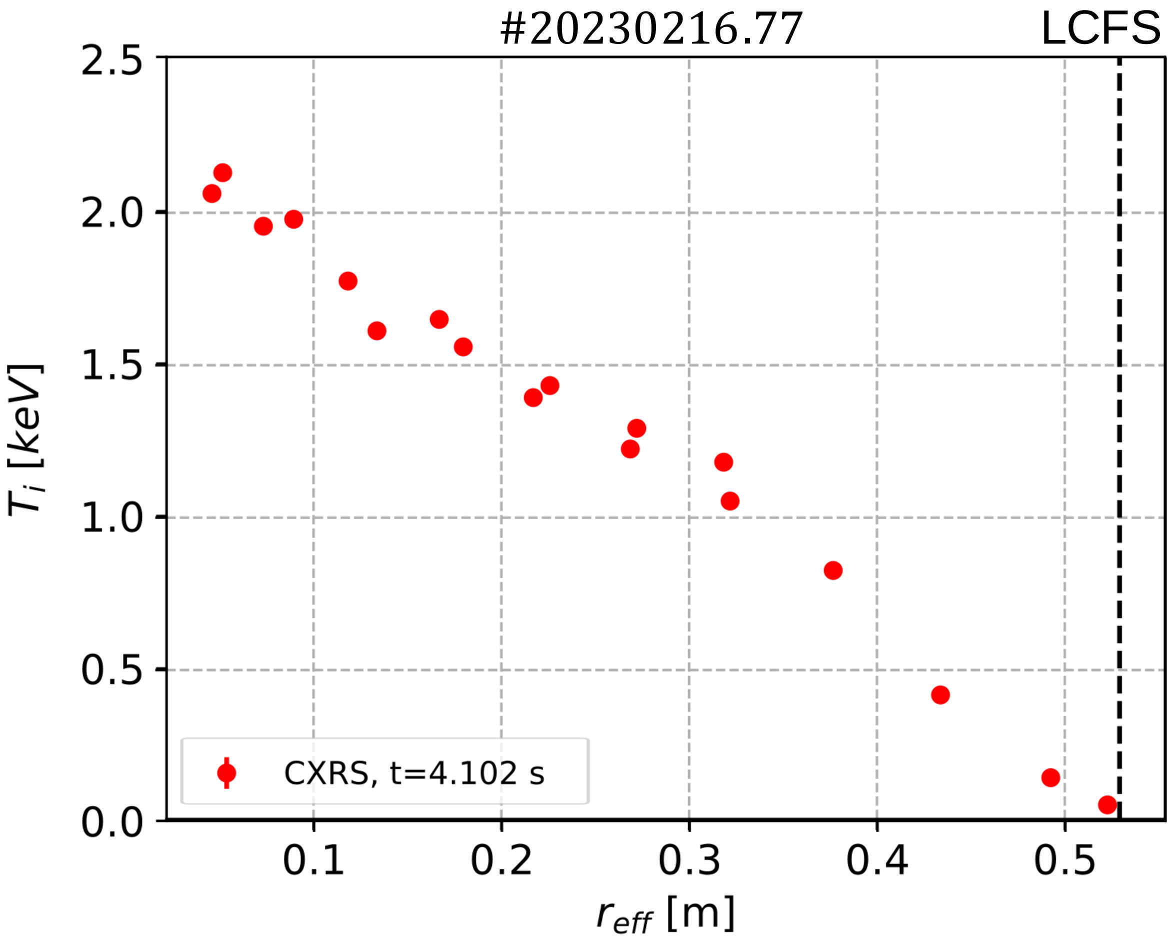

Coherence Imaging Charge Exchange Recombination Spectroscopy

- **CICERS** → Analysis of CX radiation with CIS:
  - 1D profiles → **2D maps**.

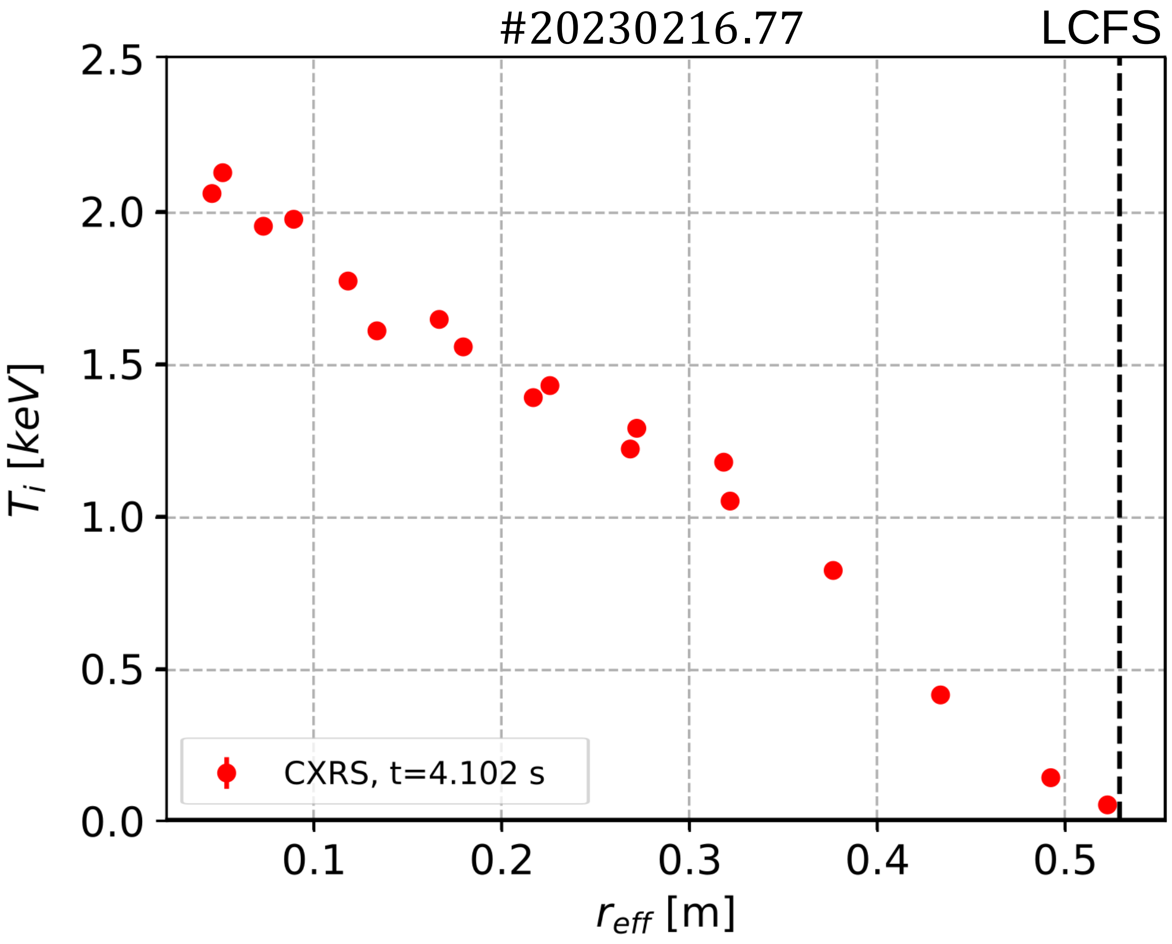

Coherence Imaging Charge Exchange Recombination Spectroscopy

- **CICERS** → Analysis of CX radiation with CIS:
  - 1D profiles → **2D maps**.

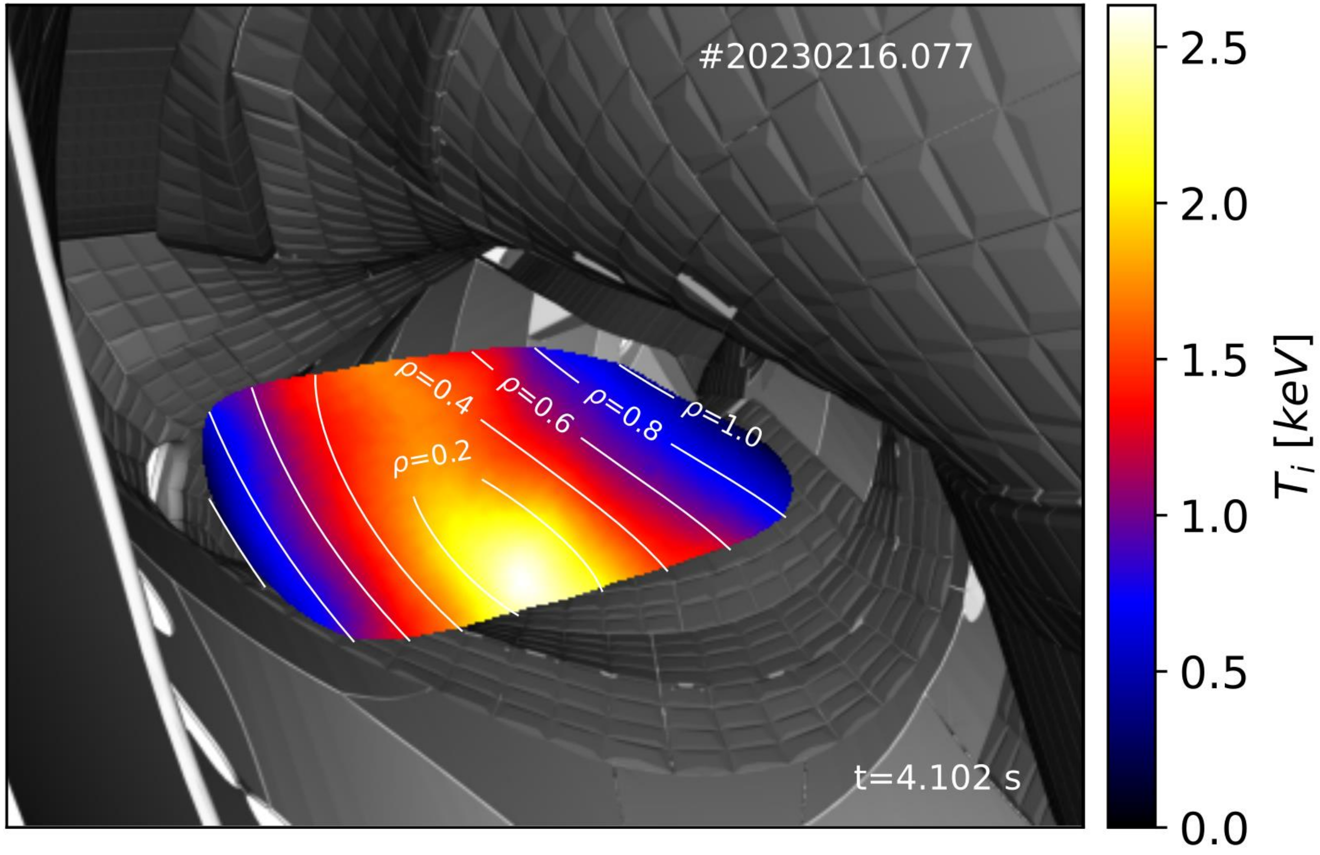

Coherence Imaging Charge Exchange Recombination Spectroscopy

- **CICERS** → Analysis of CX radiation with CIS:

  - 1D profiles → **2D maps**.
    - Enhanced **spatial resolution.**

    → ~ $\mathbf{10^5}$ **LOS**

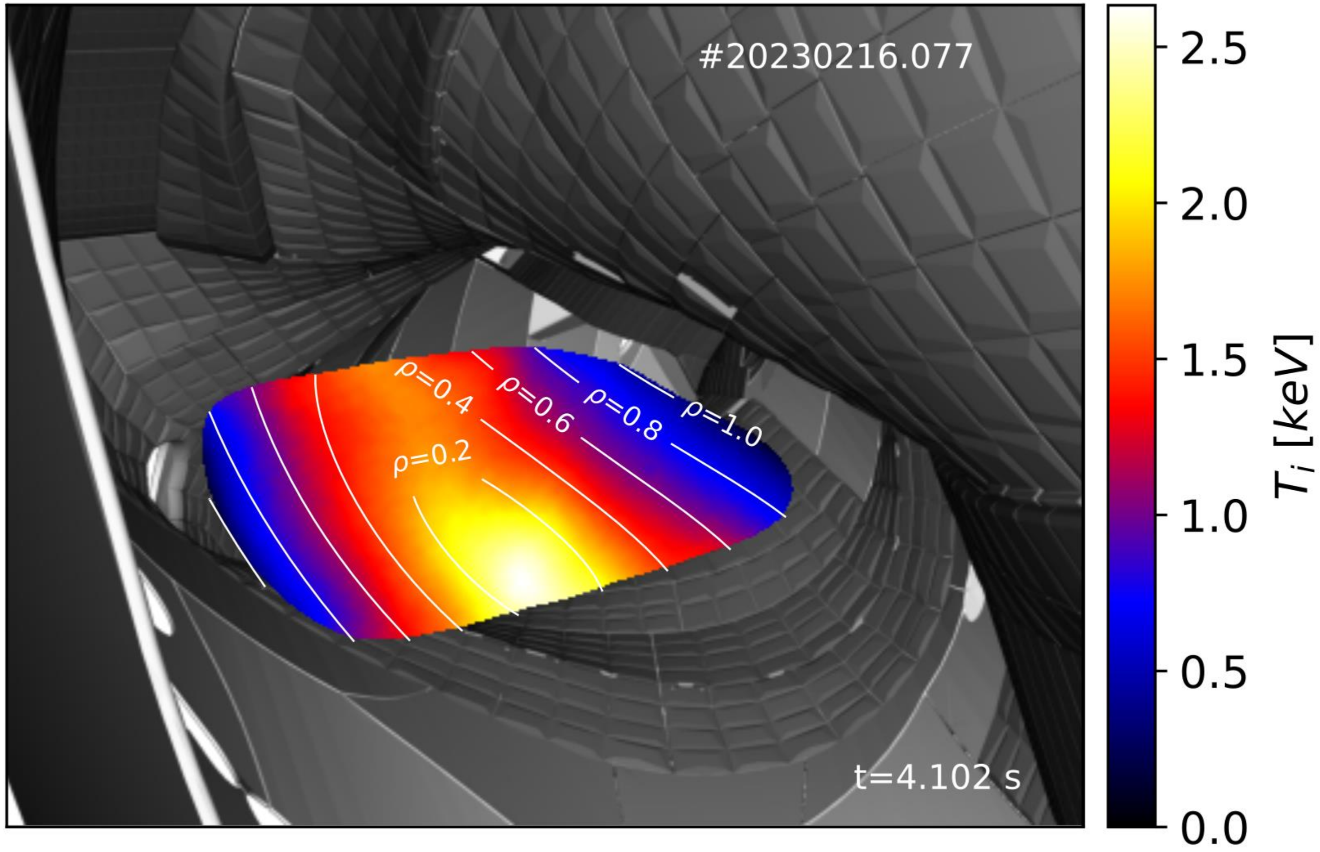

Coherence Imaging Charge Exchange Recombination Spectroscopy

- **CICERS** → Analysis of CX radiation with CIS:

  - 1D profiles → **2D maps**.
    - Enhanced **spatial resolution.**
    → ~ $\mathbf{10^5}$ **LOS**
    - Imaging **large part of poloidal cross section.**

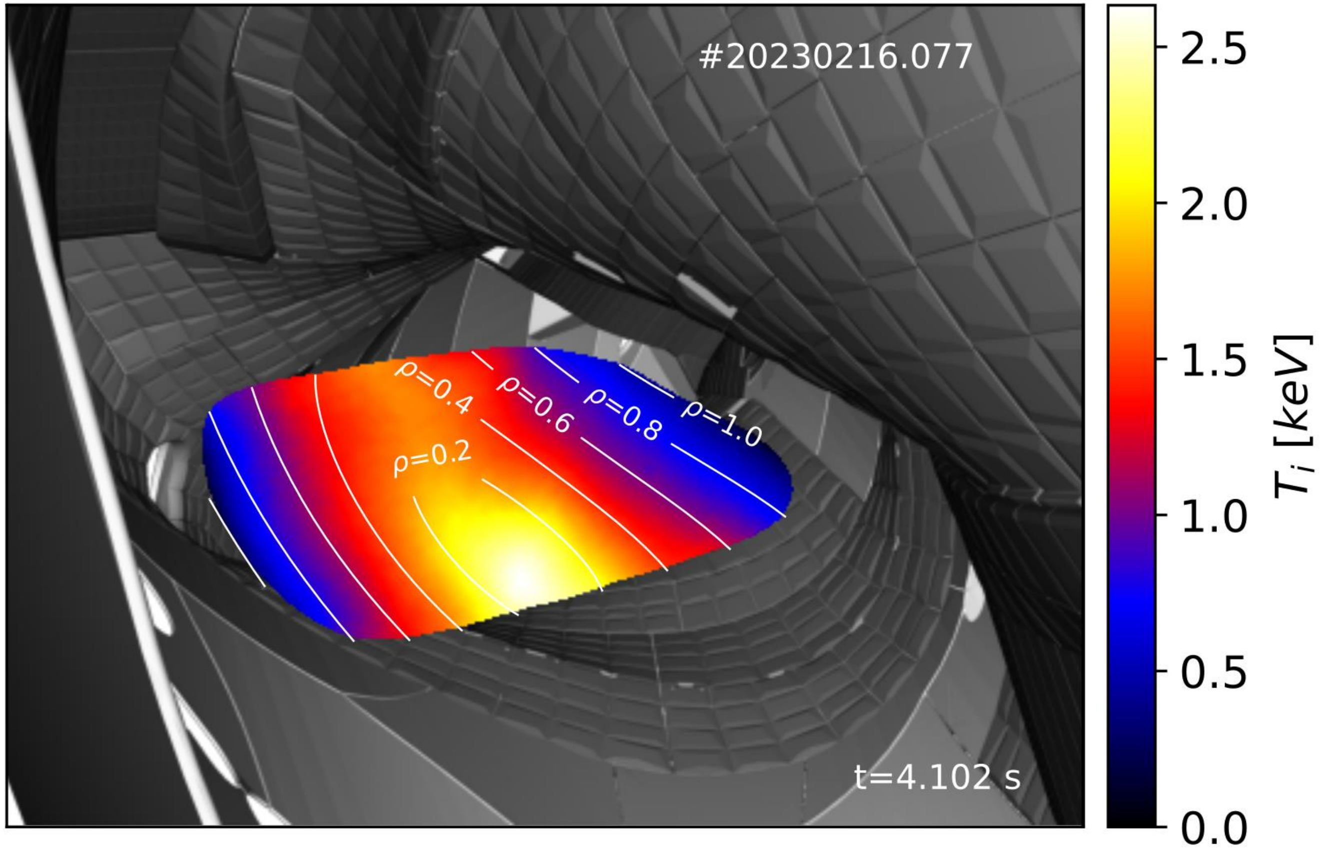

Coherence Imaging Charge Exchange Recombination Spectroscopy

- **CICERS** → Analysis of CX radiation with CIS:
  - 1D profiles → **2D maps**.
    - Enhanced **spatial resolution.** → ~ $\mathbf{10^5}$ **LOS**
    - Imaging **large part of poloidal cross section.**
  - **Poor spectral resolution.**

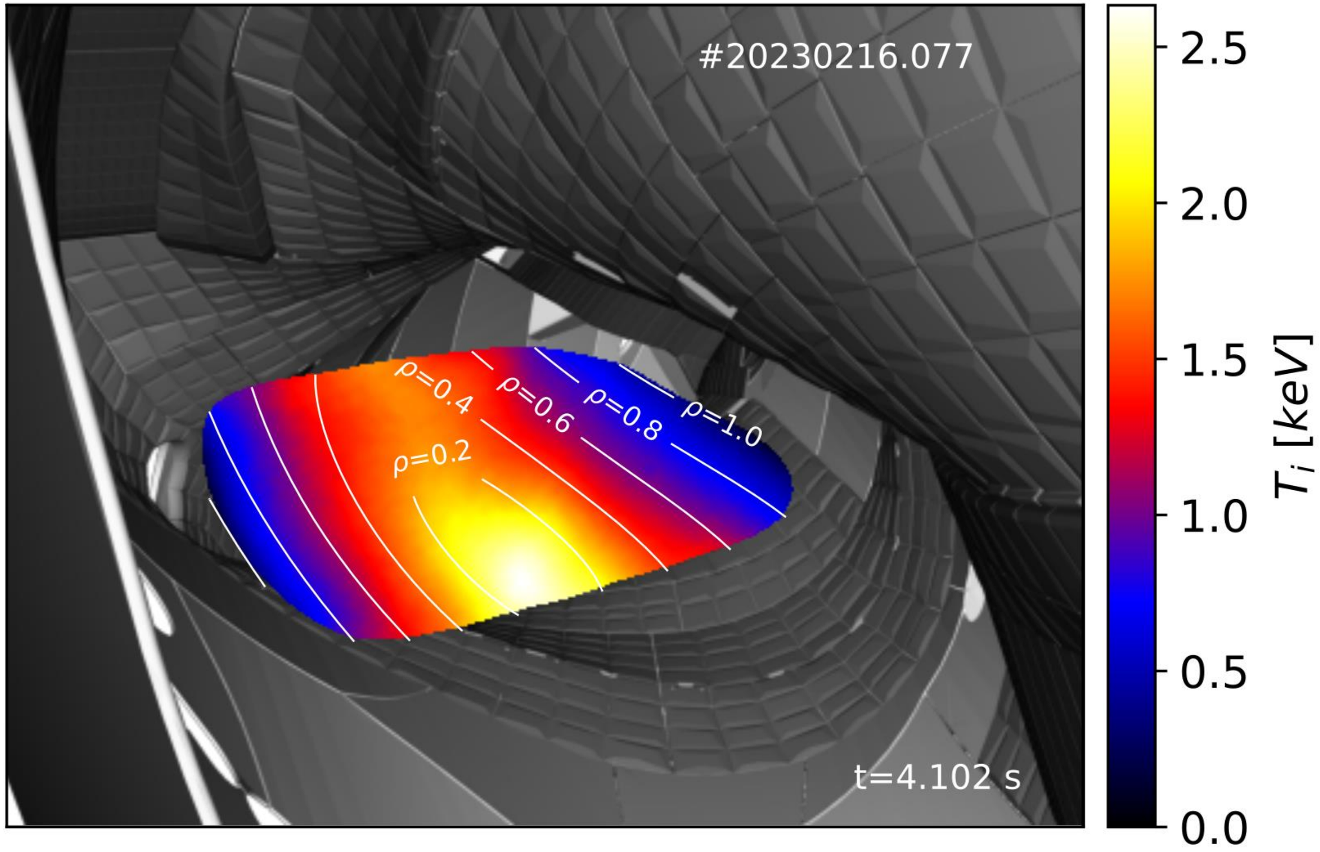

Overview

- Working principle
- Experimental arrangement
- Background radiation
- Ion temperature measurements
- Carbon impurity density measurements

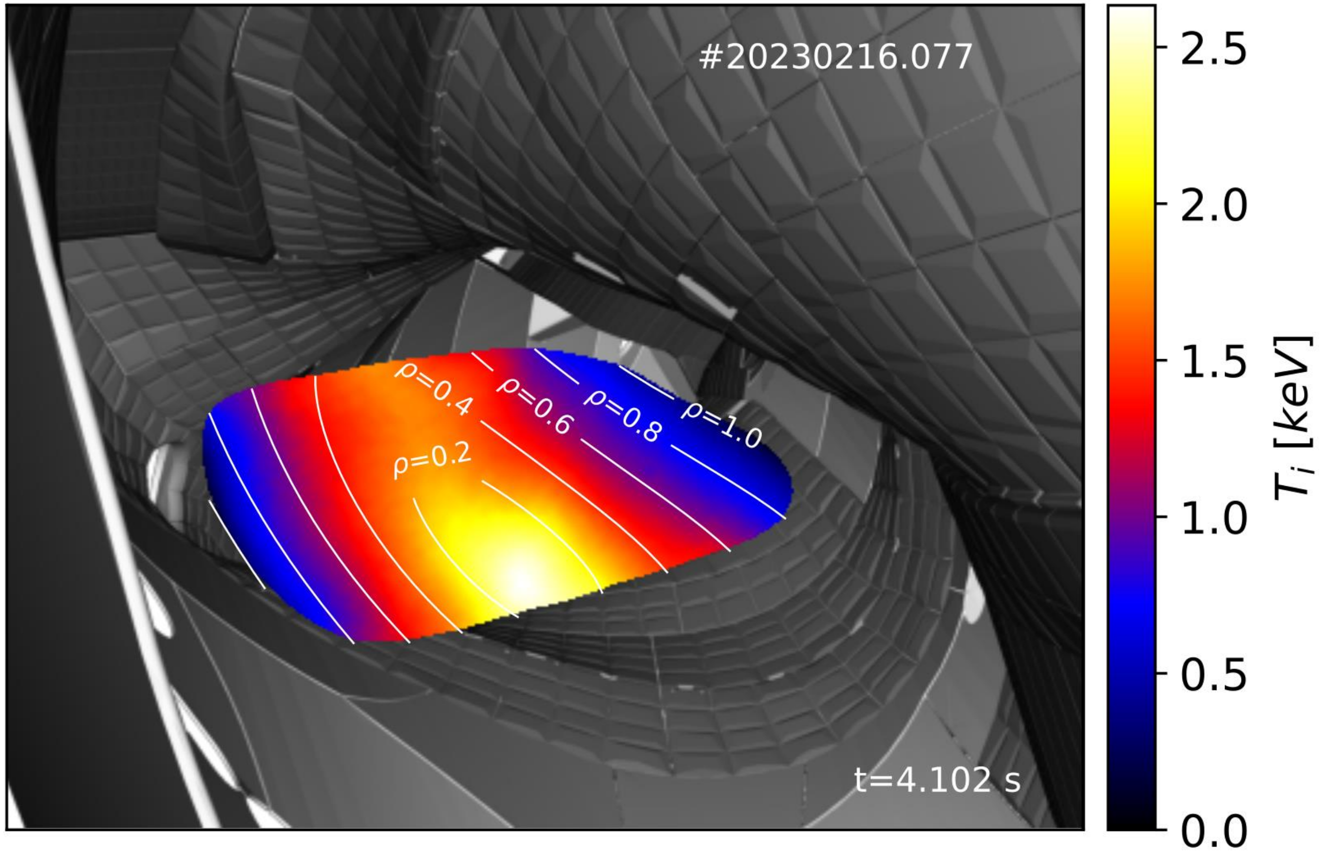

Coherence Imaging Spectroscopy (CIS)

- **CIS** → Polarization interferometry with birefringent crystals.
  - **Single-delay** approach: Birefringent **crystal(s)** + **polarizers** + **sCMOS** camera
    → Single **interference pattern**

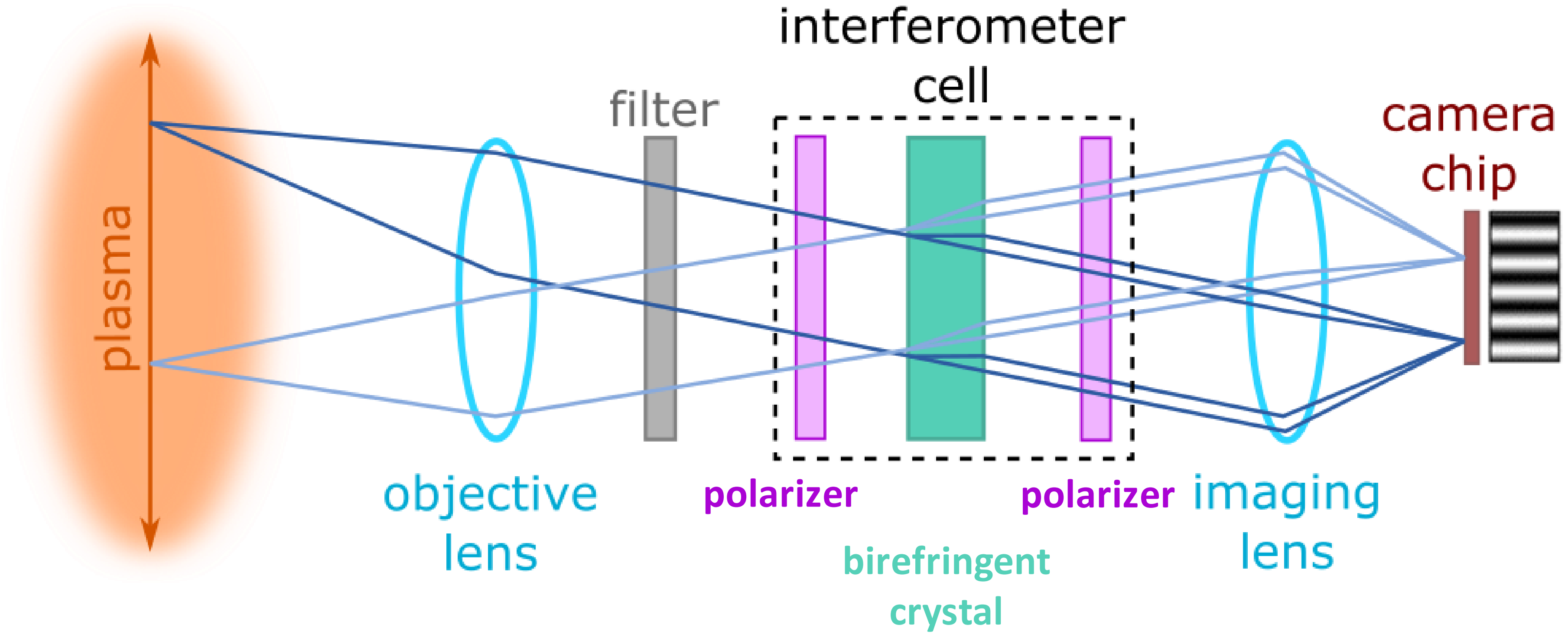

[Courtesy of V. Perseo]

Interference pattern

- **Parallel fringe pattern**:

$$S(x,y) = \frac{I_0(x,y)}{2}[1 + \zeta(x,y)\cos\Phi(\mathrm{x},\mathrm{y})]$$

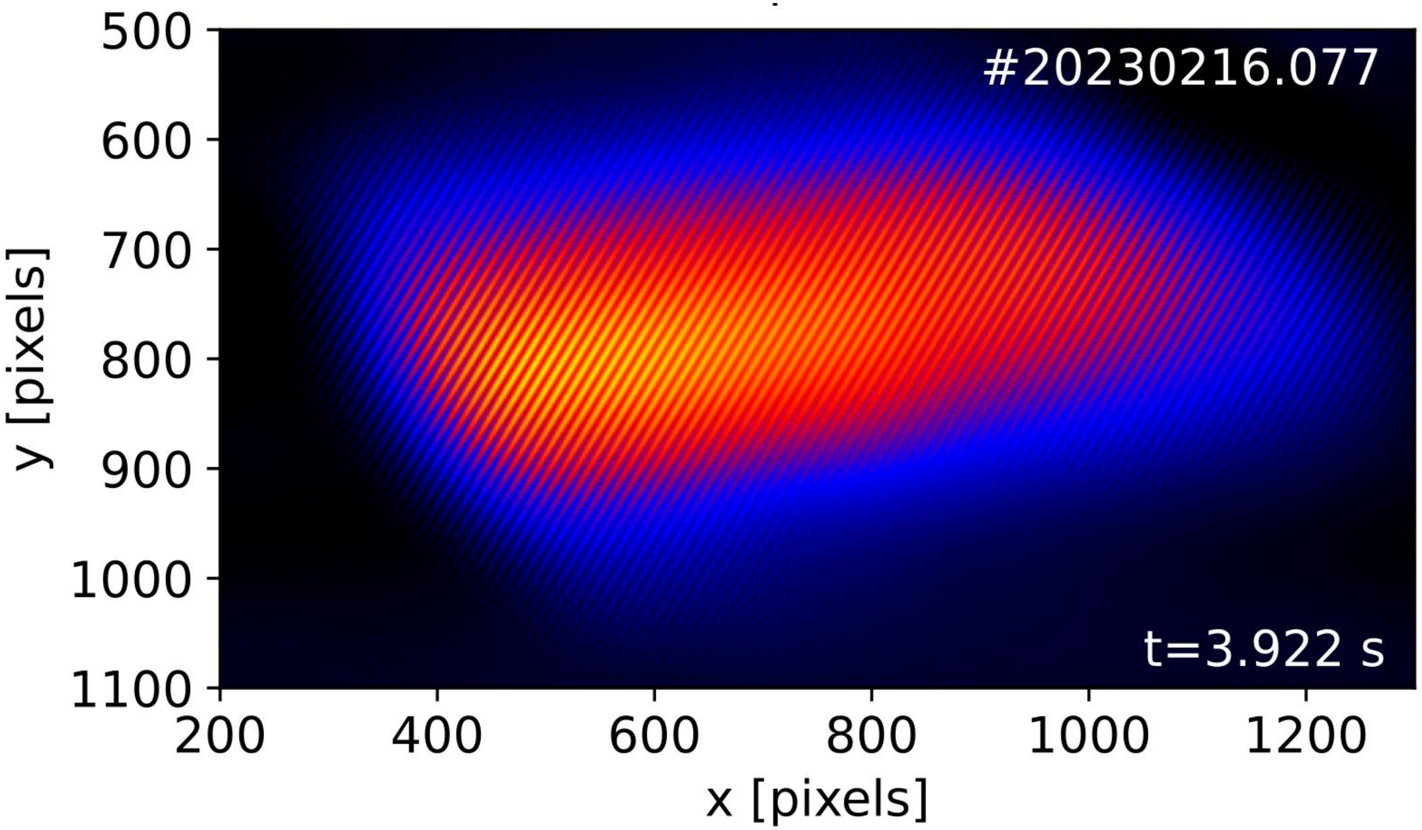

Interference pattern

- **Parallel fringe pattern**:

$$S(x,y) = \frac{I_0(x,y)}{2}[1 + \zeta(x,y)\cos\Phi(\mathrm{x},\mathrm{y})]$$

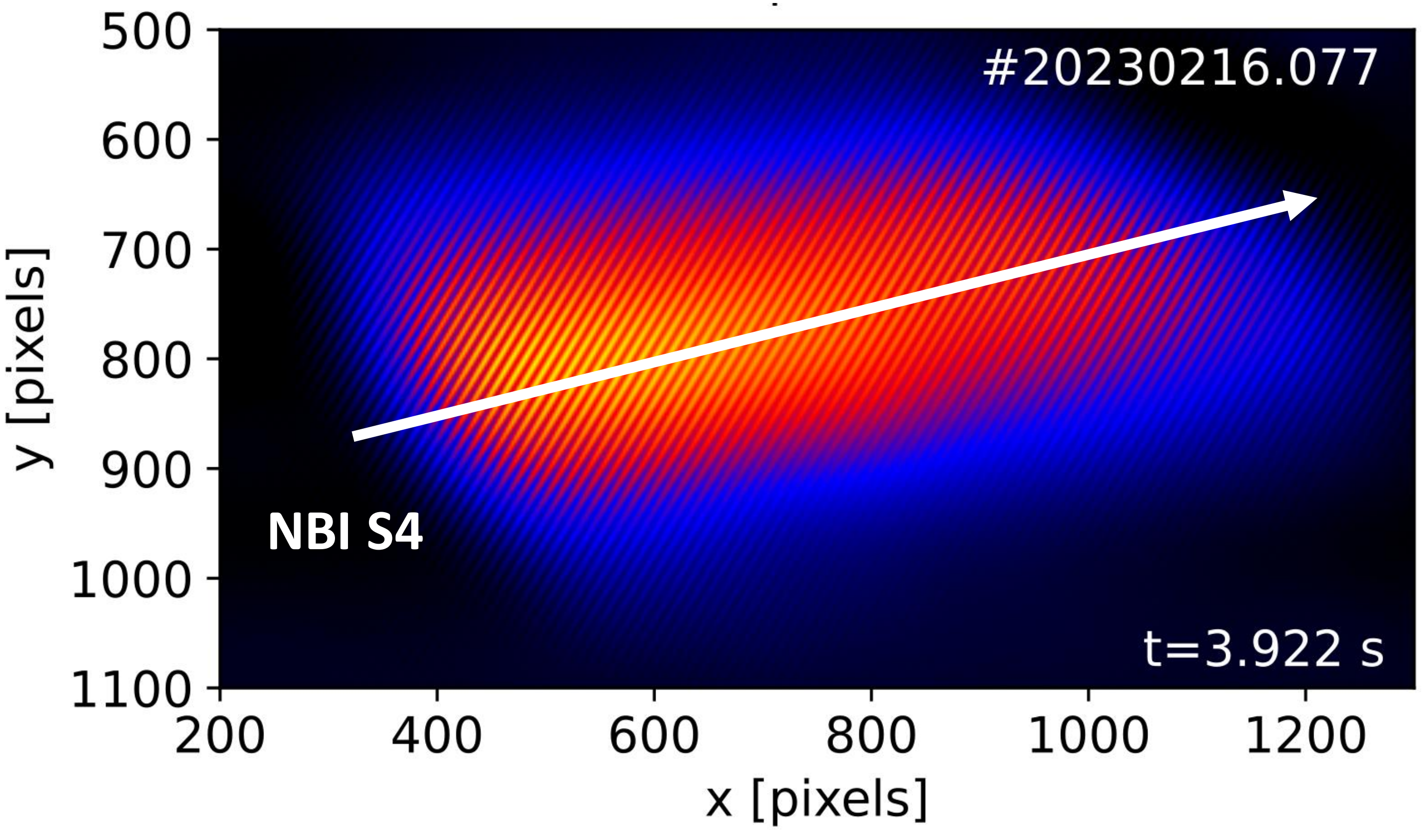

Interference pattern

- **Parallel fringe pattern**:

$$S(x,y) = \frac{I_0(x,y)}{2}[1+\zeta(x,y)\cos\Phi(x,y)]$$

- I_0, ζ, Φ retrieved via **2DFFT**

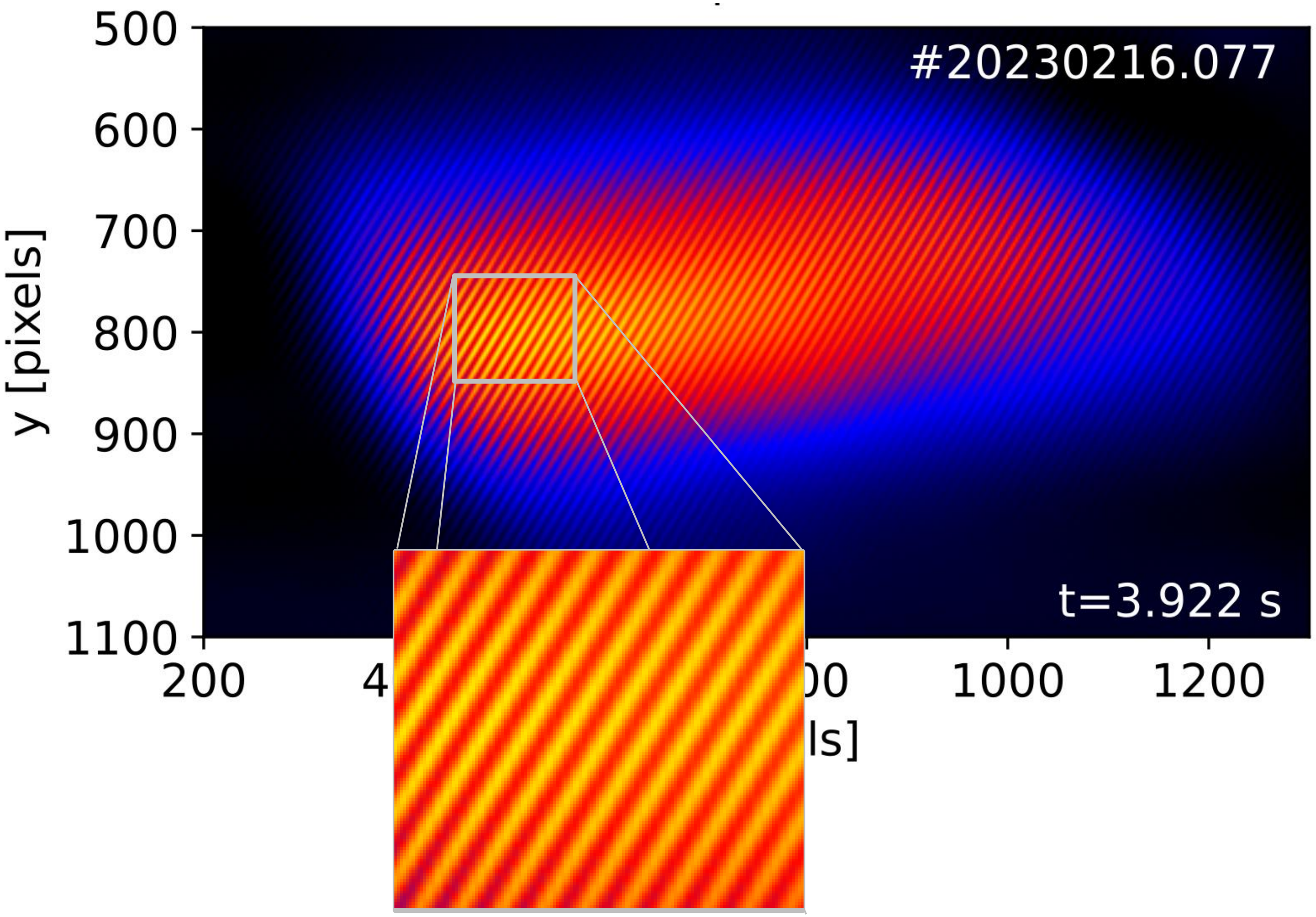

Interference pattern

- **Parallel fringe pattern**:

$$S(x,y) = \frac{\boldsymbol{I_0(x,y)}}{2}\left[1 + \zeta(x,y)\cos\Phi(\mathrm{x},\mathrm{y})\right]$$

- I_0, ζ, Φ retrieved via **2DFFT**

I_0: **Intensity** of CX radiation $\sim\propto$ $\boldsymbol{n_Z}$

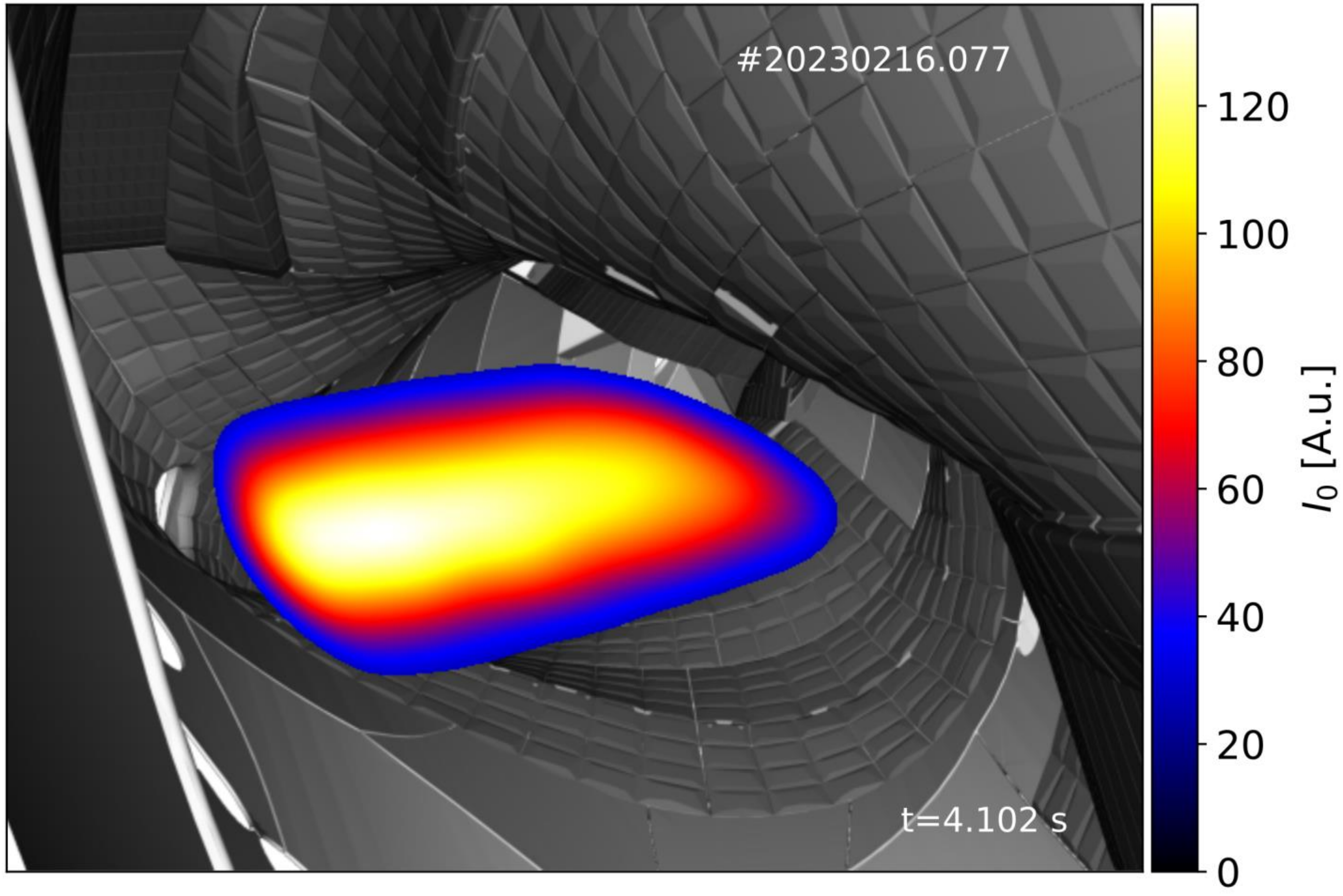

Interference pattern

- **Parallel fringe pattern**:

$$S(x,y) = \frac{I_0(x,y)}{2}[1 + \boldsymbol{\zeta(x,y)} \cos\Phi(\mathrm{x},\mathrm{y})]$$

- I_0, ζ, Φ retrieved via **2DFFT**

I_0: **Intensity** of CX radiation $\sim\propto \boldsymbol{n_Z}$

ζ: **Contrast** → Spectral broadening $\propto e^{-\boldsymbol{T_i}}$

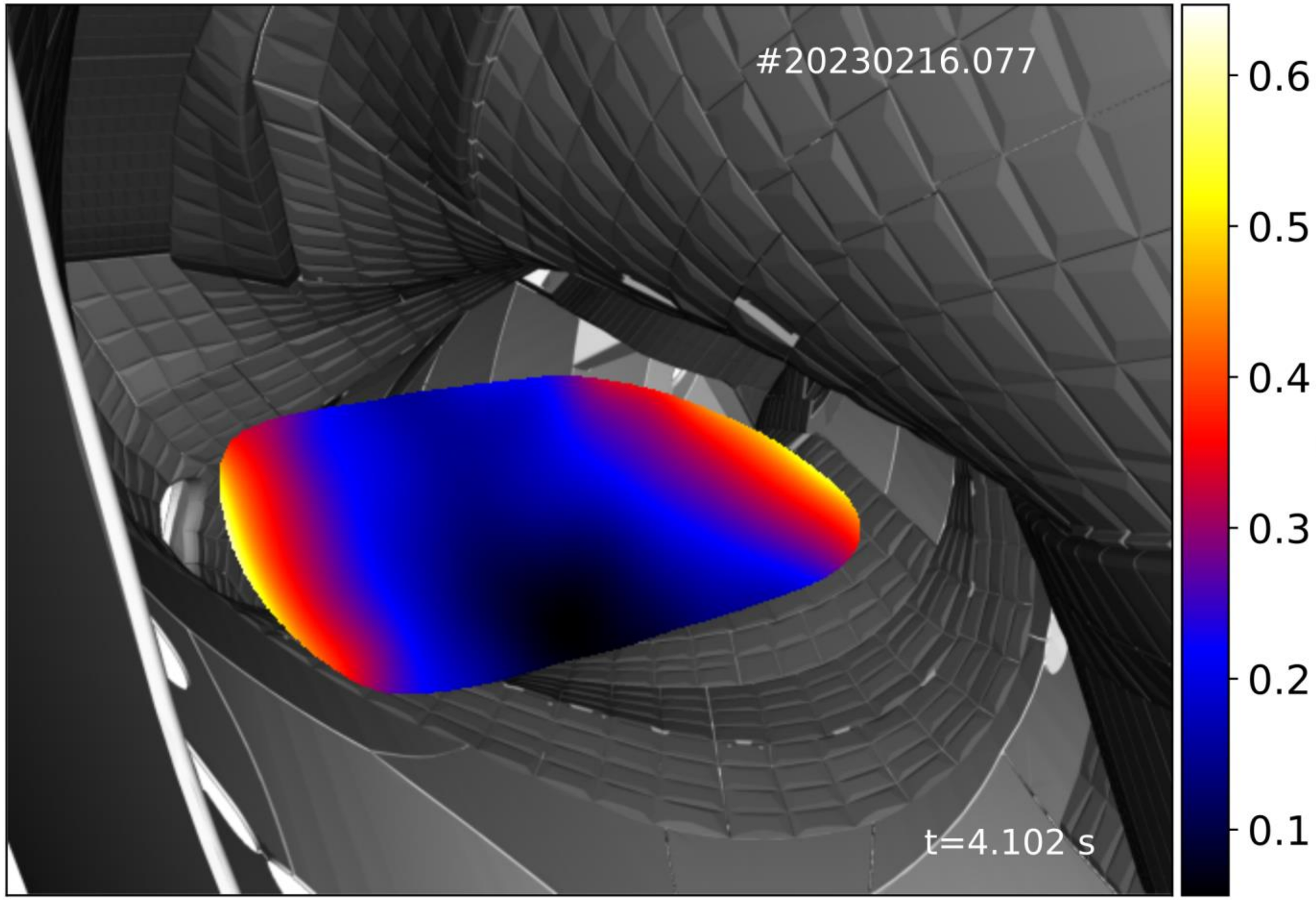

Interference pattern

- **Parallel fringe pattern**:

$$S(x,y) = \frac{I_0(x,y)}{2}[1 + \zeta(x,y)\cos\mathbf{\Phi}(\mathbf{x},\boldsymbol{y})]$$

- I_0, ζ, Φ retrieved via **2DFFT**

I_0: **Intensity** of CX radiation $\sim\propto$ $\boldsymbol{n_Z}$

ζ: **Contrast** → Spectral broadening $\propto e^{-\boldsymbol{T_i}}$

Φ: **Phase shift** → Wavelength shift $\propto$ $\boldsymbol{v_Z}$

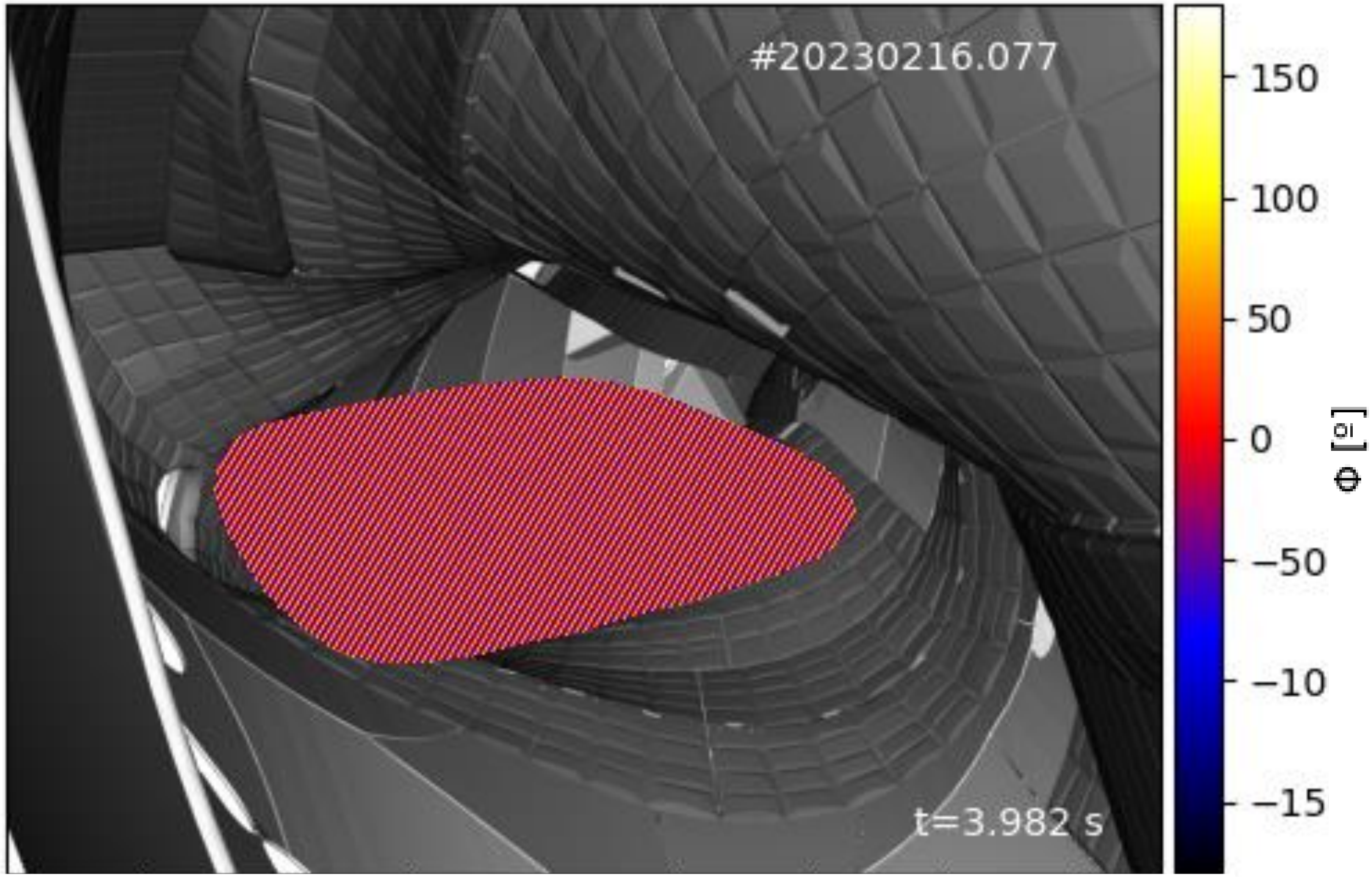

Experimental arrangement

- **Toroidal** view → NBI sources **S3**, **S4**

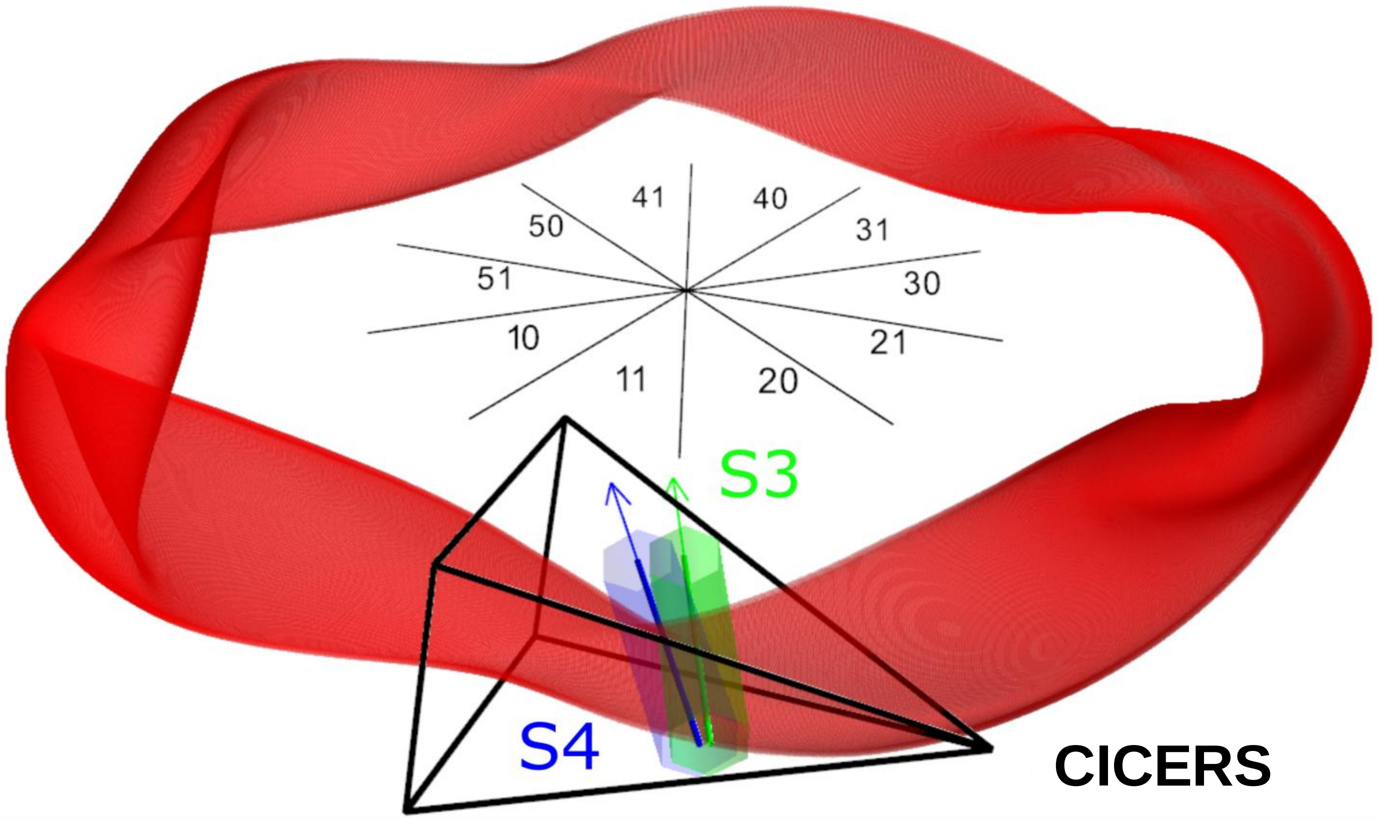

CICERS

Experimental arrangement

- **Toroidal** view → NBI sources **S3**, **S4**
- **Single-delay** approach:
  - Crystals optimized for high T_i (~ 2 keV)
    → Delay (2.5 mm)+ Savart (10+10 mm)
  - Emission line → CVI($\lambda = 529.05$ nm)

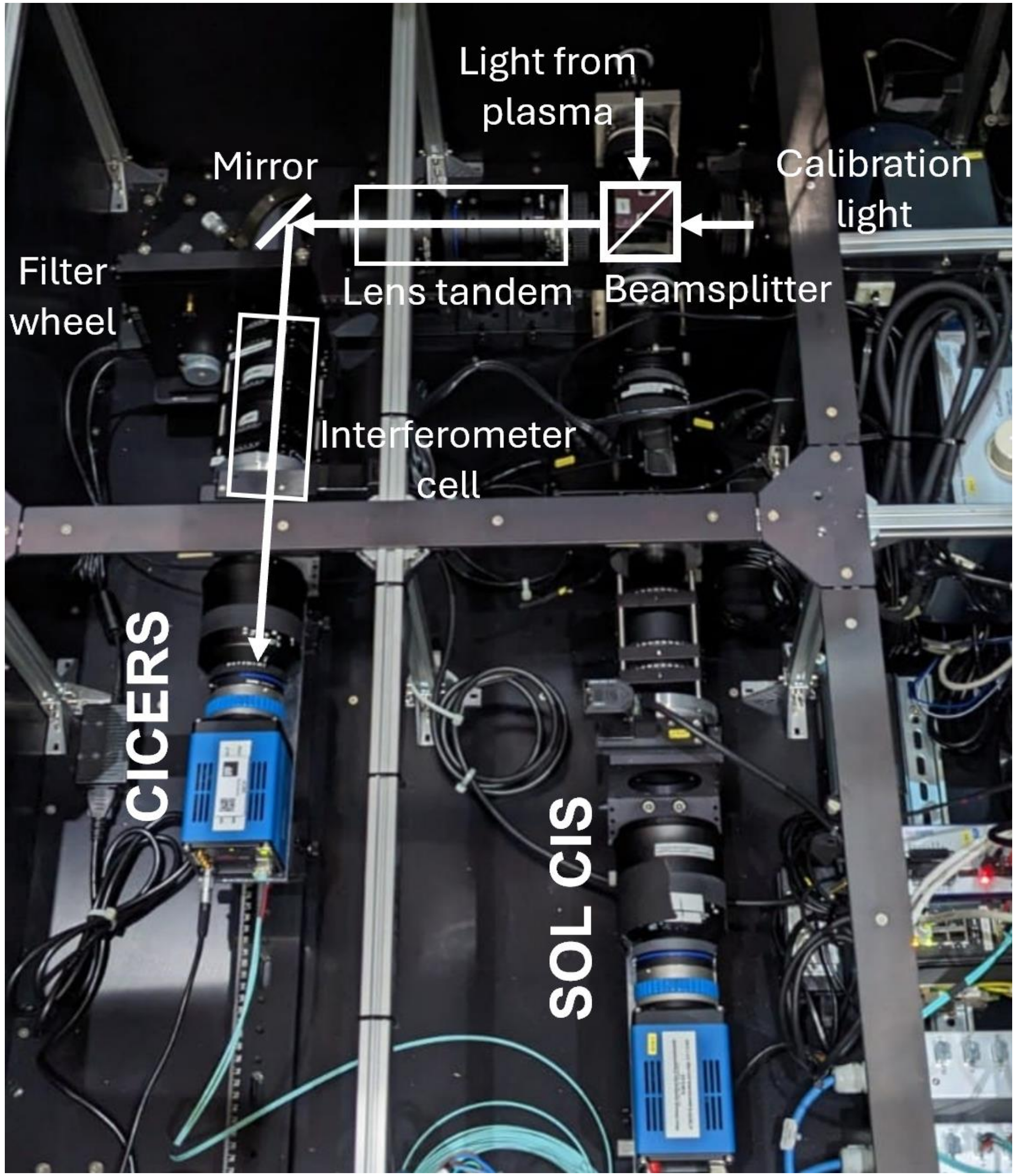

Experimental arrangement

- **Toroidal** view → NBI sources **S3**, **S4**
- **Single-delay** approach:
  - Crystals optimized for high T_i (~ 2 keV)
    → Delay (2.5 mm)+ Savart (10+10 mm)
  - Emission line → CVI($\lambda = 529.05$ nm)
- Calibrations carried out with **C-WAVE tunable laser:**
  - V. Perseo et al., this conference, **1.2.30**
  - S. Akhundzada et al., this conference, **1.4.26**
  - R. Lopez-Cansino et al., PPCF 2024

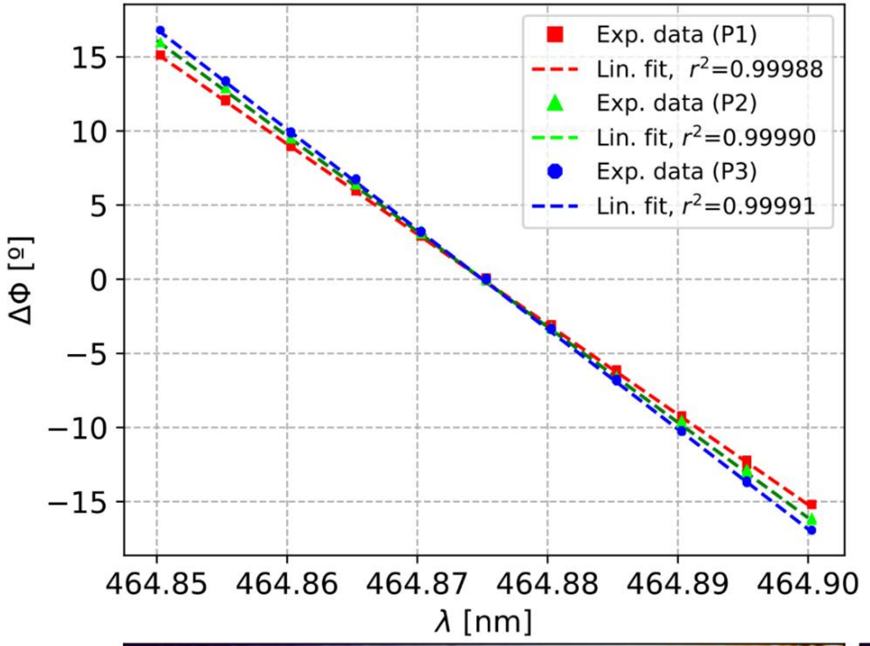

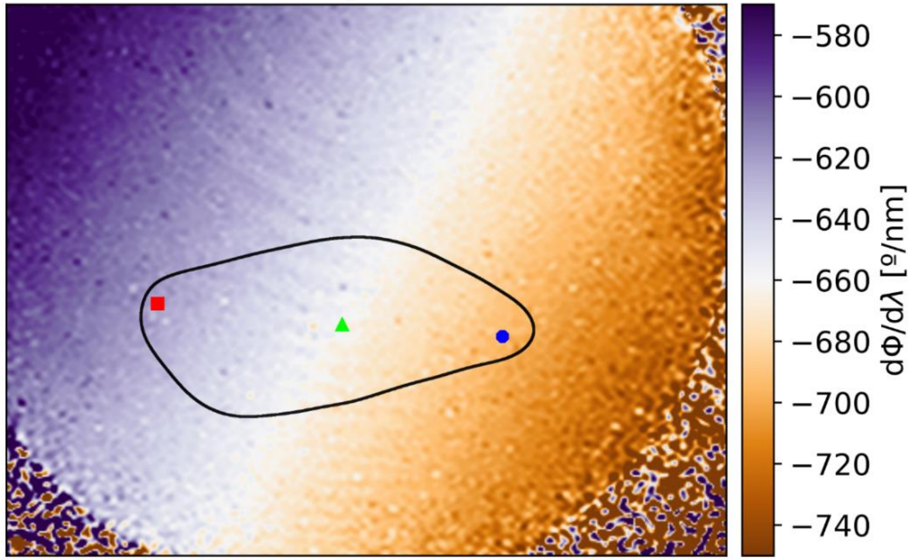

Background radiation

- Typical **CXRS spectrum**:

Background radiation

- Typical **CXRS spectrum**:
  - **Active CX**
    - **CX** with **NBI neutrals**

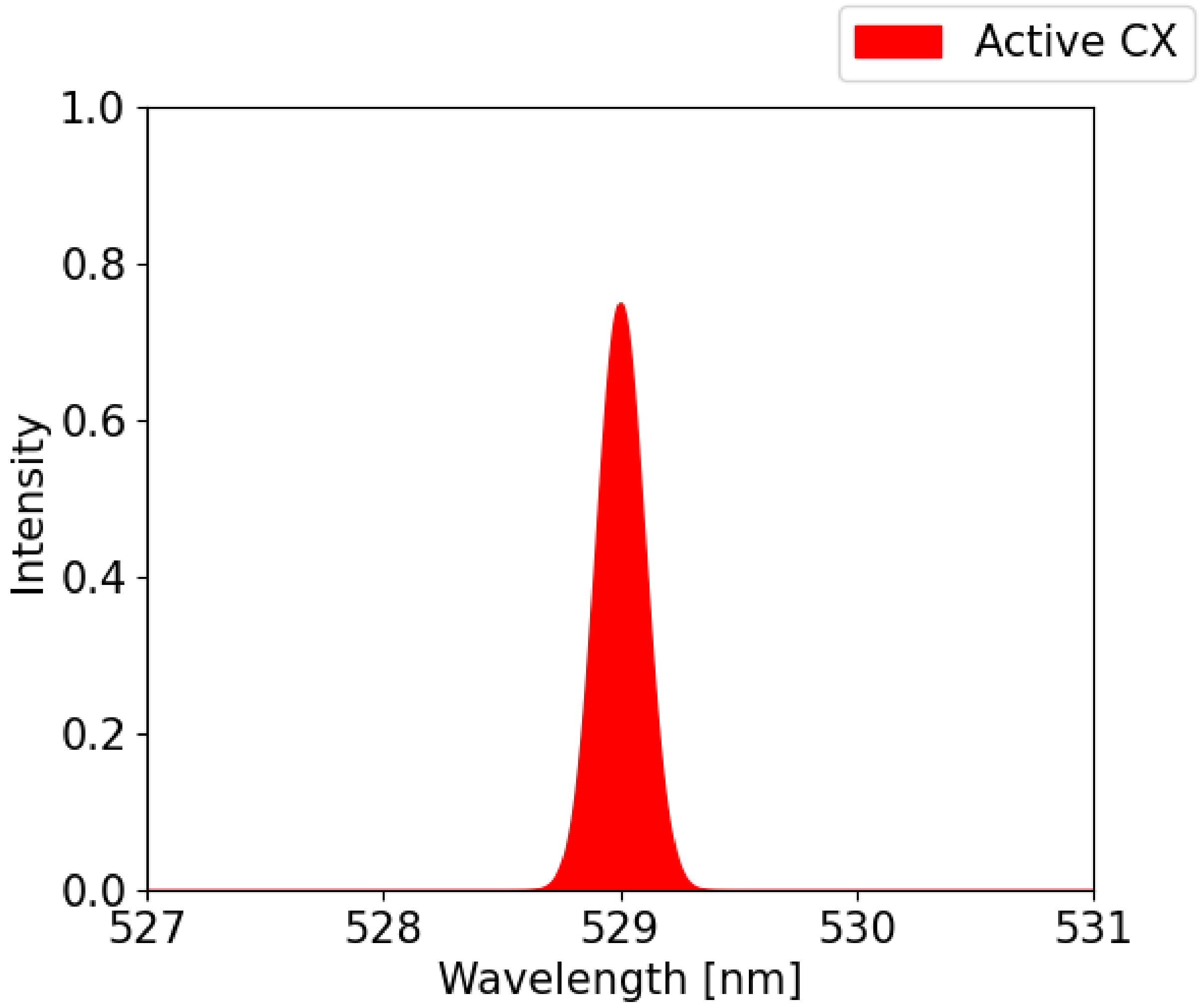

Background radiation

- Typical **CXRS spectrum**:
  - **Active CX**
    - **CX** with **NBI neutrals**
  - **Passive**
    - **CX** with **edge neutrals**
    - **Electron-Impact excitation**

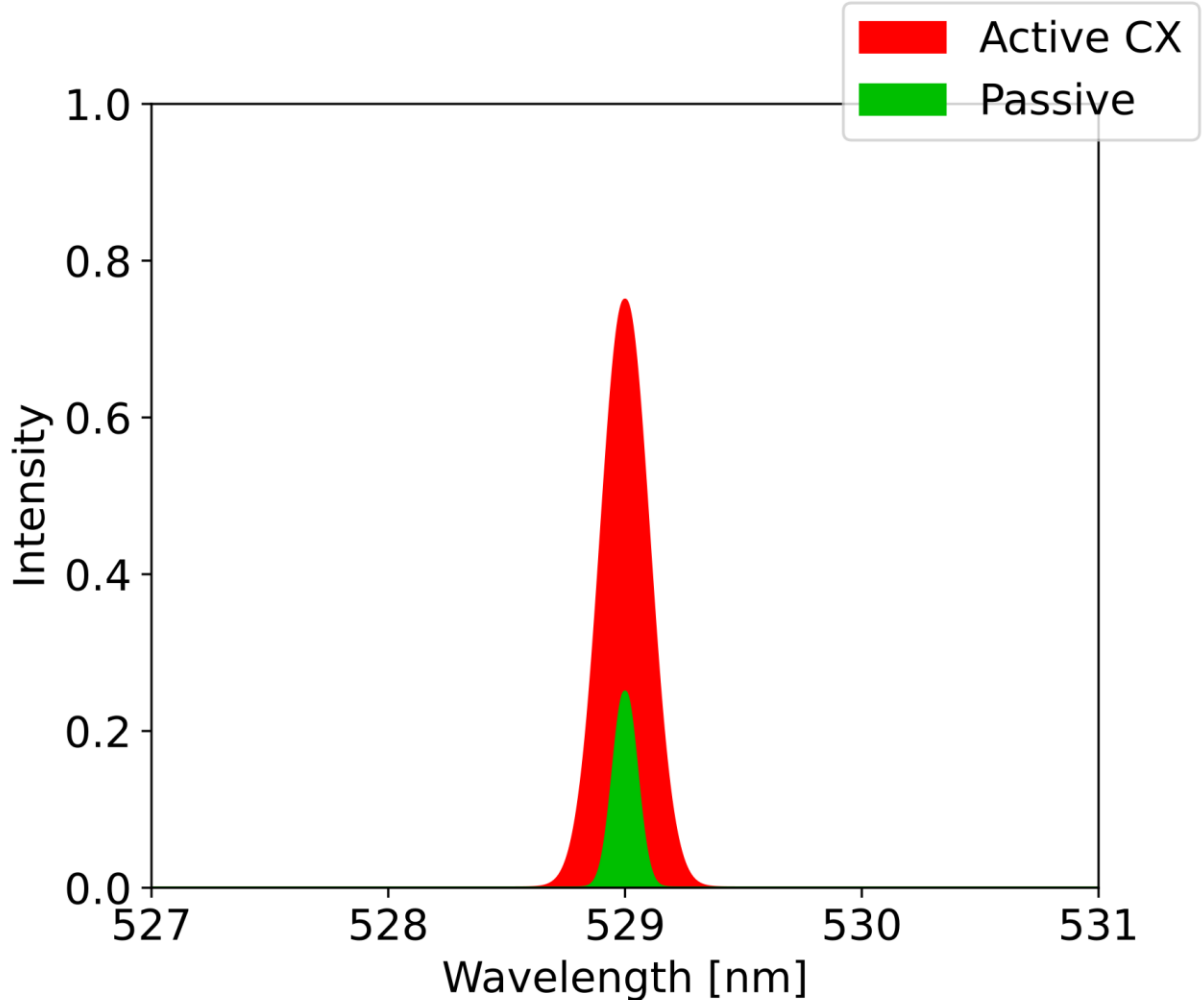

Background radiation

- Typical **CXRS spectrum**:
    - **Active CX**
        - **CX** with **NBI neutrals**
    - **Passive**
        - **CX** with **edge neutrals**
        - **Electron-Impact excitation**
    - **Bremsstrahlung**

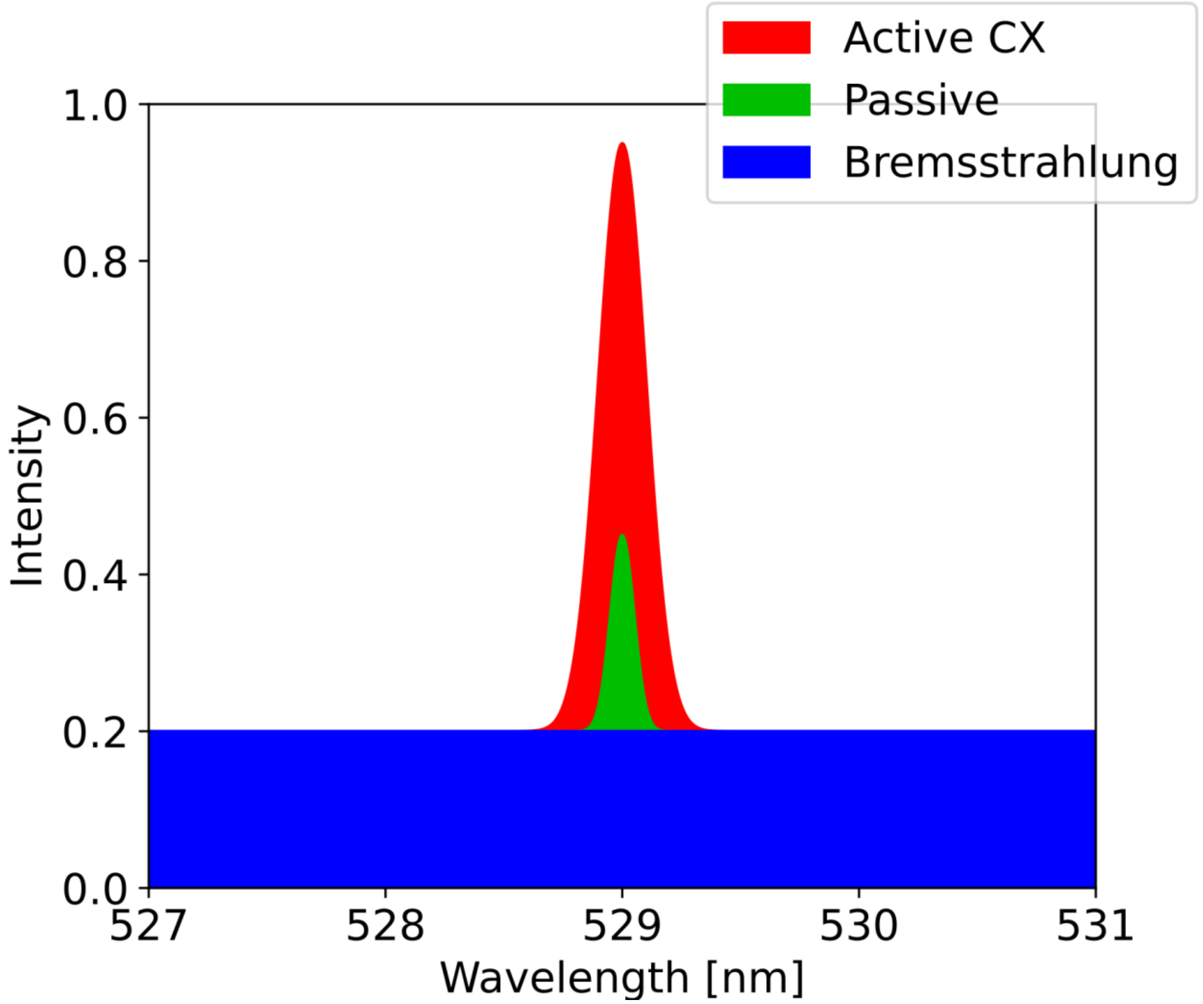

Background radiation

- Typical **CXRS spectrum**:
  - Active CX
    - **CX** with **NBI neutrals**
  - Passive
    - **CX** with **edge neutrals**
    - **Electron-Impact excitation**
  - Bremsstrahlung

- CICERS:
  - **Total spectrum** encoded in fringe pattern.

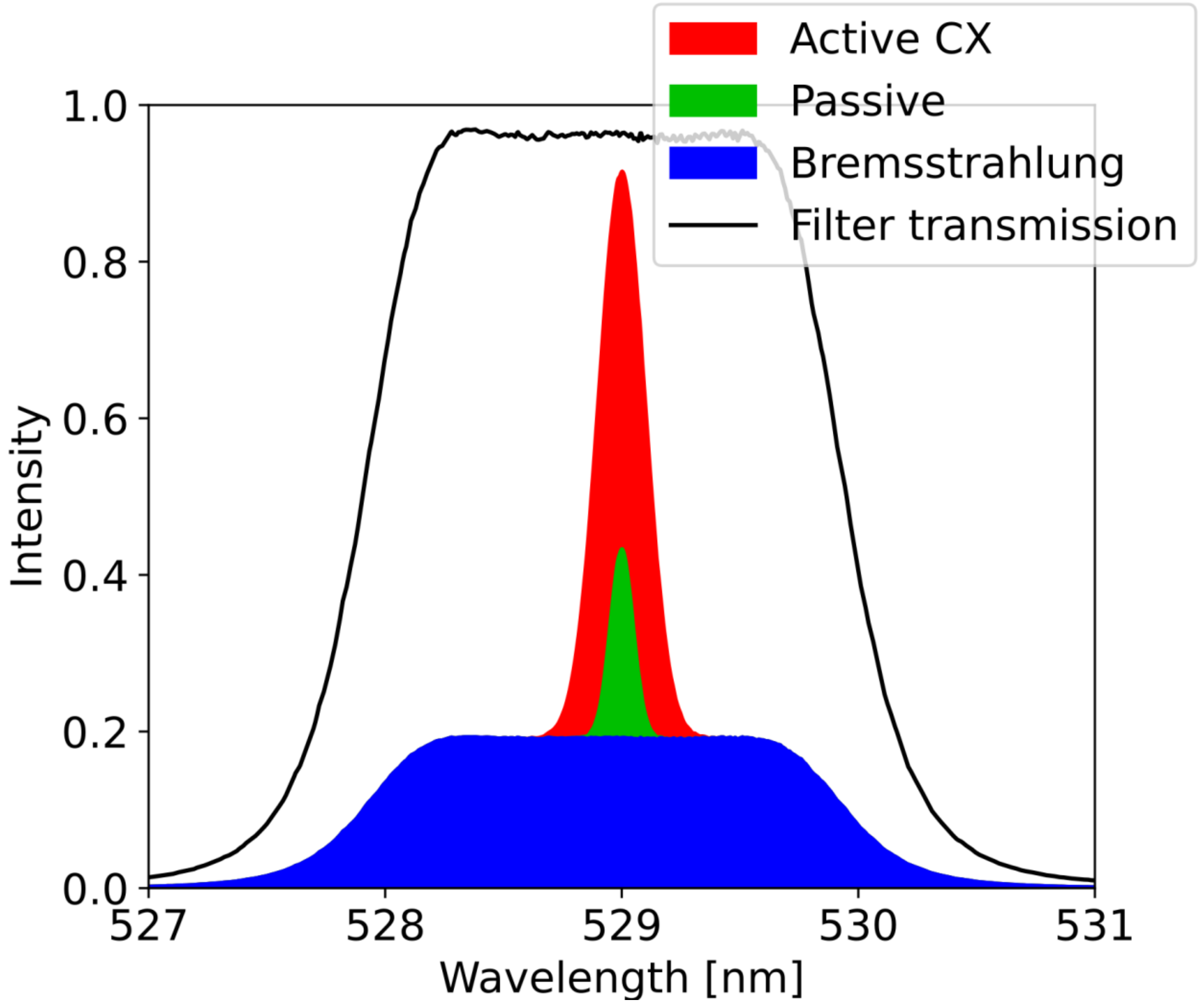

Background radiation

- Typical **CXRS spectrum**:
  - **Active CX**
    - **CX** with **NBI neutrals**
  - **Passive**
    - **CX** with **edge neutrals**
    - **Electron-Impact excitation**
  - **Bremsstrahlung**
- CICERS:
  - **Total spectrum** encoded in fringe pattern**.**

→ Need strategies to **isolate the CX contribution** from contaminants!

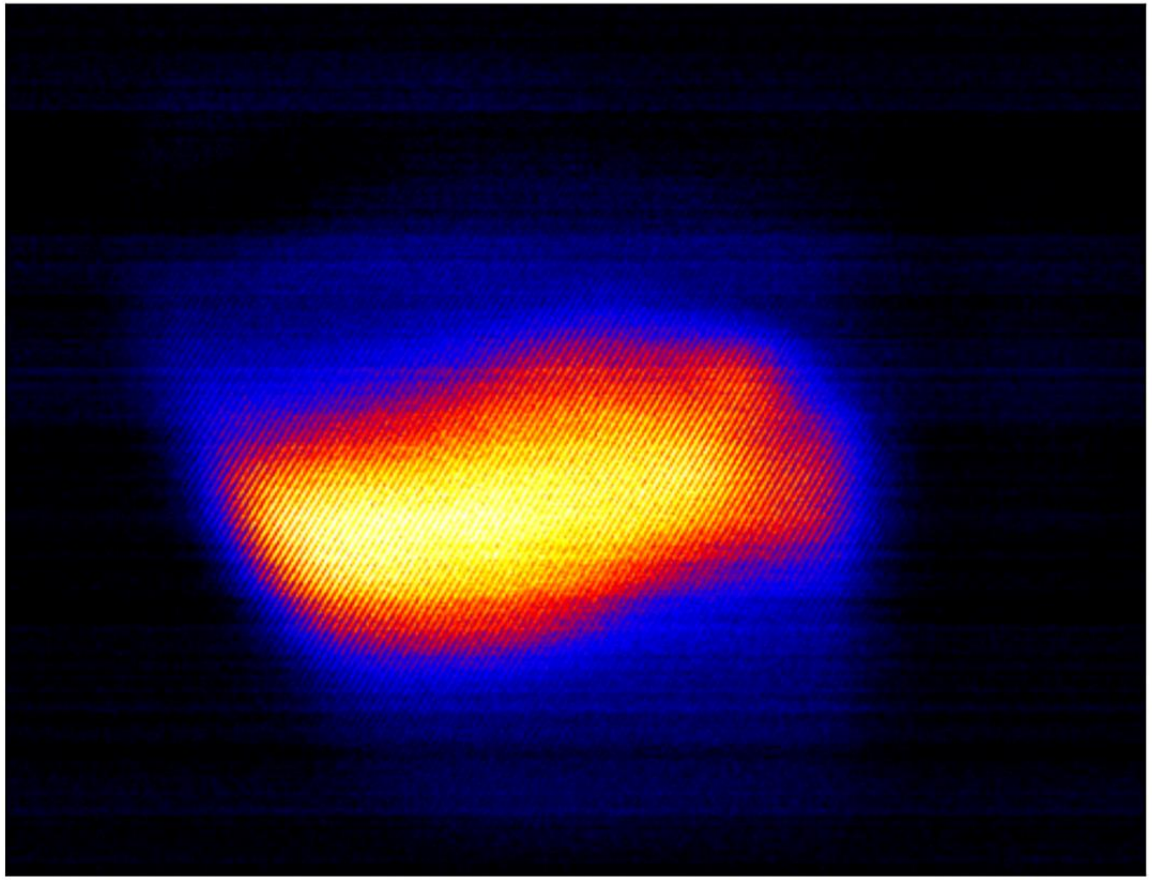

How to isolate the active CX contribution

- $\boldsymbol{S}$ is **linear** w.r.t each individual radiation component.

$$\boldsymbol{S} = \boldsymbol{S_{CX}} + \boldsymbol{S_{pas}} + \boldsymbol{S_{B}}$$

$$S_i = \frac{I_i}{2}(1 + \zeta_i \cos \Phi_i)$$

How to isolate the active CX contribution

- $\boldsymbol{S}$ is **linear** w.r.t each individual radiation component.

$$\boldsymbol{S} = \boldsymbol{S_{CX}} + \boldsymbol{S_{pas}} + \boldsymbol{S_{B}} \qquad S_i = \frac{I_i}{2}(1 + \zeta_i \cos \Phi_i)$$

- **Active CX** only appears with NBI → **Interpolation of background radiation** before and after injection and subtraction from total signal[4]

[4] R. Lopez-Cansino et al., PPCF 2024

How to isolate the active CX contribution

- $\boldsymbol{S}$ is **linear** w.r.t each individual radiation component.

$$\boldsymbol{S} = \boldsymbol{S_{CX}} + \boldsymbol{S_{pas}} + \boldsymbol{S_B} \qquad\qquad S_i = \frac{I_i}{2}(1 + \zeta_i \cos\Phi_i)$$

- **Active CX** only appears with NBI → **Interpolation of background radiation** before and after injection and subtraction from total signal[4]

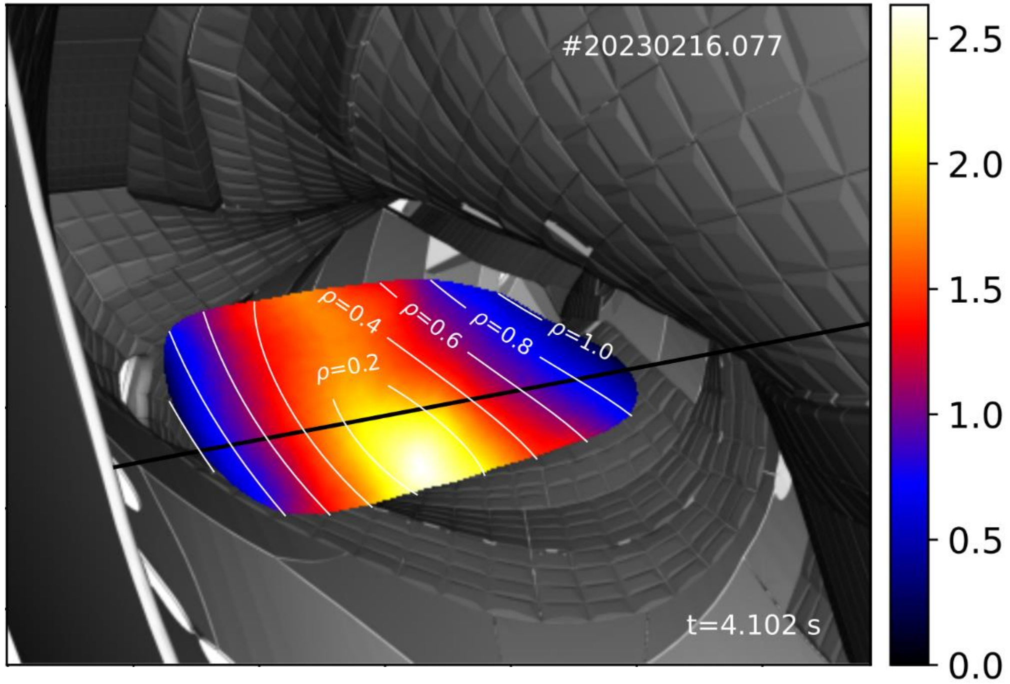

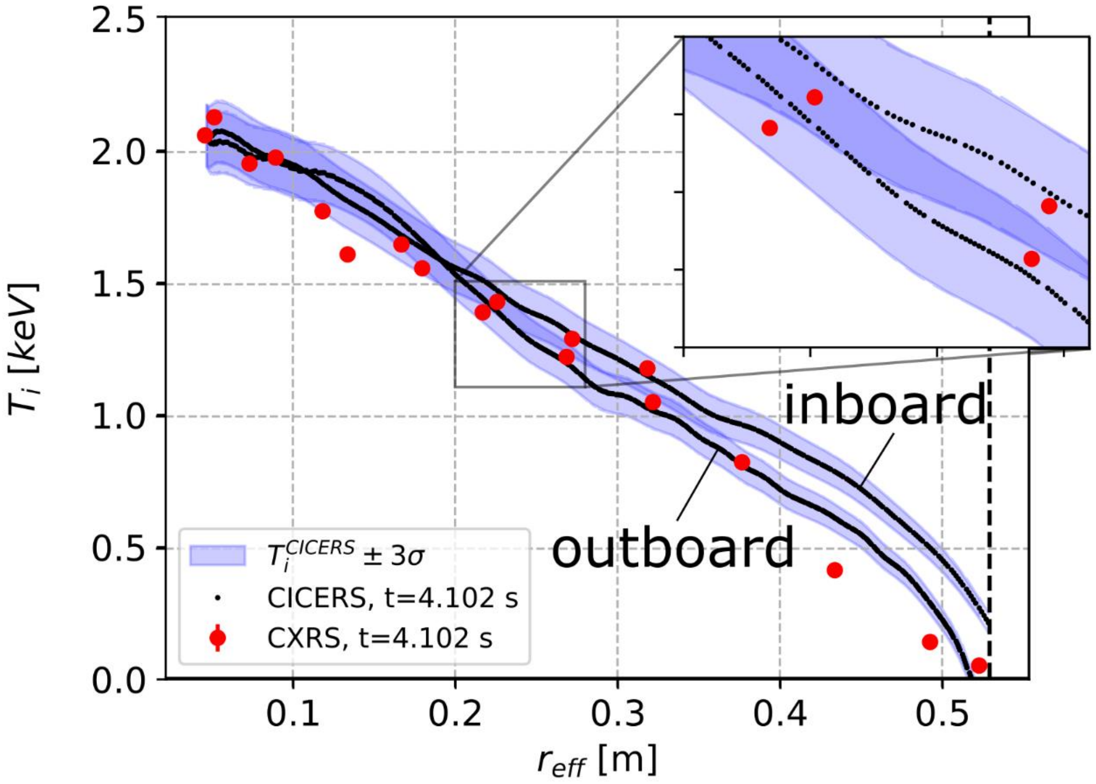

[4] R. Lopez-Cansino et al., PPCF 2024

How to isolate the active CX contribution

- $\boldsymbol{S}$ is **linear** w.r.t each individual radiation component.

$$\boldsymbol{S} = \boldsymbol{S_{CX}} + \boldsymbol{S_{pas}} + \boldsymbol{S_{B}} \qquad S_i = \frac{I_i}{2}(1 + \zeta_i \cos \Phi_i)$$

- **Active CX** only appears with NBI → **Interpolation of background radiation** before and after injection and subtraction from total signal[4]

- **Modelling background** radiation:

[4] R. Lopez-Cansino et al., PPCF 2024

How to isolate the active CX contribution

- $\boldsymbol{S}$ is **linear** w.r.t each individual radiation component.

$$\boldsymbol{S} = \boldsymbol{S_{CX}} + \boldsymbol{S_{pas}} + \boldsymbol{S_B} \qquad S_i = \frac{I_i}{2}(1 + \zeta_i \cos\Phi_i)$$

- **Active CX** only appears with NBI → **Interpolation of background radiation** before and after injection and subtraction from total signal[4]

- **Modelling background** radiation:

$$\boldsymbol{I_{CX}} = \boldsymbol{I_{eff}} - (\boldsymbol{I_{pas}} + \boldsymbol{I_B})$$

$$\boldsymbol{\zeta_{CX}} = \frac{\boldsymbol{\zeta_{eff} I_{eff}} - \boldsymbol{\zeta_{pas} I_{pas}}}{\boldsymbol{I_{eff}} - (\boldsymbol{I_{pas}} + \boldsymbol{I_B})}$$

[4] R. Lopez-Cansino et al., PPCF 2024

How to isolate the active CX contribution

- $\boldsymbol{S}$ is **linear** w.r.t each individual radiation component.

$$\boldsymbol{S} = \boldsymbol{S_{CX}} + \boldsymbol{S_{pas}} + \boldsymbol{S_B} \qquad S_i = \frac{I_i}{2}(1 + \zeta_i \cos\Phi_i)$$

- **Active CX** only appears with NBI → **Interpolation of background radiation** before and after injection and subtraction from total signal[4]

- **Modelling background** radiation:

$$\boldsymbol{I_{CX}} = \boldsymbol{I_{eff}} - (\boldsymbol{I_{pas}} + \boldsymbol{I_B})$$

$$\boldsymbol{\zeta_{CX}} = \frac{\boldsymbol{\zeta_{eff} I_{eff}} - \boldsymbol{\zeta_{pas} I_{pas}}}{\boldsymbol{I_{eff}} - (\boldsymbol{I_{pas}} + \boldsymbol{I_B})}$$

- $\mathbf{I_{eff}}, \boldsymbol{\zeta_{eff}}$: effective parameters from raw signal
- $\mathbf{I_B}$: Bremsstrahlung line-integrated intensity
- $\mathbf{I_{pas}}, \boldsymbol{\zeta_{pas}}$: Passive line-integrated intensity and contrast

[4] R. Lopez-Cansino et al., PPCF 2024

Modelling workflow

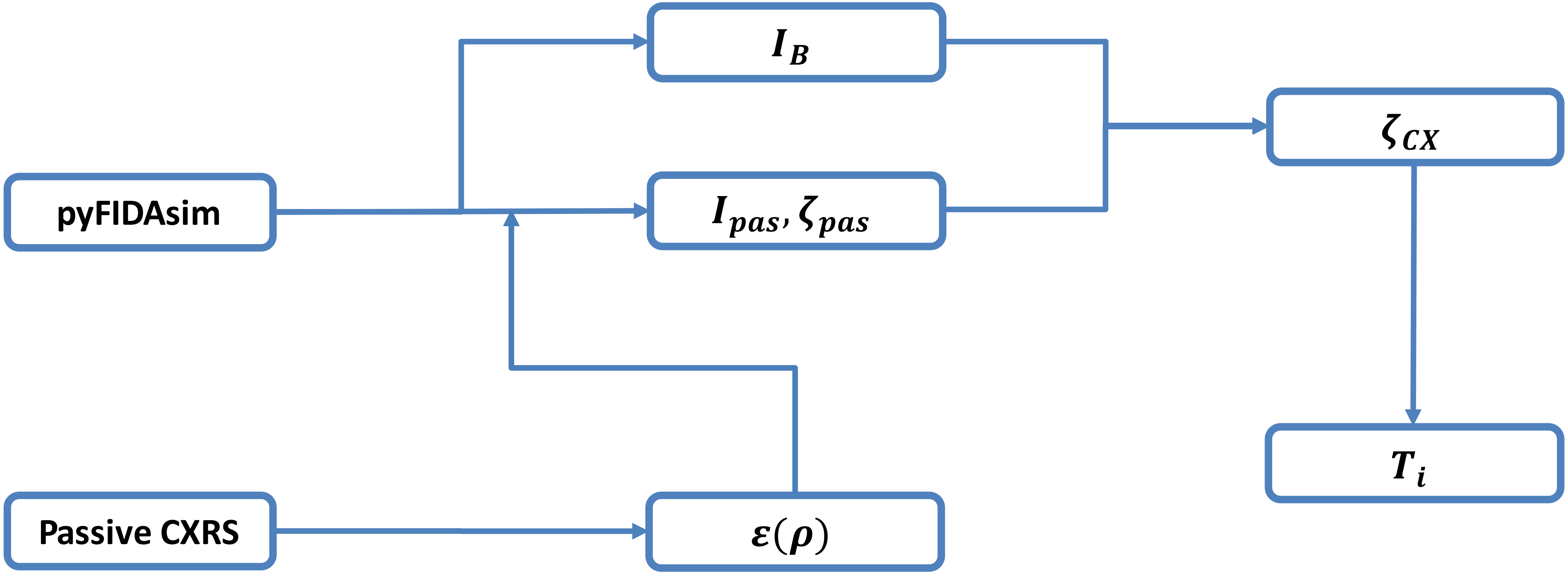

Modelling workflow: Grid

- **3D** grid
- Local $\boldsymbol{B}$ → **VMEC**
- Intersections with LOS

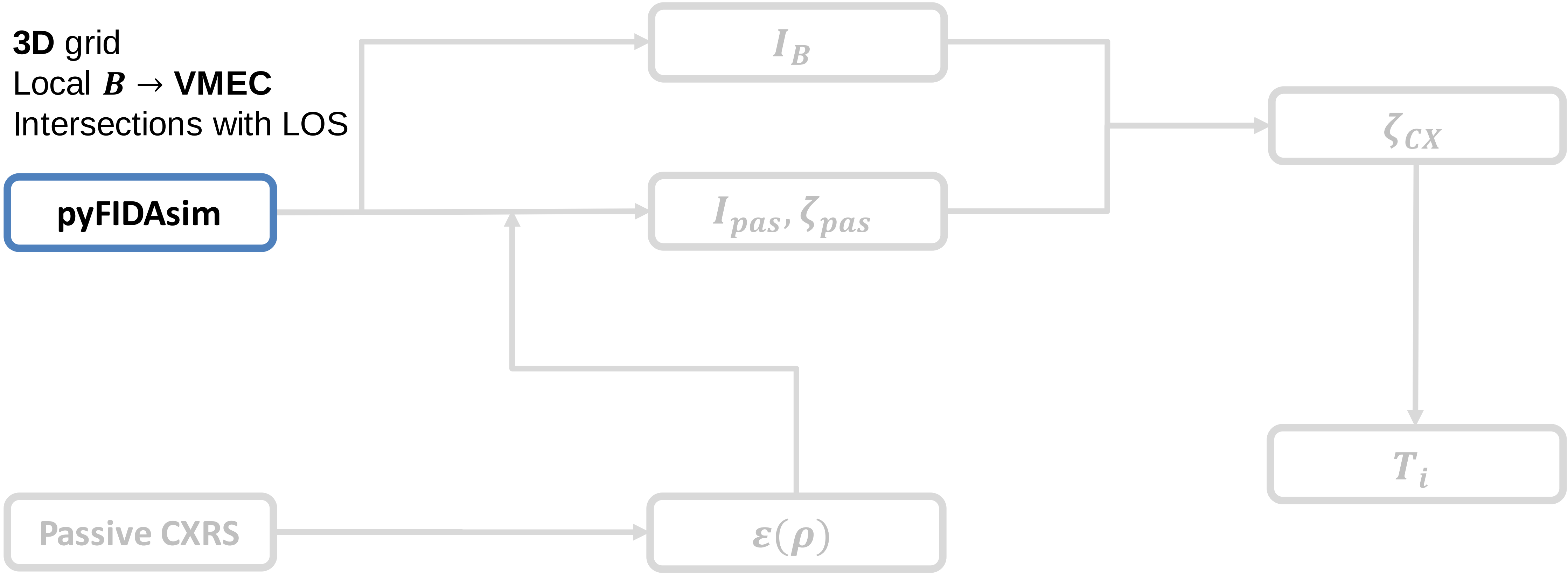

Modelling workflow: Bremsstrahlung contribution

- **3D** grid
- Local $\boldsymbol{B}$ → **VMEC**
- Intersections with LOS

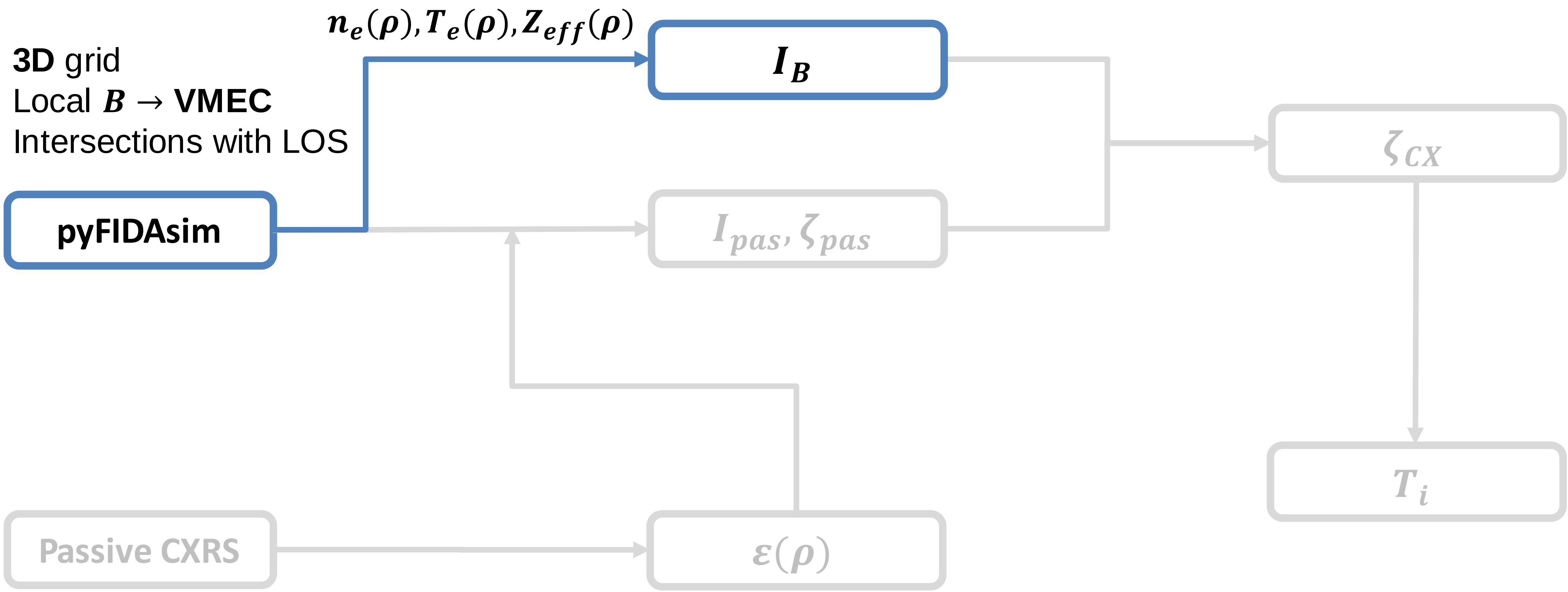

Bremsstrahlung intensity

- $\boldsymbol{I_B} \rightarrow n_e, T_e, Z_{eff}$ profiles:

$$\frac{dN_B}{d\lambda} = 7.59 \cdot 10^{-9} g \frac{n_e^2 Z_{eff}}{\lambda T_e^{\frac{1}{2}}} e^{-\frac{hc}{\lambda}T_e}$$

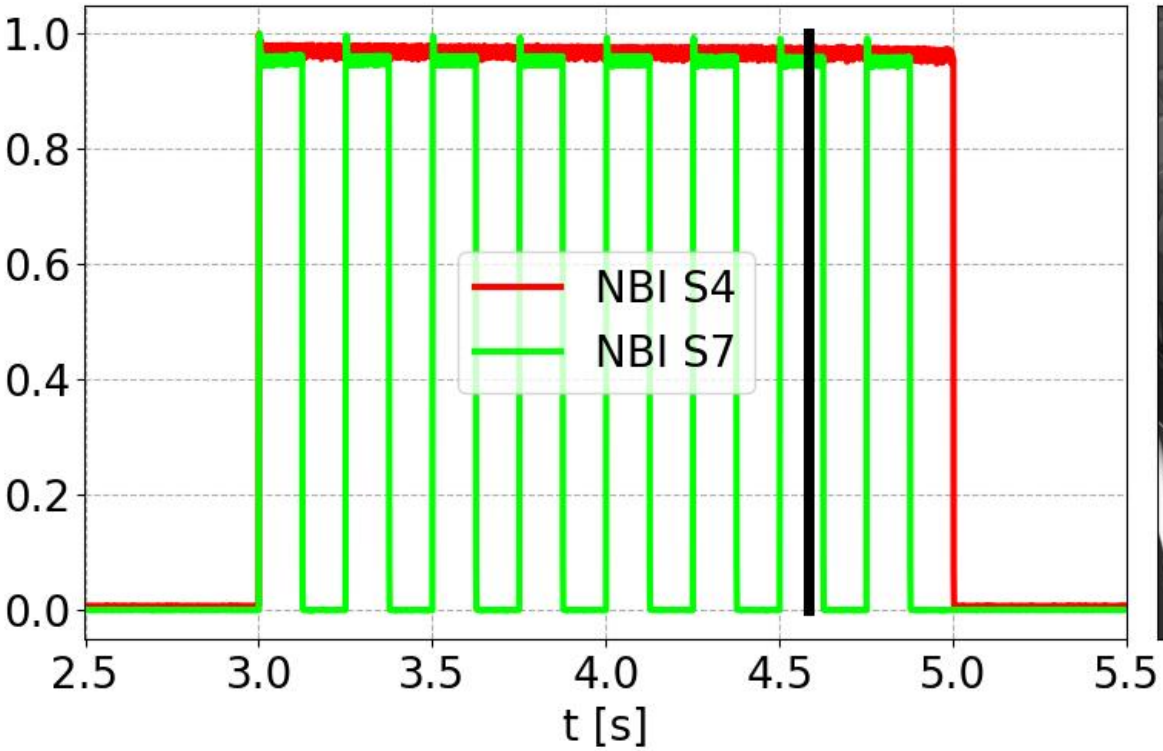

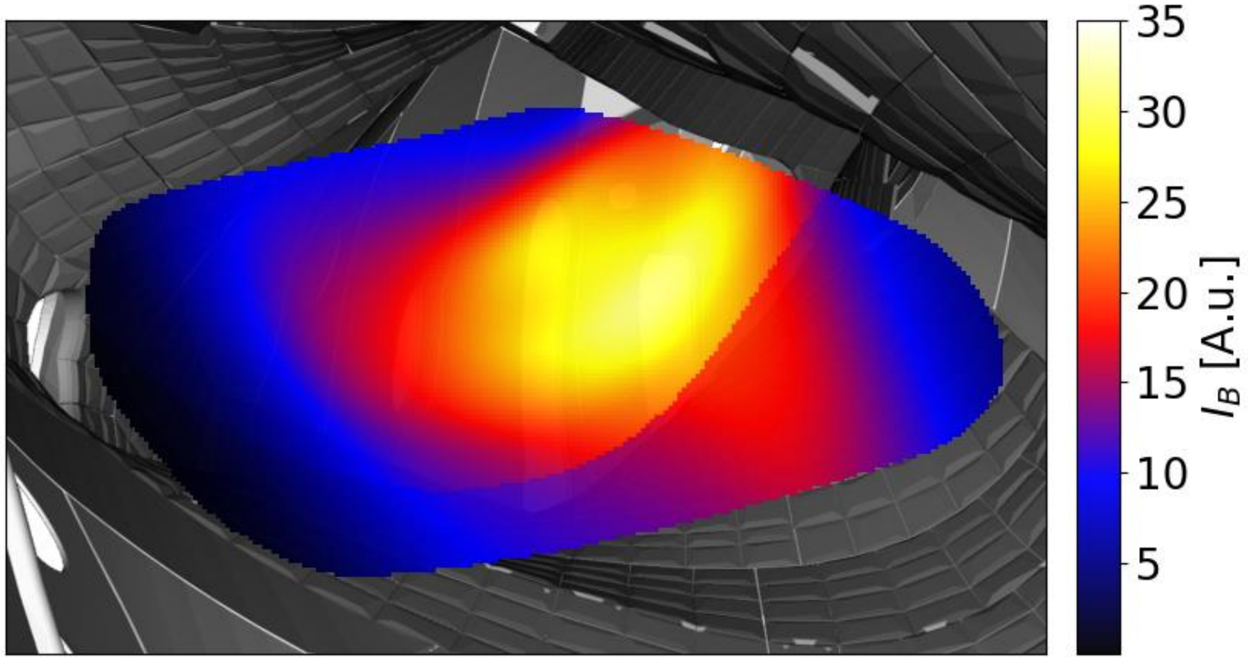

Bremsstrahlung intensity

- $\boldsymbol{I_B} \rightarrow n_e, T_e, Z_{eff}$ profiles:

$$\frac{dN_B}{d\lambda} = 7.59 \cdot 10^{-9} g \frac{n_e^2 Z_{eff}}{\lambda T_e^{\frac{1}{2}}} e^{-\frac{hc}{\lambda} T_e}$$

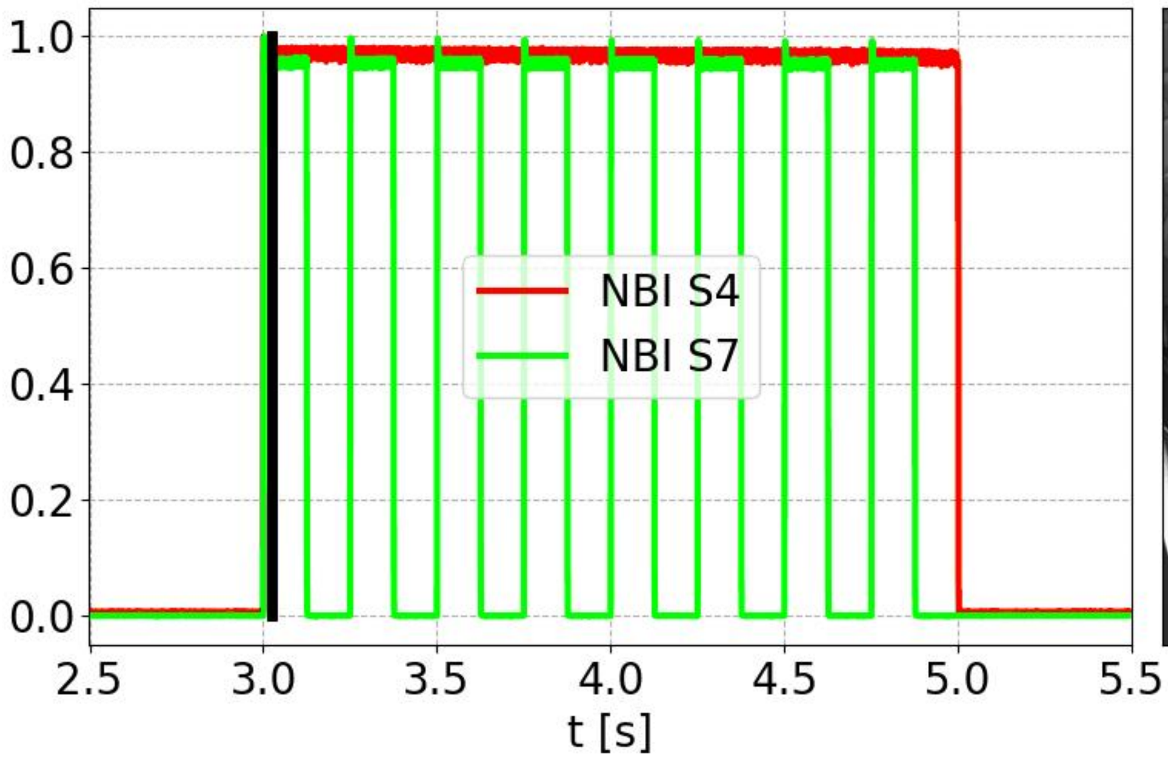

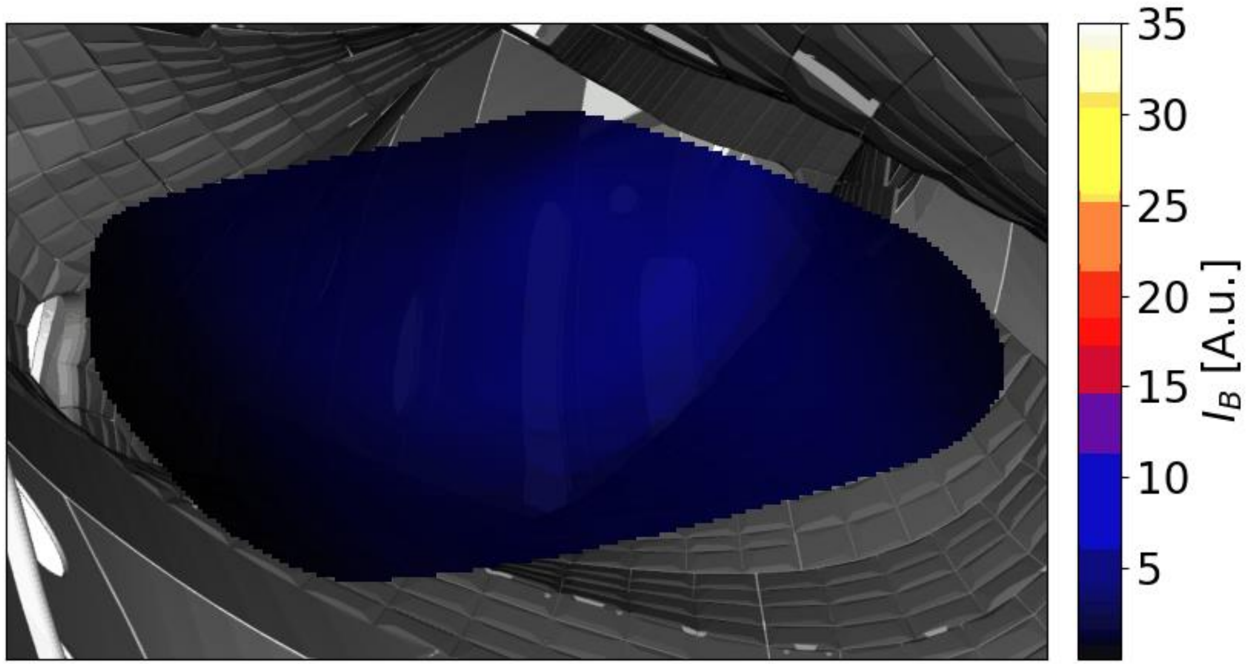

Bremsstrahlung evolution along discharge

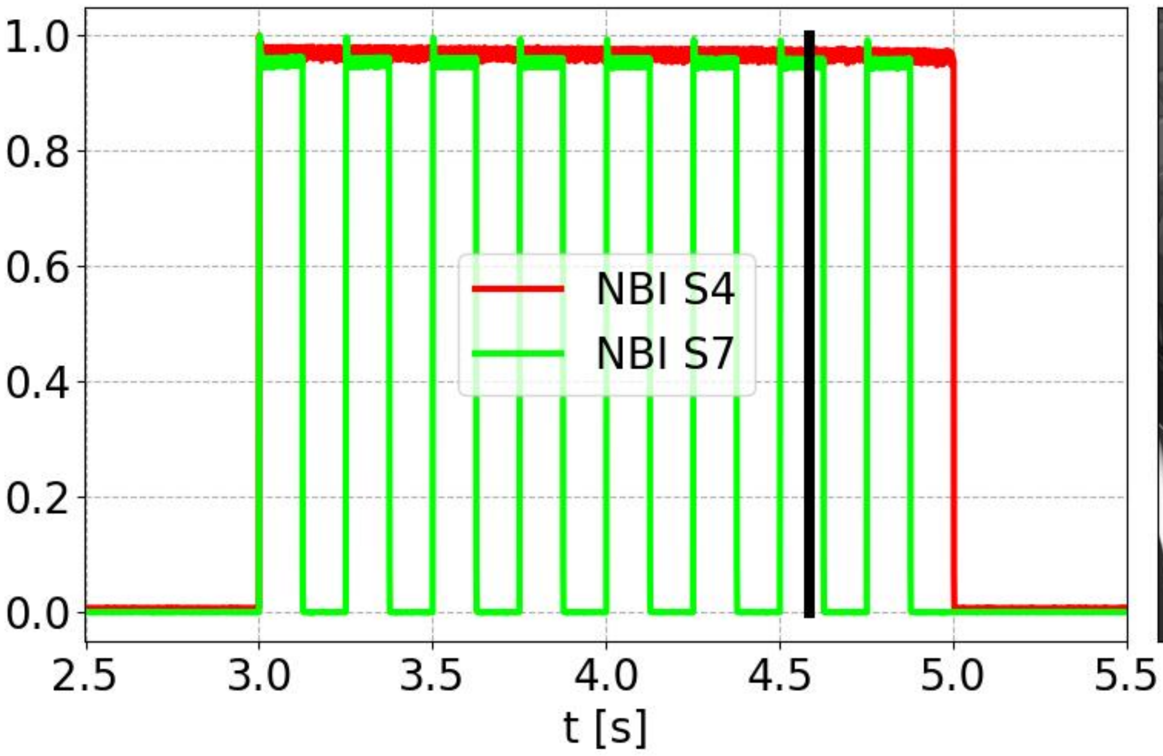

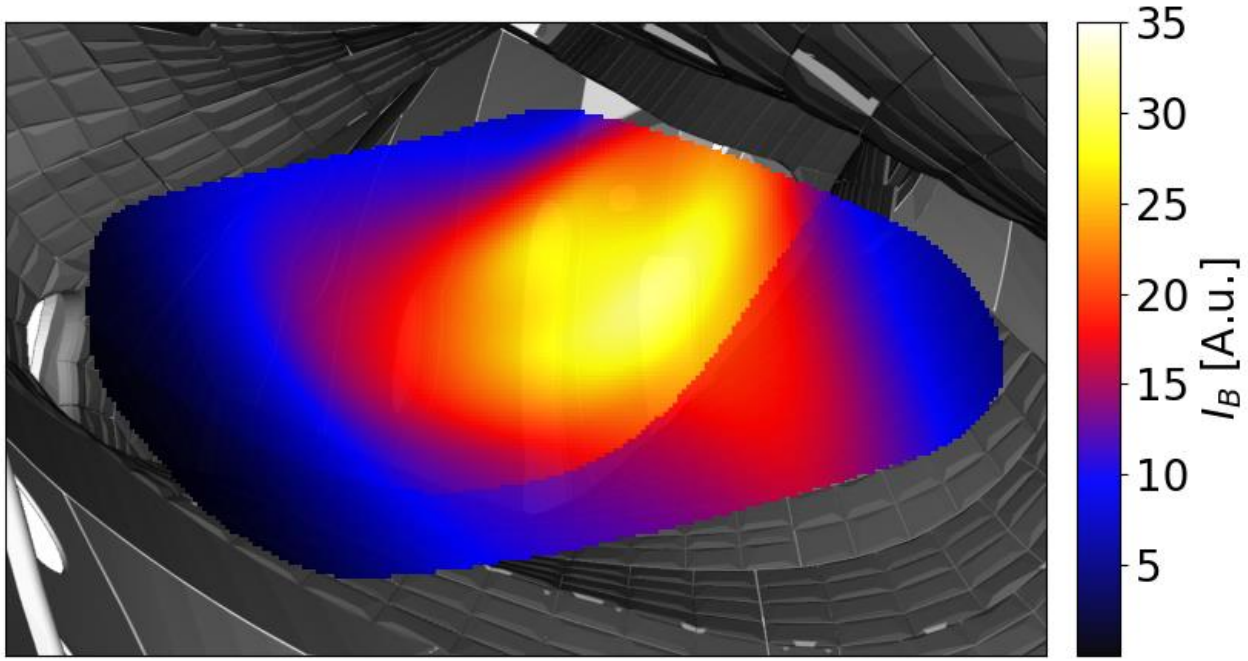

Able to predict $\boldsymbol{I_B}$ within 25% accuracy → Quality of profiles

Modelling workflow: Bremsstrahlung contribution

- **3D** grid
- Local $\boldsymbol{B}$ → **VMEC**
- Intersections with LOS

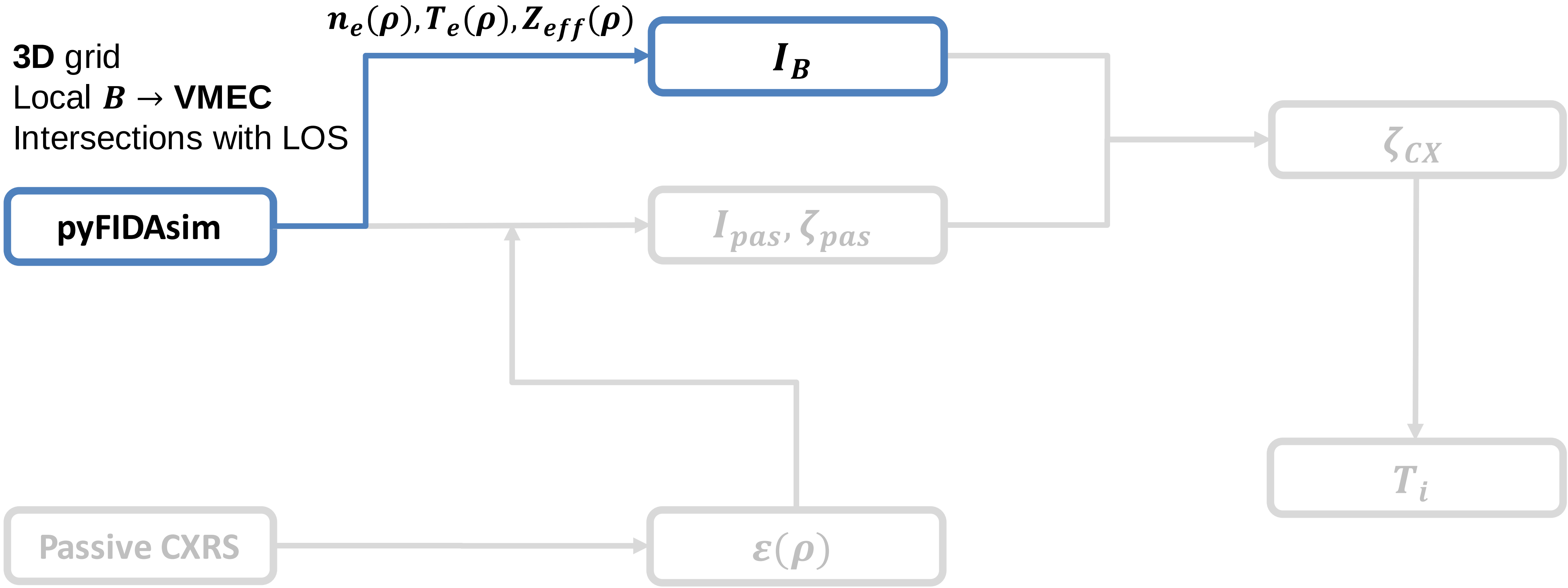

Modelling workflow: Passive contribution

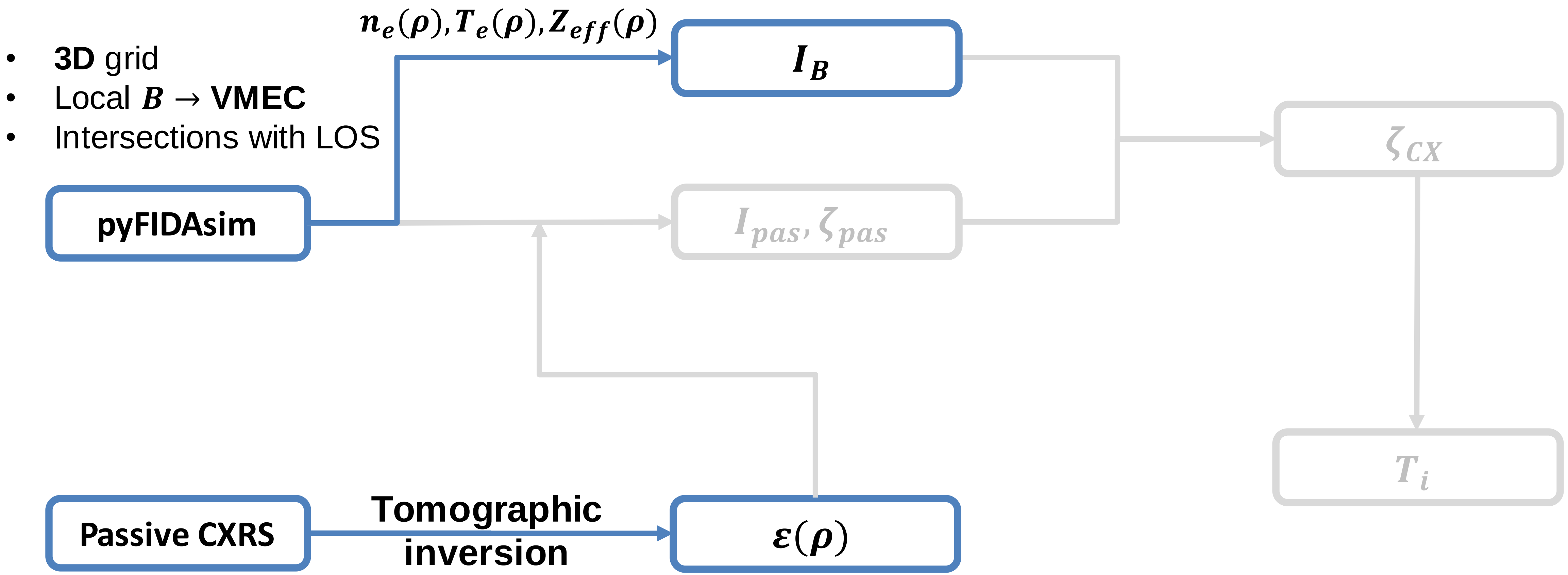

Passive radiation

- Dedicated spectrometer for passive CVI at W7-X.
  → O.P Ford et al, this conference, **3.4.33**

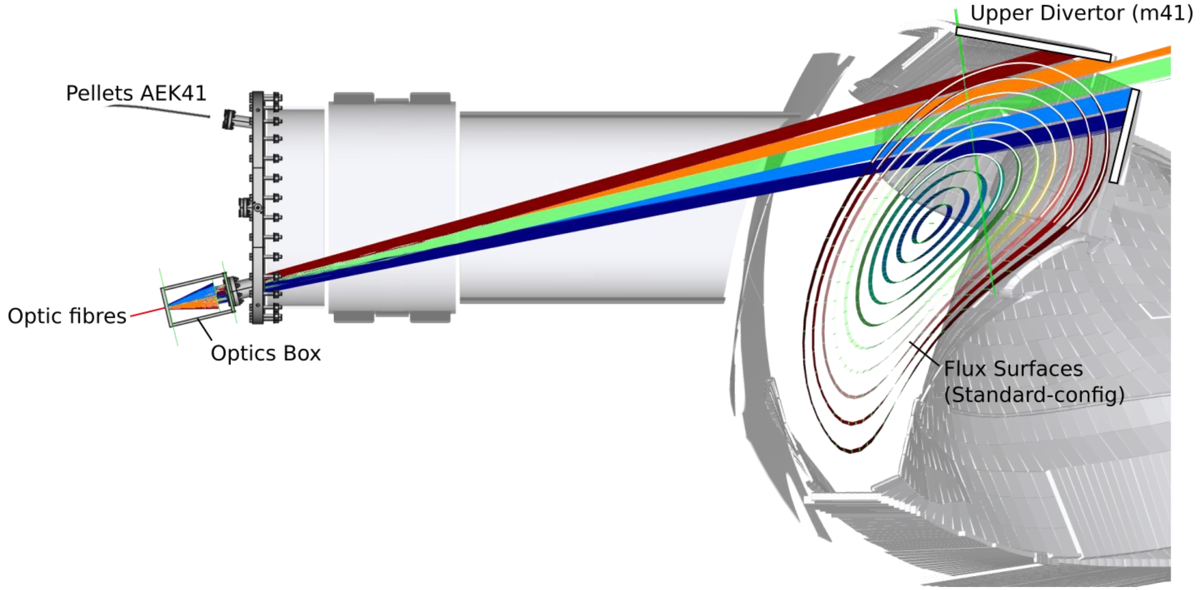

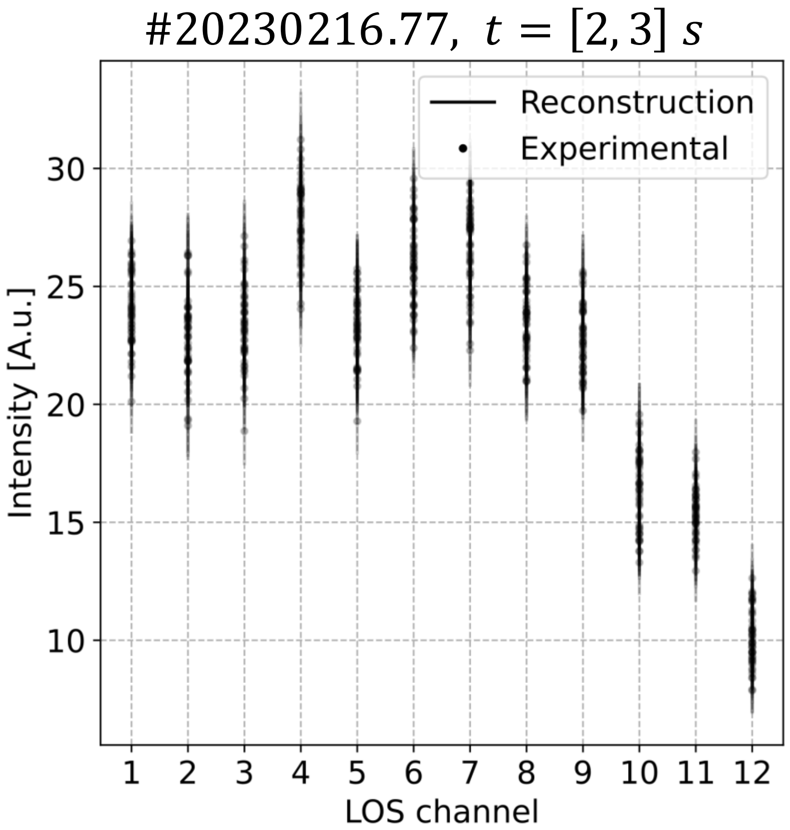

Passive radiation

- Dedicated spectrometer for passive CVI at W7-X.
  - → O.P Ford et al, this conference, **3.4.33**
- Tomographic inversion on CVI passive intensity:

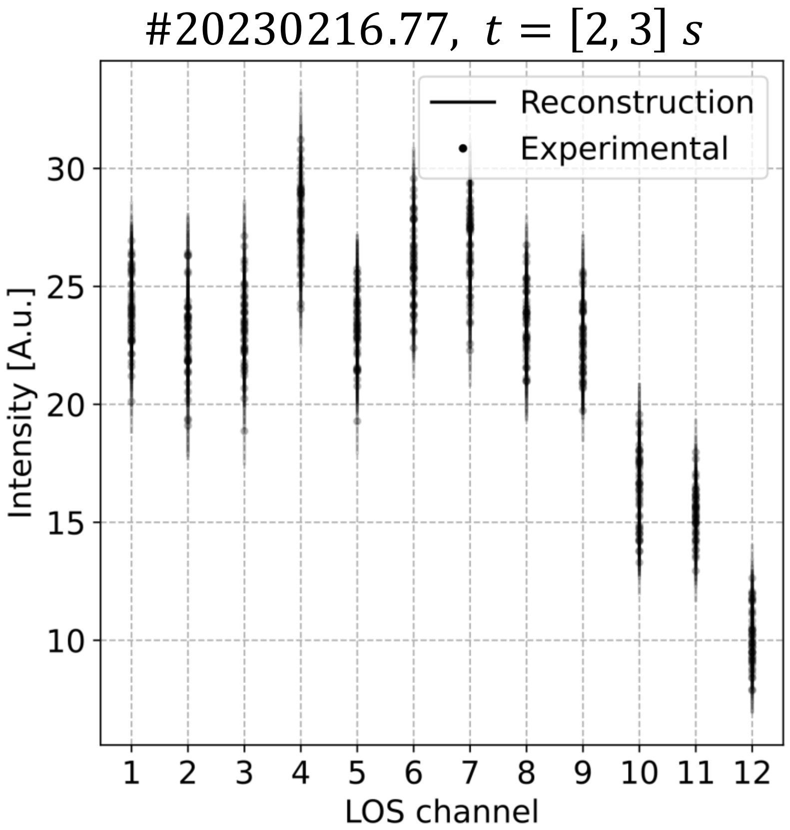

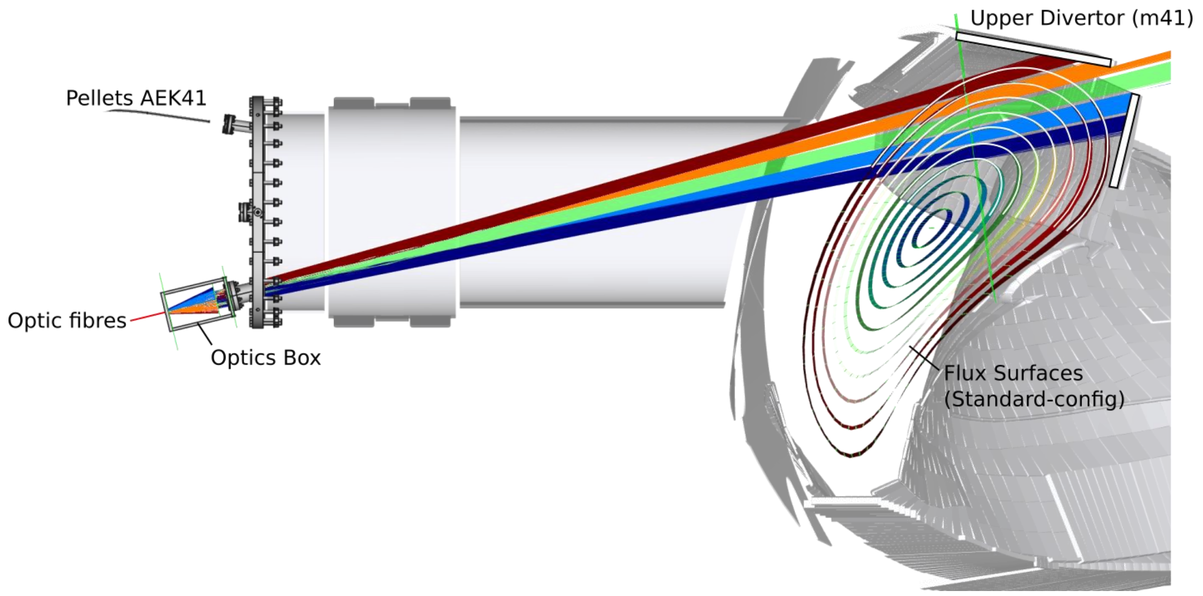

Passive radiation

- Dedicated spectrometer for passive CVI at W7-X.
  → O.P Ford et al, this conference, **3.4.33**
- Tomographic inversion on CVI passive intensity:

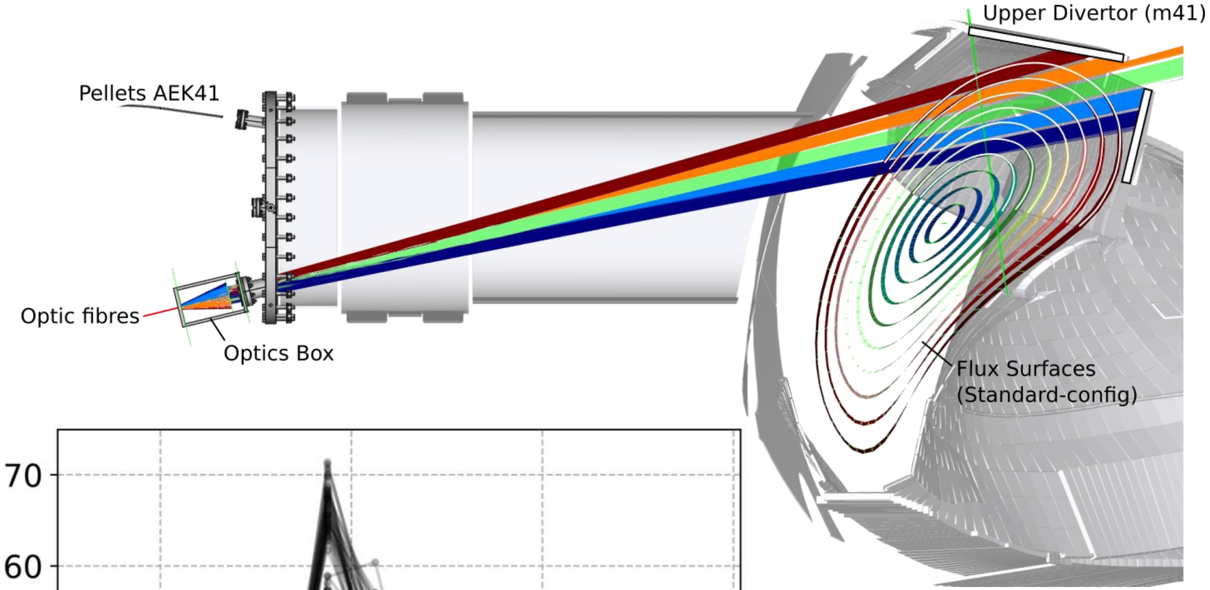

$\#20230216.77,\ t = [2,3]\ s$

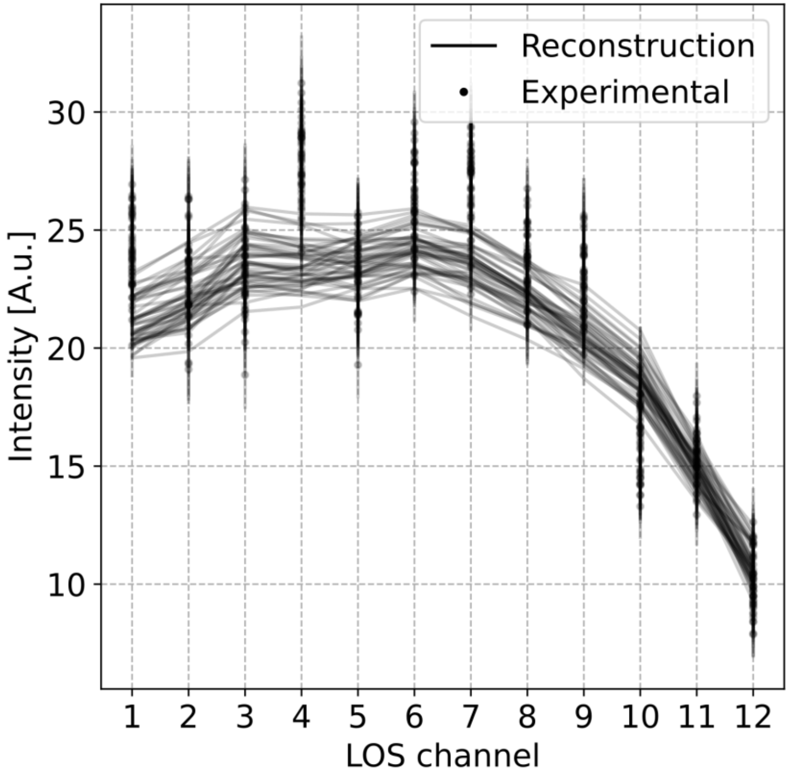

$$I_i = w_\alpha \varepsilon_i^\alpha$$

0^{th} Tikhonov

$$\mathcal{C}(\boldsymbol{E}|\alpha) = ||\boldsymbol{w\varepsilon} - \boldsymbol{I}||_2^2 + \alpha||\boldsymbol{\varepsilon}||_2^2$$

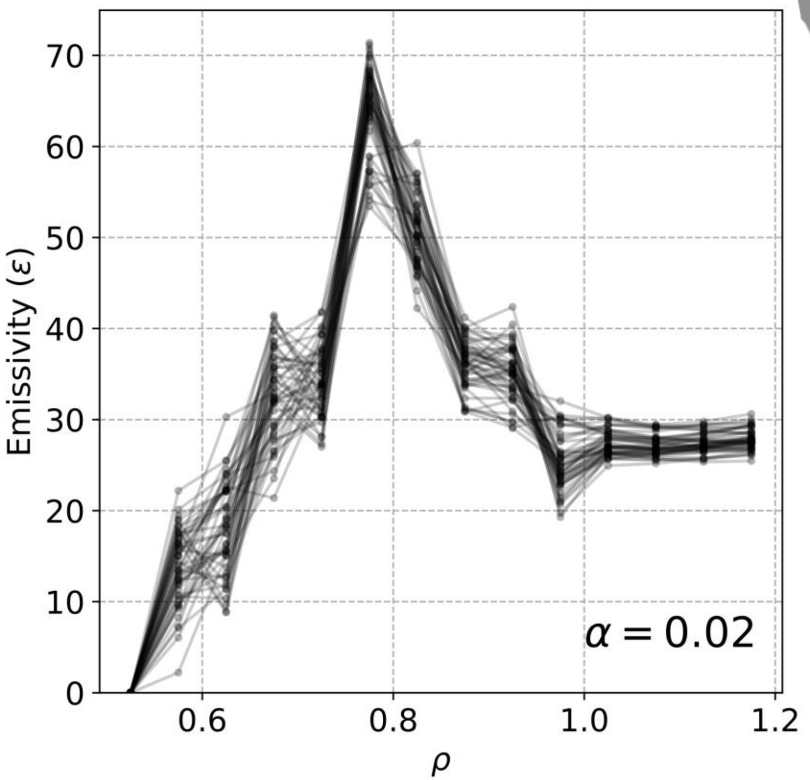

Passive radiation

- Dedicated spectrometer for passive CVI at W7-X.
  - → O.P Ford et al, this conference, **3.4.33**
- Tomographic inversion on CVI passive intensity:
  - ○ 1^{st} order estimation of emissivity → $\boldsymbol{\varepsilon}(\boldsymbol{\rho})$

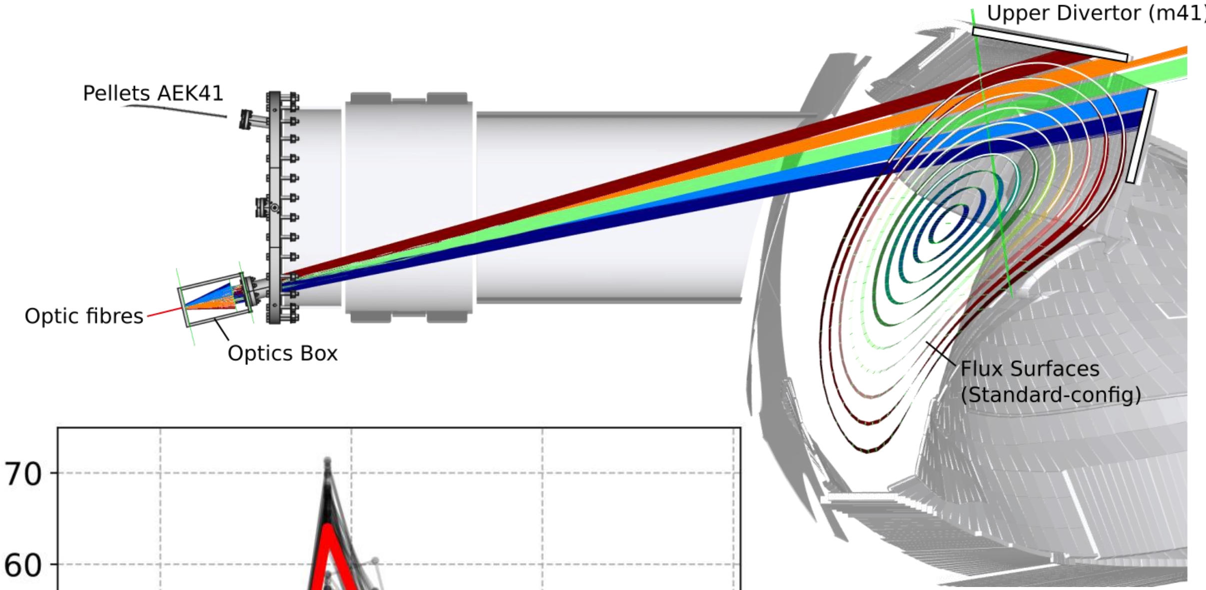

$\#20230216.77,\ t = [2,3]\ s$

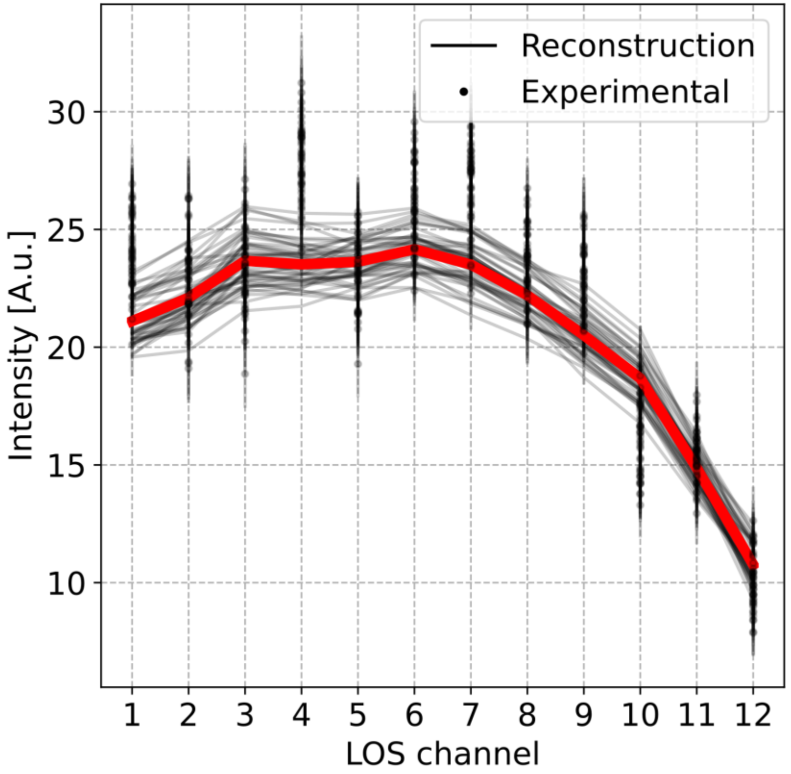

$$I_i = w_\alpha \varepsilon_i^\alpha$$

0^{th} Tikhonov

$$\mathcal{C}(\boldsymbol{E}|\alpha) = \left|\left|\boldsymbol{w\varepsilon} - \boldsymbol{I}\right|\right|_2^2 + \alpha\left|\left|\boldsymbol{\varepsilon}\right|\right|_2^2$$

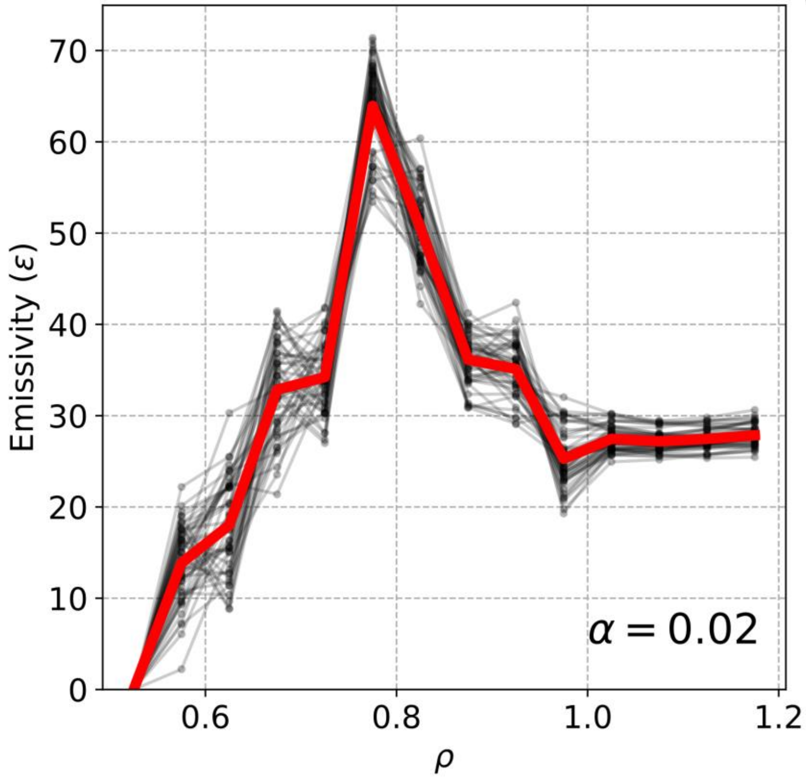

Modelling workflow: Passive contribution

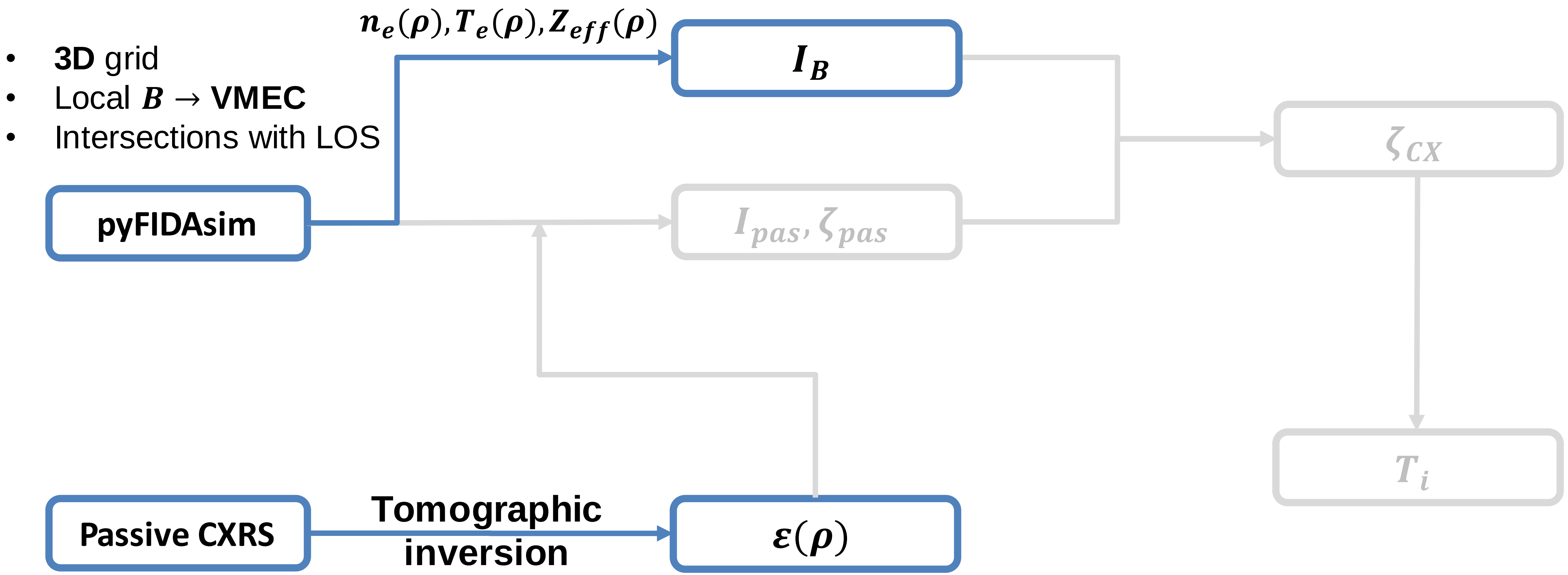

Modelling workflow: Passive contribution

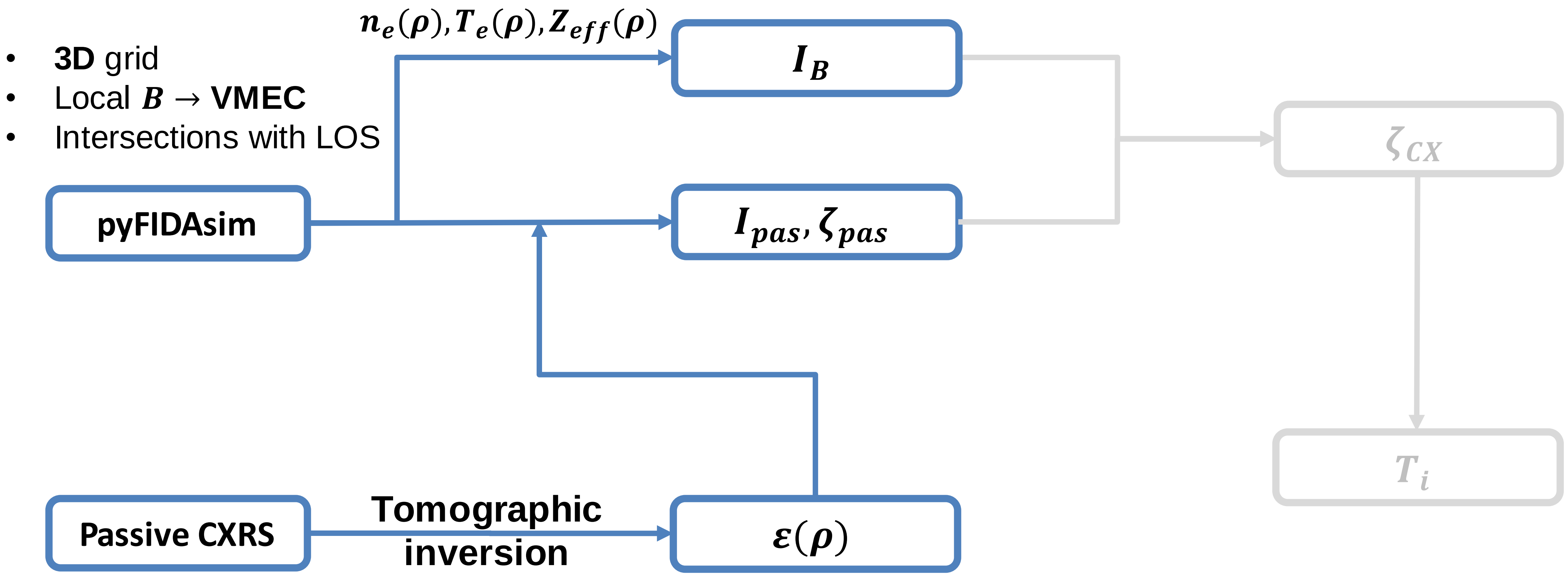

Passive radiation

- Dedicated spectrometer for passive CVI at W7-X.
  → O.P Ford et al, this conference, **3.4.33**
- Tomographic inversion on CXRS CVI passive intensity.
  - 1^{st} order estimation of CVI passive emissivity
- I_{pas}, ζ_{pas} :

$$I_{pas} = \int_{LOS} \varepsilon(\rho) dl$$

$$\zeta_{pas} = \frac{\int_{LOS} \zeta(T_i, \boldsymbol{B}) \varepsilon(\rho) dl}{\int_{LOS} \varepsilon(\rho) dl}$$

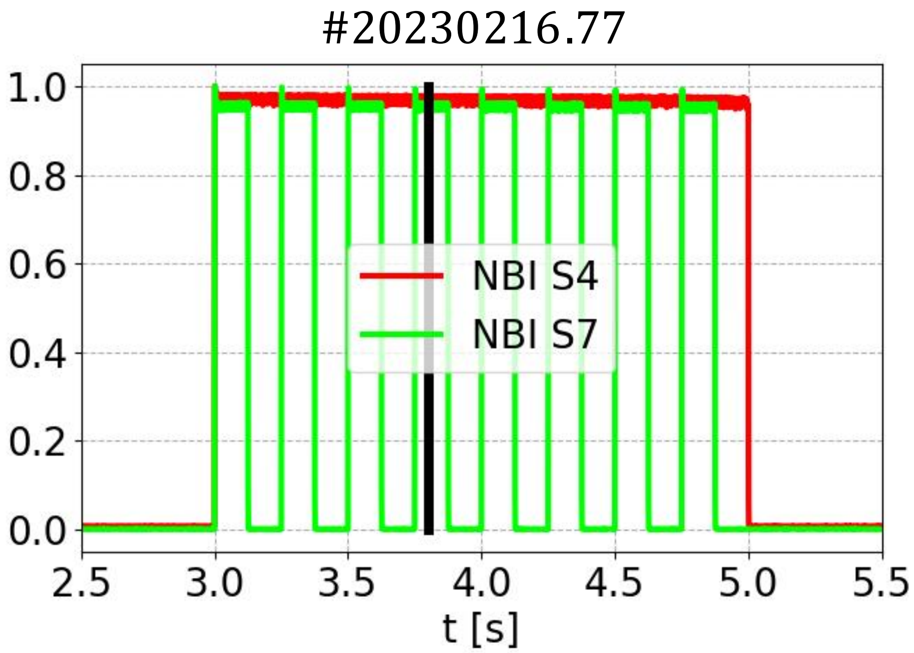

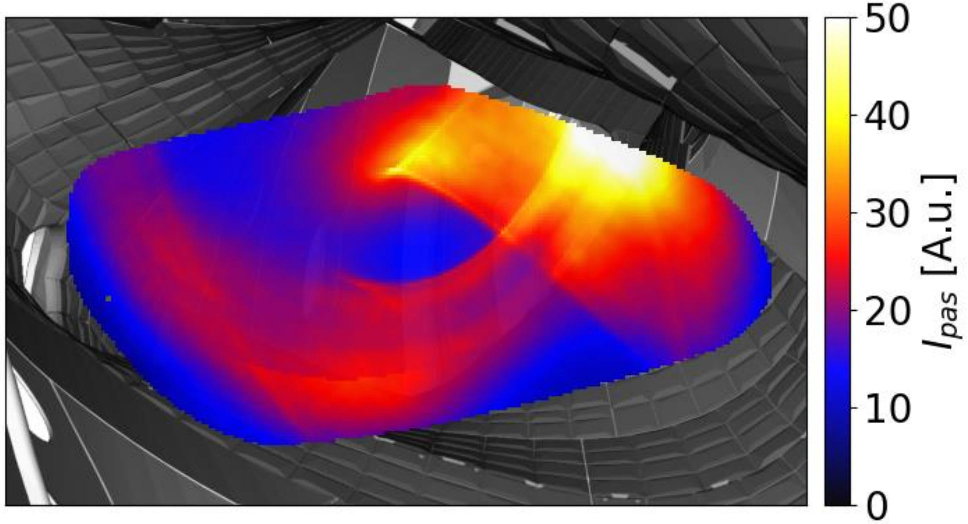

Passive radiation

- Dedicated spectrometer for passive CVI at W7-X.
  → O.P Ford et al, this conference, **3.4.33**
- Tomographic inversion on CXRS CVI passive intensity.
  - 1^{st} order estimation of CVI passive emissivity
- I_{pas}, ζ_{pas} :

$$I_{pas} = \int_{LOS} \varepsilon(\rho) dl$$

$$\zeta_{pas} = \frac{\int_{LOS} \zeta(T_i, \boldsymbol{B}) \varepsilon(\rho) dl}{\int_{LOS} \varepsilon(\rho) dl}$$

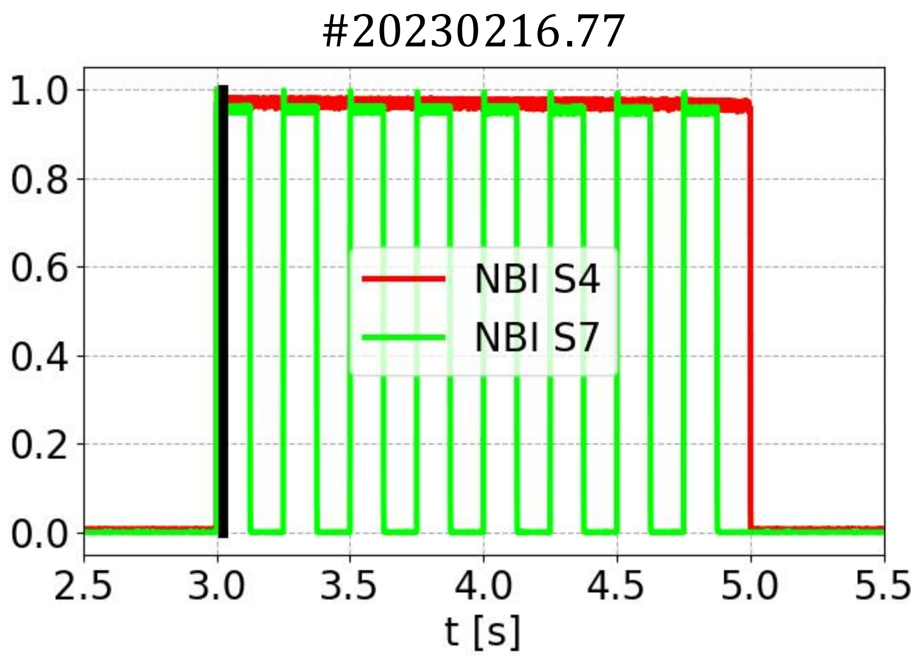

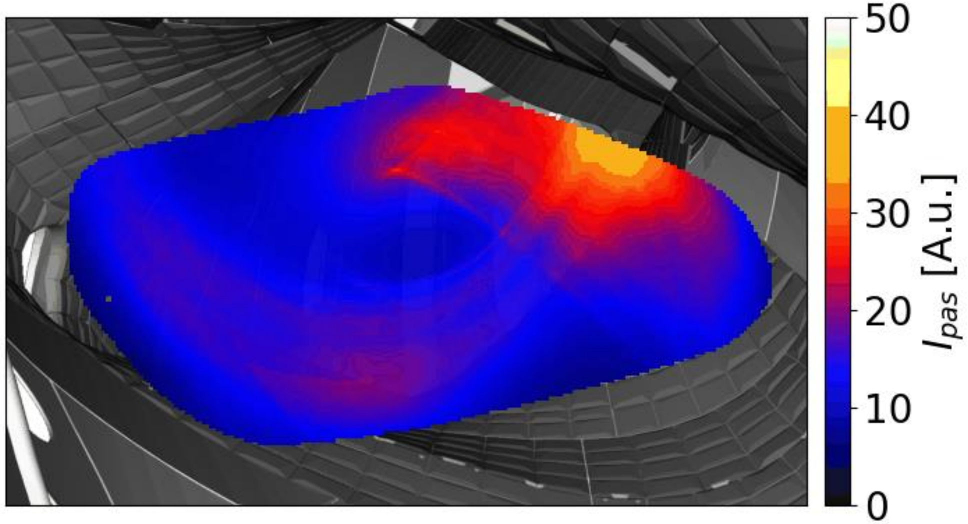

Passive radiation

- Dedicated spectrometer for passive CVI at W7-X.
  → O.P Ford et al, this conference, **3.4.33**
- Tomographic inversion on CXRS CVI passive intensity.

  - 1^{st} order estimation of CVI passive emissivity

- I_{pas}, ζ_{pas} :

$$I_{pas} = \int_{LOS} \varepsilon(\rho) dl$$

$$\zeta_{pas} = \frac{\int_{LOS} \zeta(T_i, \boldsymbol{B}) \varepsilon(\rho) dl}{\int_{LOS} \varepsilon(\rho) dl}$$

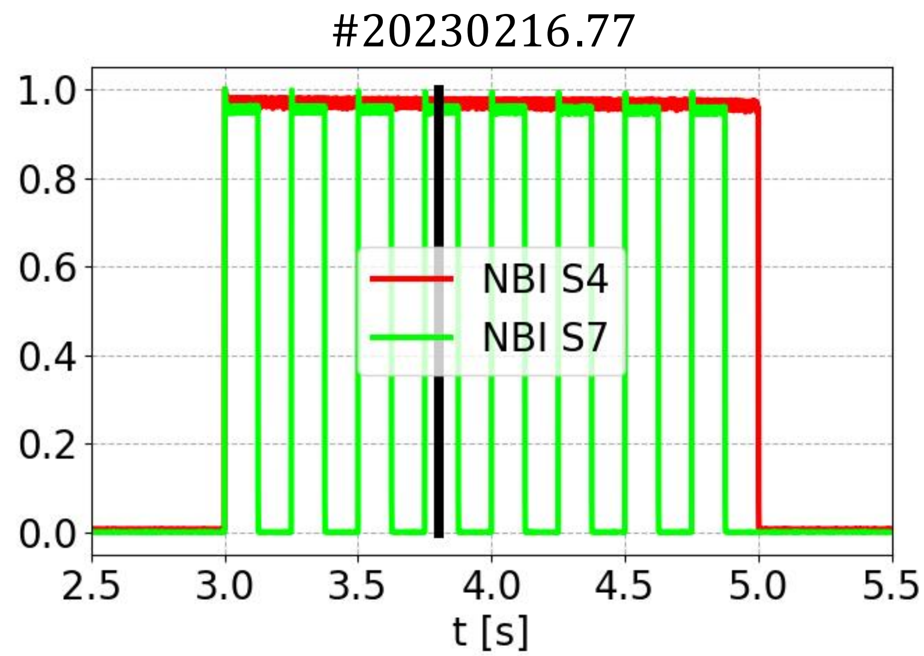

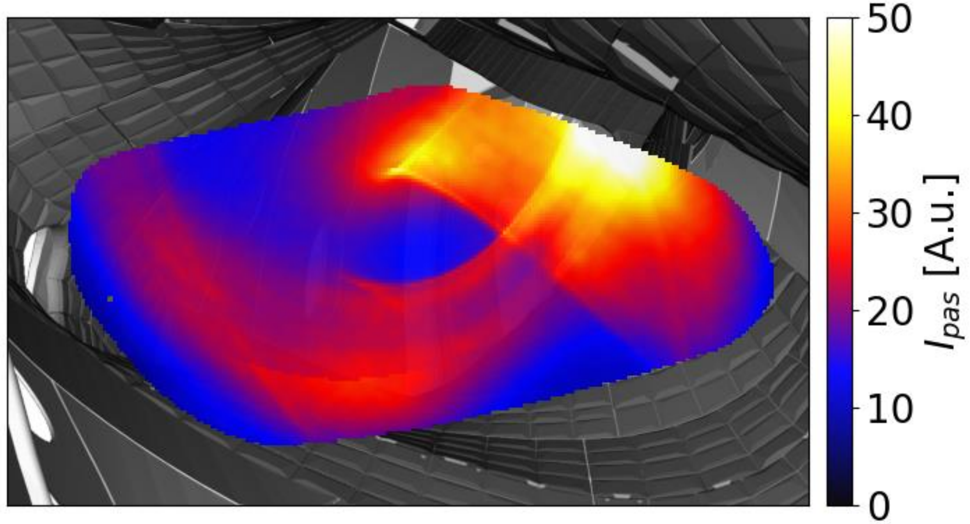

Modelling workflow: Passive contribution

- **3D** grid
- Local $\boldsymbol{B}$ → **VMEC**
- Intersections with LOS

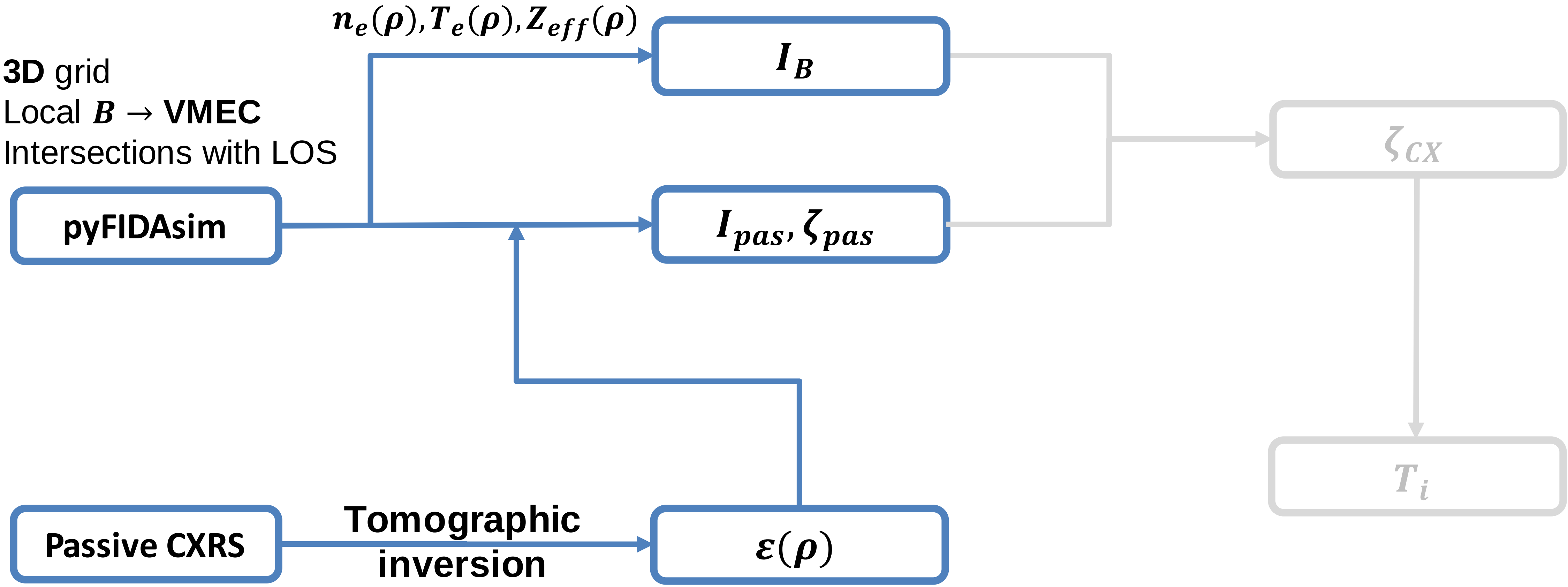

Modelling workflow: T_i

$$\zeta_{CX} = \frac{\zeta_{eff} I_{eff} - \zeta_{pas} I_{pas}}{I_{eff} - (I_{pas} + I_B)}$$

- **3D** grid
- Local B → **VMEC**
- Intersections with LOS

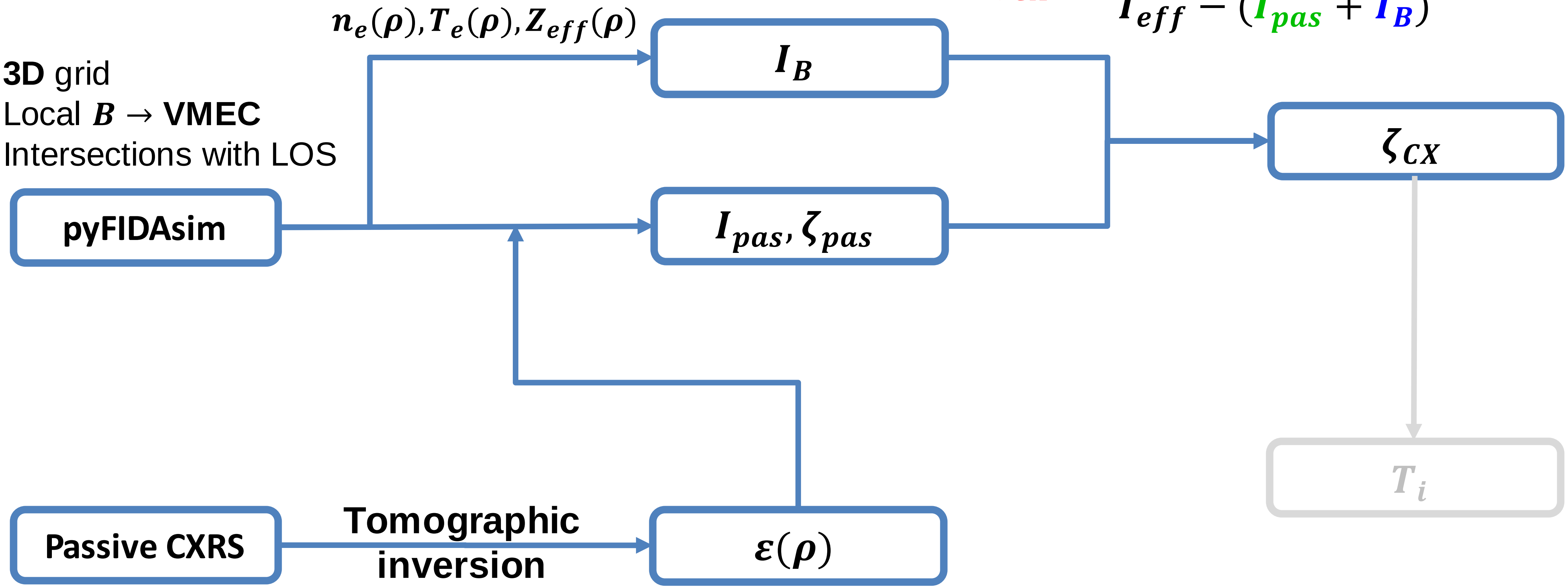

Modelling workflow: T_i

$$\zeta_{CX} = \frac{\zeta_{eff} I_{eff} - \zeta_{pas} I_{pas}}{I_{eff} - (I_{pas} + I_B)}$$

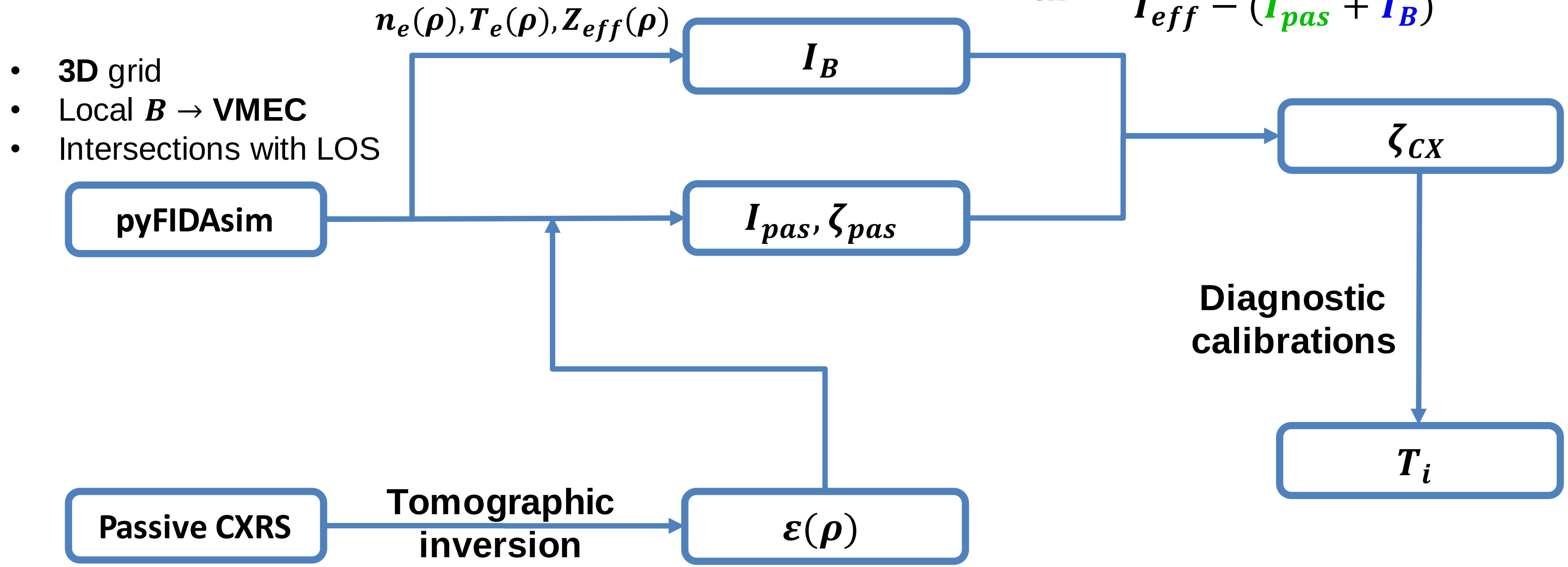

Modelling workflow: T_i

$$\zeta_{CX} = \frac{\zeta_{eff} I_{eff} - \zeta_{pas} I_{pas}}{I_{eff} - (I_{pas} + I_B)}$$

- **3D** grid
- Local B → **VMEC**
- Intersections with LOS

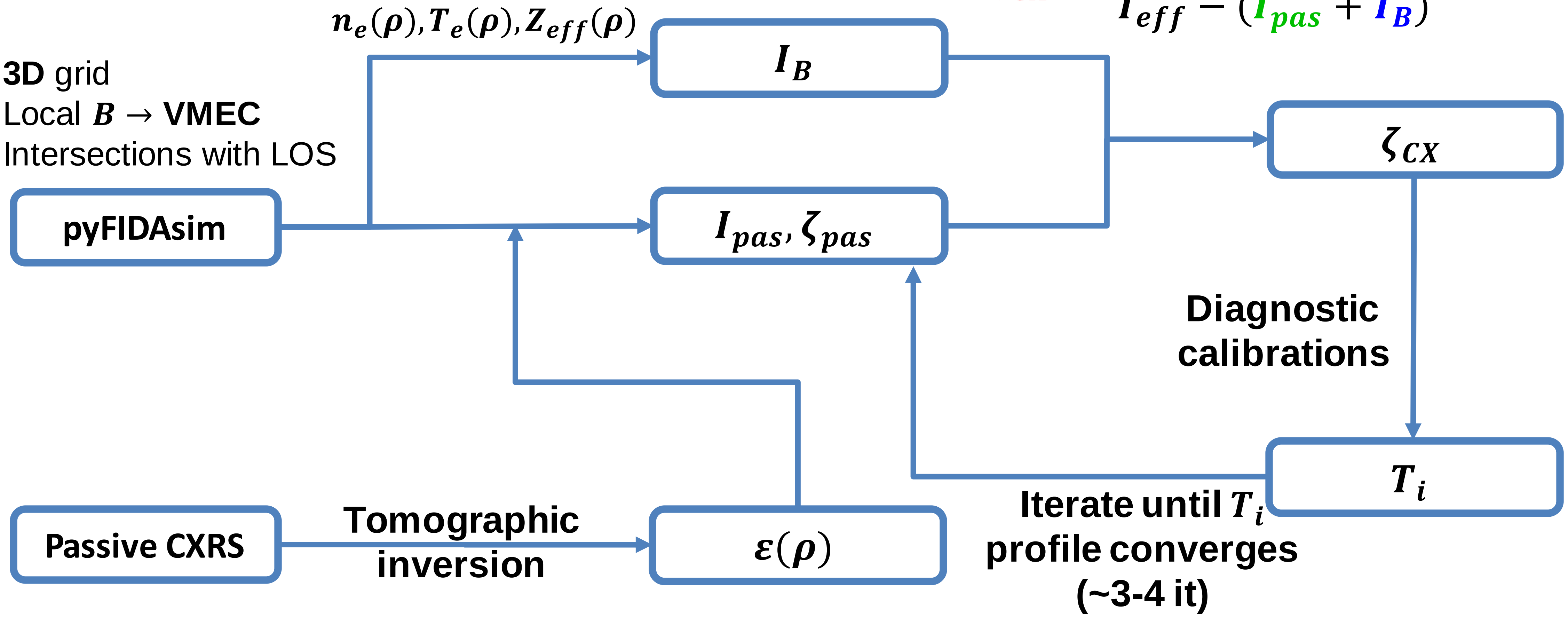

Good agreement with CXRS

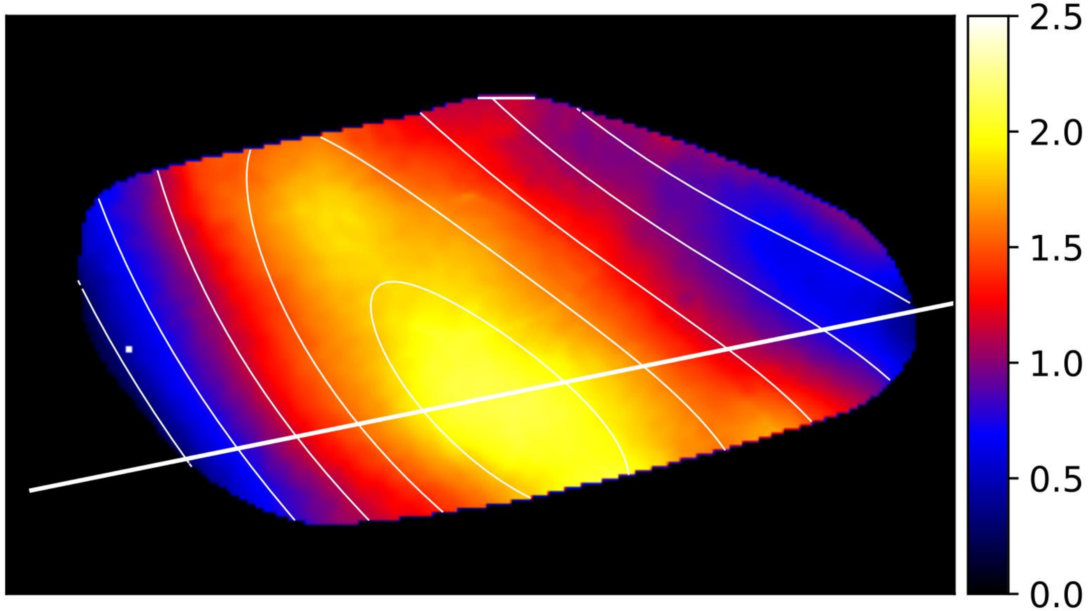

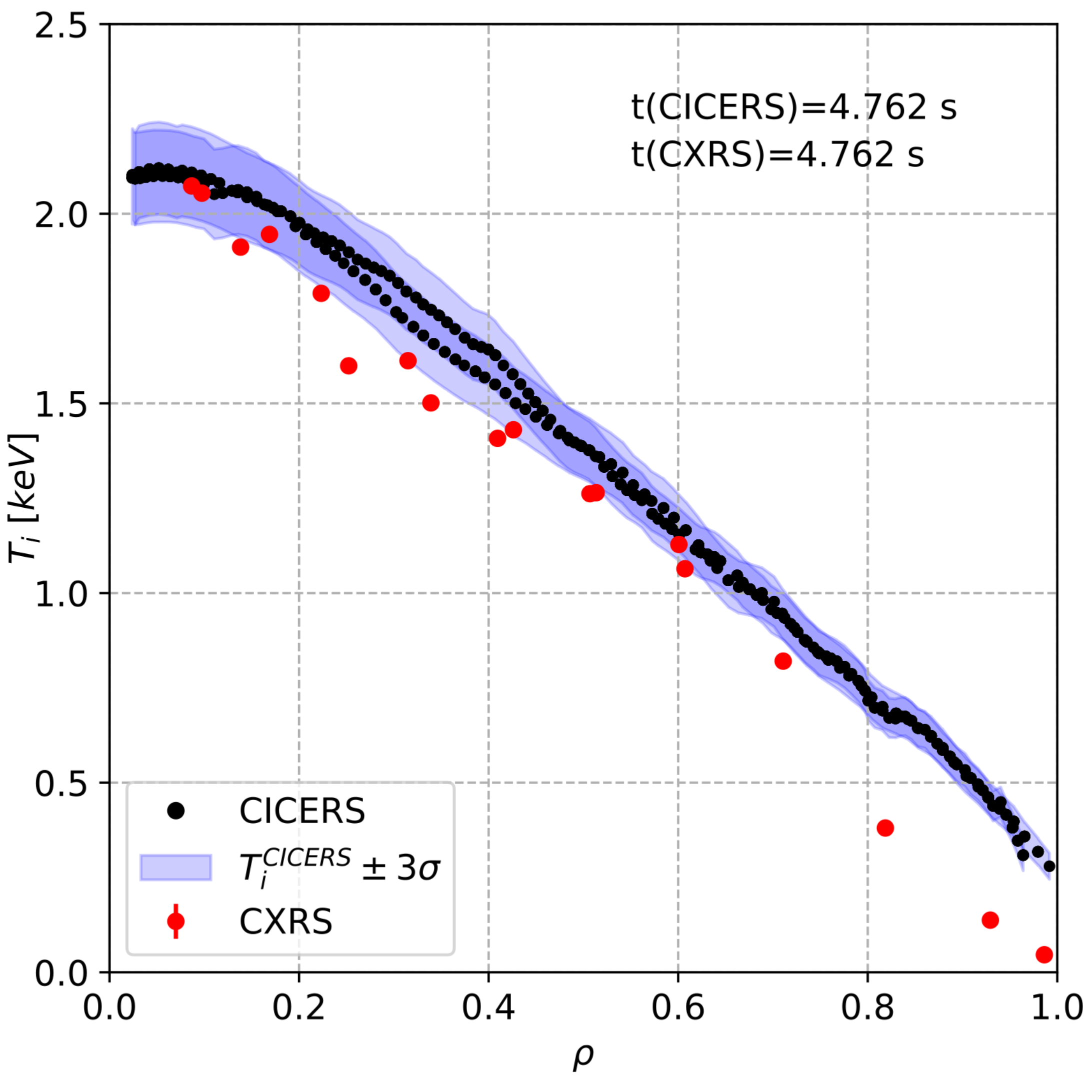

- Overall **good agreement** with **CXRS** T_i profiles
- Slightly **higher T_i** towards the Edge
  → Background radiation becomes more important
- Errors on I_B limits measurements with **continuous NBI** to **low n_e** plasmas.
- Higher **n_e plasmas** → **NBI blips**

T_i from ζ_{CX}

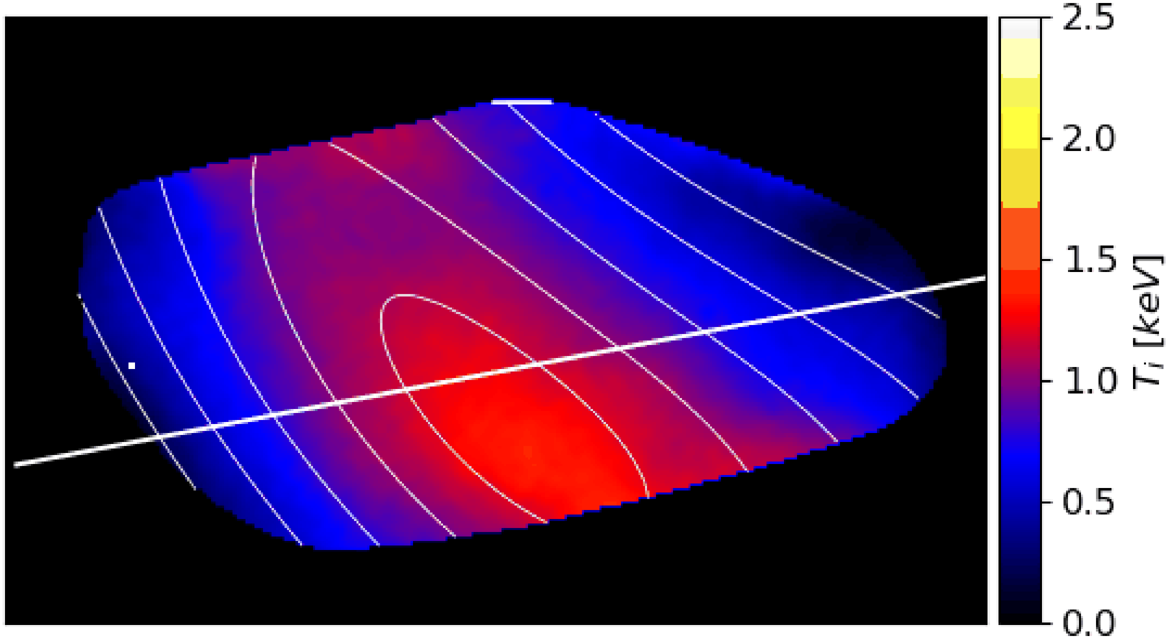

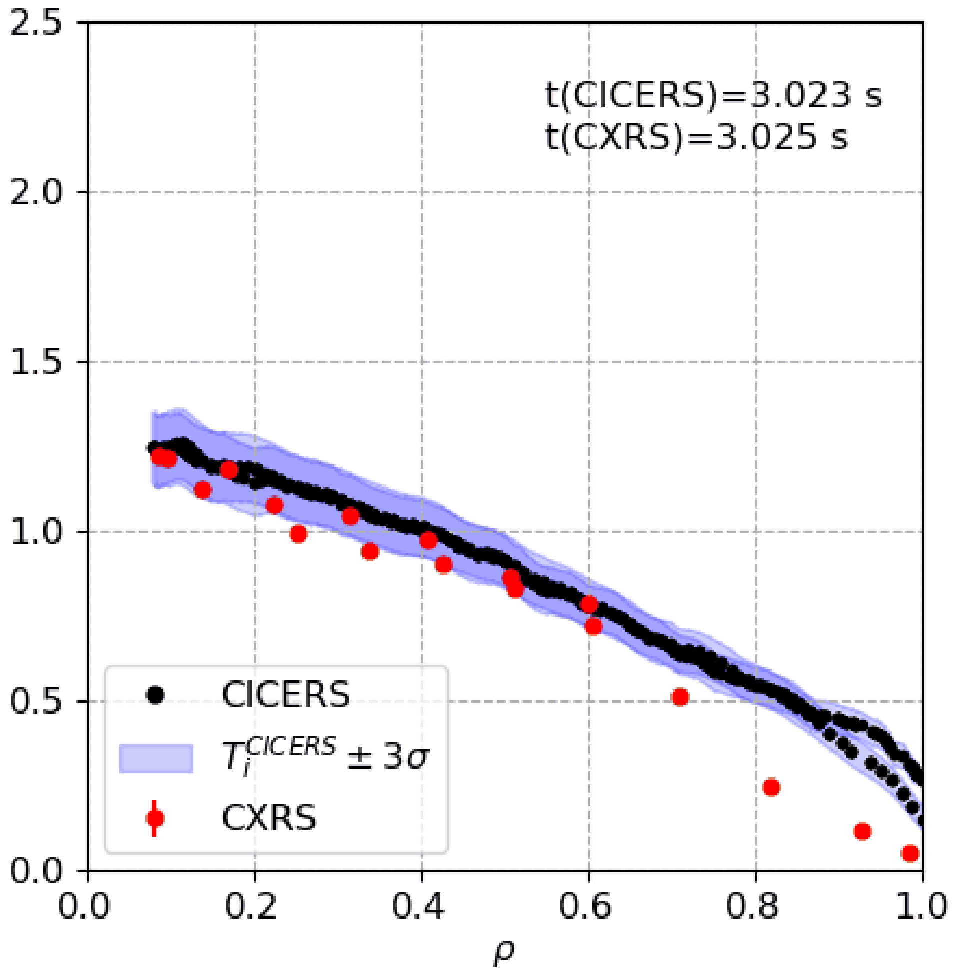

T_i from ζ_{CX}

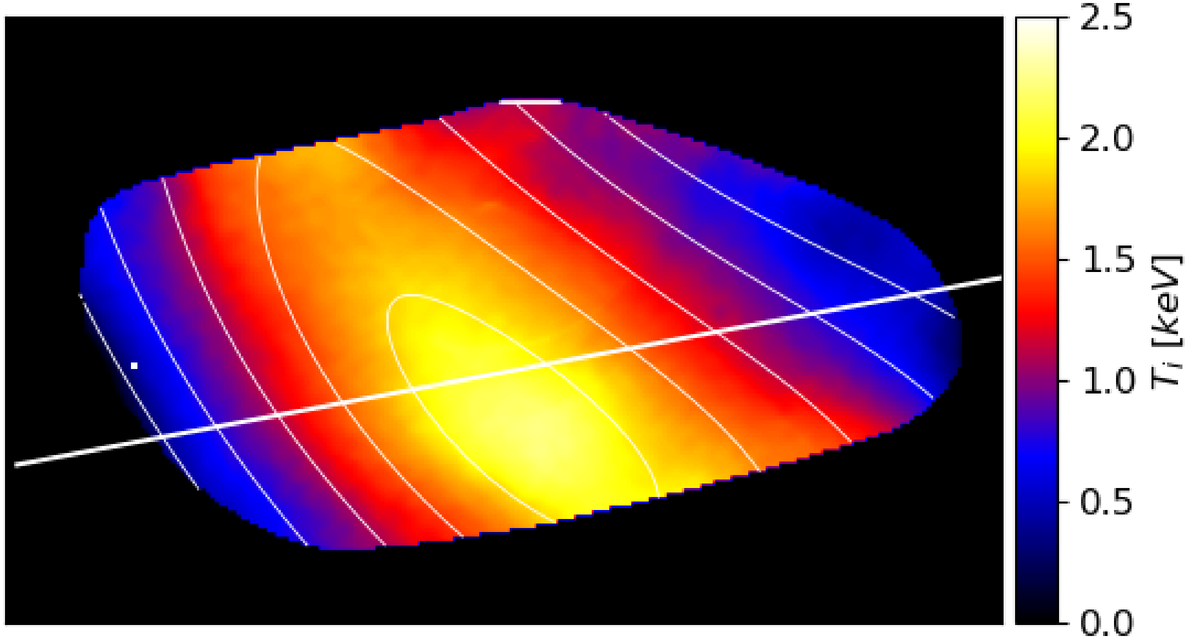

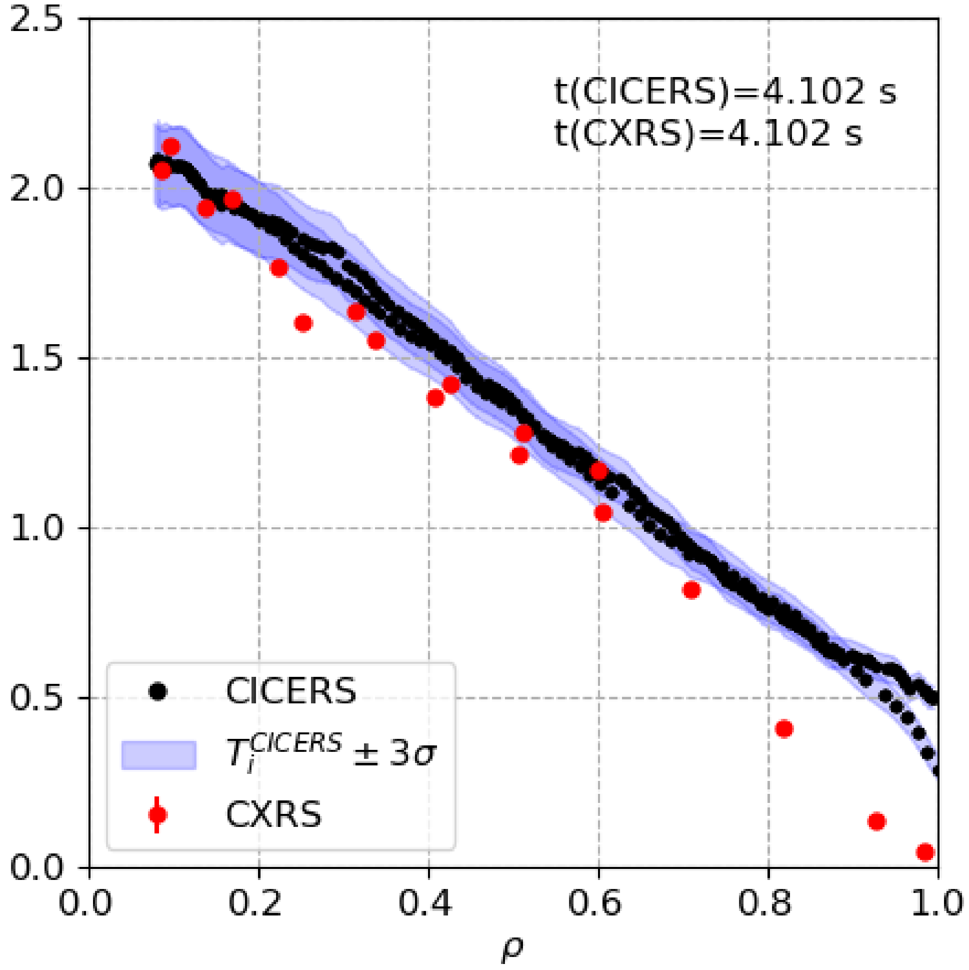

Modelling provides better T_i results than ROI-scaled interp.

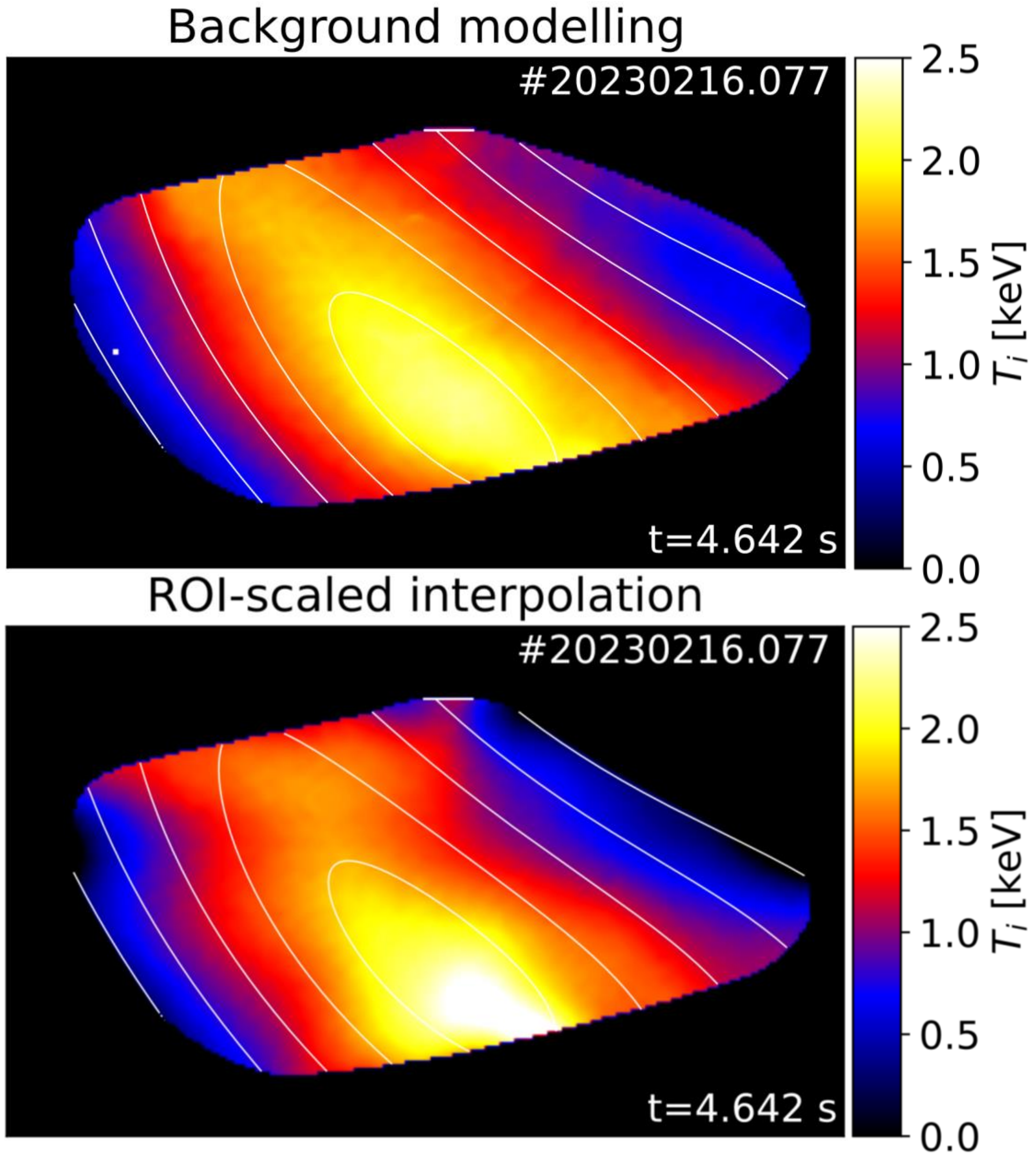

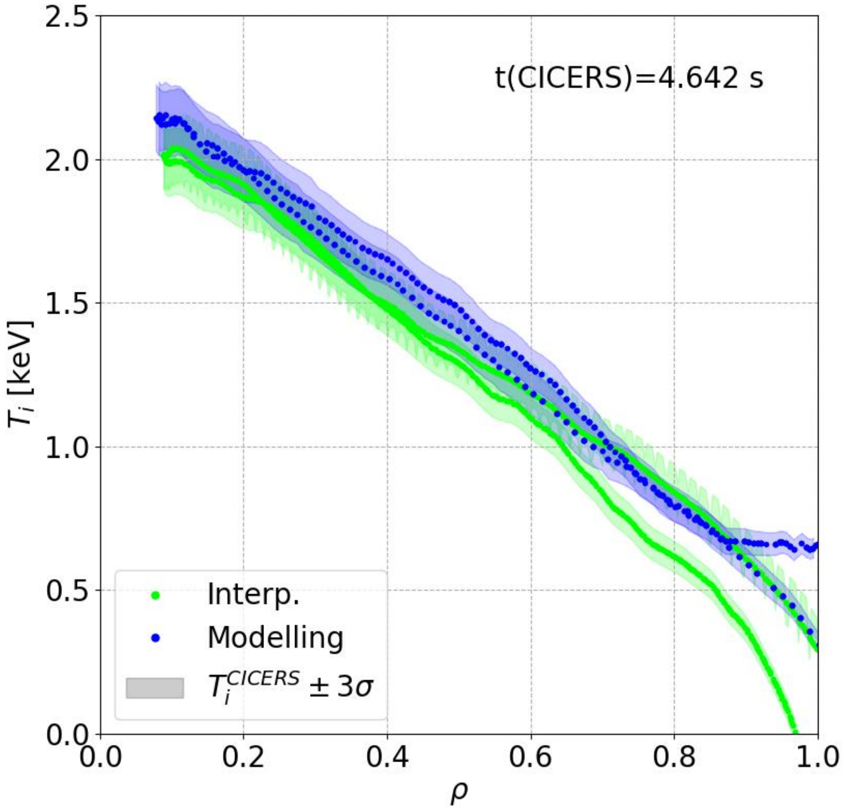

- **Better** adjustment to **Flux Surface contours**
- Overall **reduced inboard-outboard** asymmetries

Modelling CICERS intensity with pyFIDAsim

- NBI MC-based modelling[5]: **neutral density** $\boldsymbol{n_H}$ for each **energy component** $\boldsymbol{E}$.

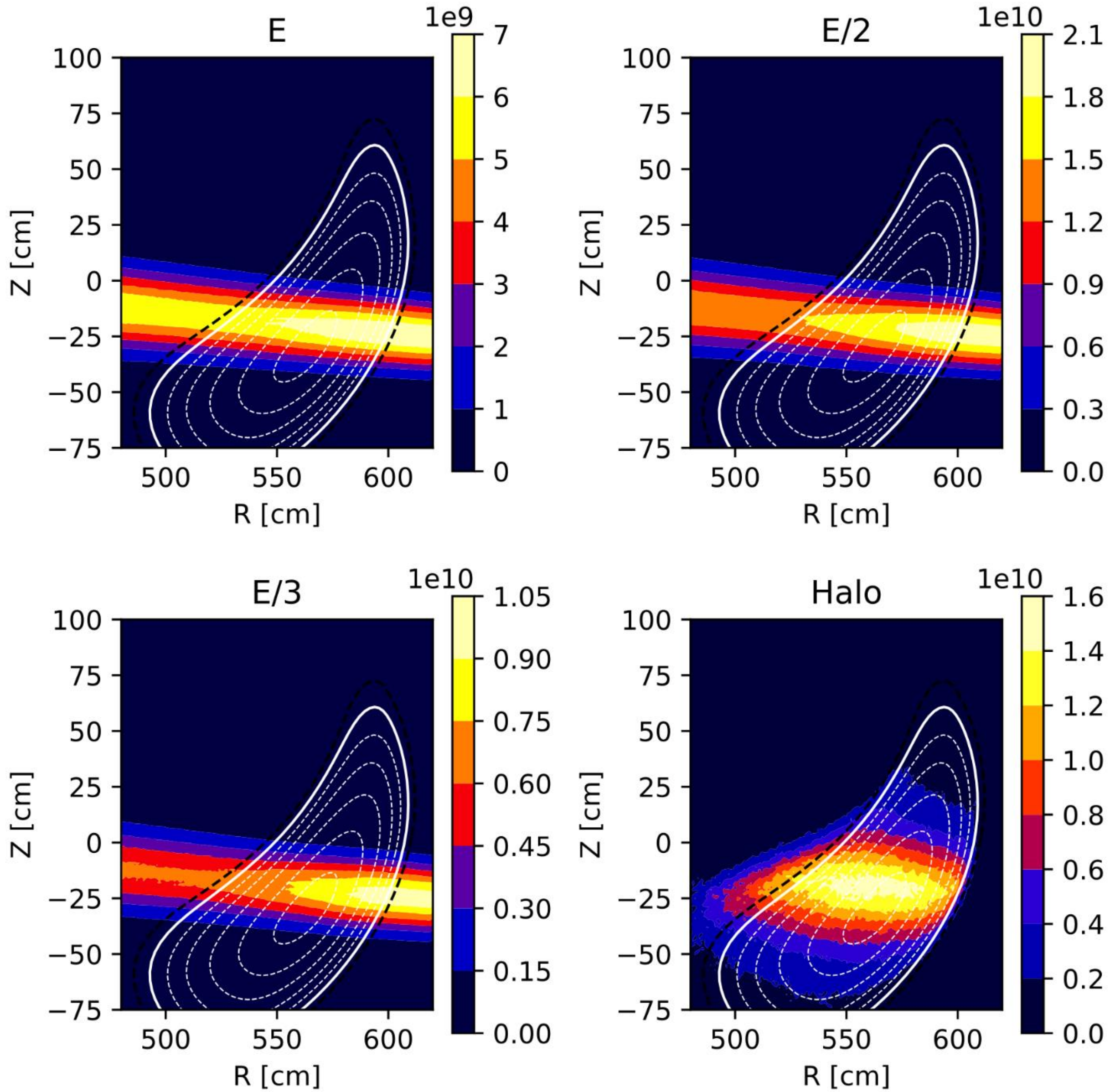

[5] C. Swee et al., PPCF 2022

Modelling CICERS intensity with pyFIDAsim

- NBI MC-based modelling[5]: **neutral density $\boldsymbol{n_H}$** for each **energy component $\boldsymbol{E}$**.

- CICERS view implemented and **recreation of $\boldsymbol{I_{CX}}$**

$$I_{C6+} = \frac{1}{4\pi}\sum_{E,i}\int_{LOS} n_H^{E,i} n_{C6+} \langle \sigma v \rangle_{CX}^{E,i} dl$$

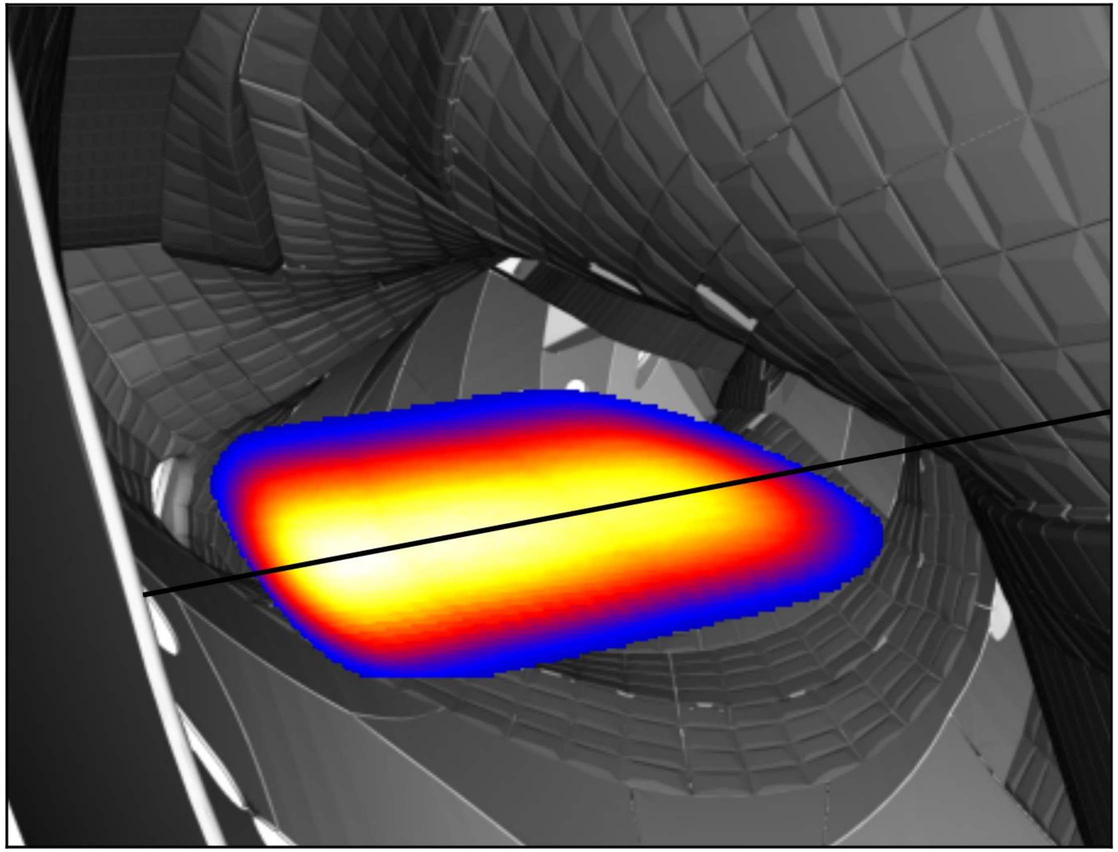

[5] C. Swee et al., PPCF 2022

Modelling CICERS intensity with pyFIDAsim

- NBI MC-based modelling[5]: **neutral density n_H** for each **energy component E**.

- CICERS view implemented and **recreation of I_{CX}**

$$I_{C6+} = \frac{1}{4\pi}\sum_{E,i}\int_{LOS} n_H^{E,i} n_{C6+} \langle\sigma v\rangle_{CX}^{E,i} dl$$

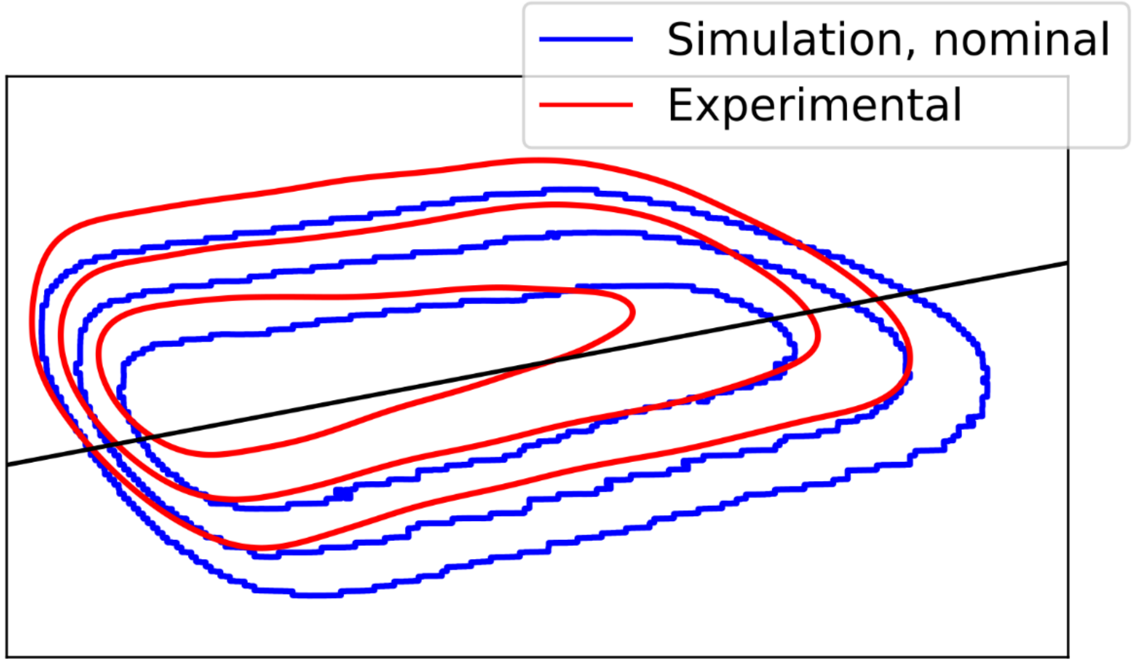

[5] C. Swee et al., PPCF 2022

Modelling CICERS intensity with pyFIDAsim

- NBI MC-based modelling[5]: **neutral density** $\boldsymbol{n_H}$ for each **energy component** $\boldsymbol{E}$.
- CICERS view implemented and **recreation of** $\boldsymbol{I_{CX}}$

$$I_{C6+} = \frac{1}{4\pi} \sum_{E,i} \int_{LOS} n_H^{E,i} n_{C6+} \langle \sigma v \rangle_{CX}^{E,i} dl$$

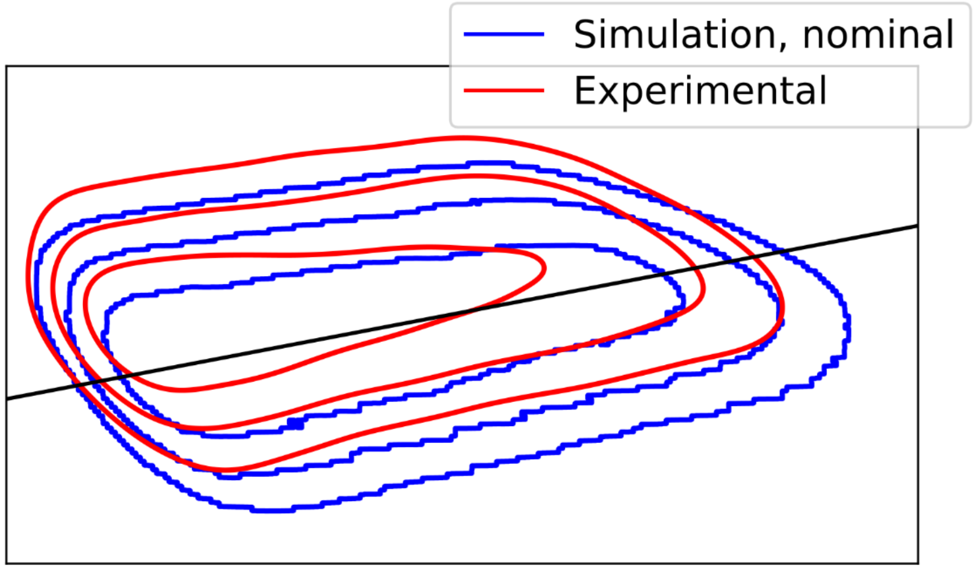

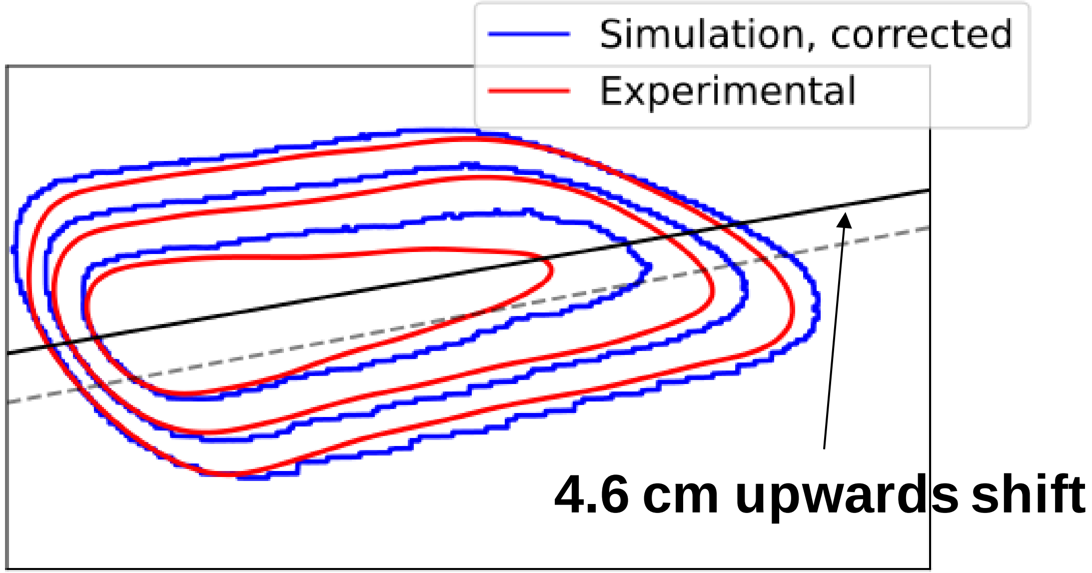

[5] C. Swee et al., PPCF 2022

Modelling CICERS intensity with pyFIDAsim

- NBI MC-based modelling[5]: **neutral density** $\boldsymbol{n_H}$ for each **energy component** $\boldsymbol{E}$.
- CICERS view implemented and **recreation of** $\boldsymbol{I_{CX}}$

$$I_{C6+} = \frac{1}{4\pi}\sum_{E,i}\int_{LOS} n_H^{E,i} n_{C6+} \langle\sigma v\rangle_{CX}^{E,i} dl$$

  - **5 cm shift** in source position reported by **bayesian BES modelling**[6] on S7/S8
  - **Shift in calorimeter loads** due to **magnetic field**[7]

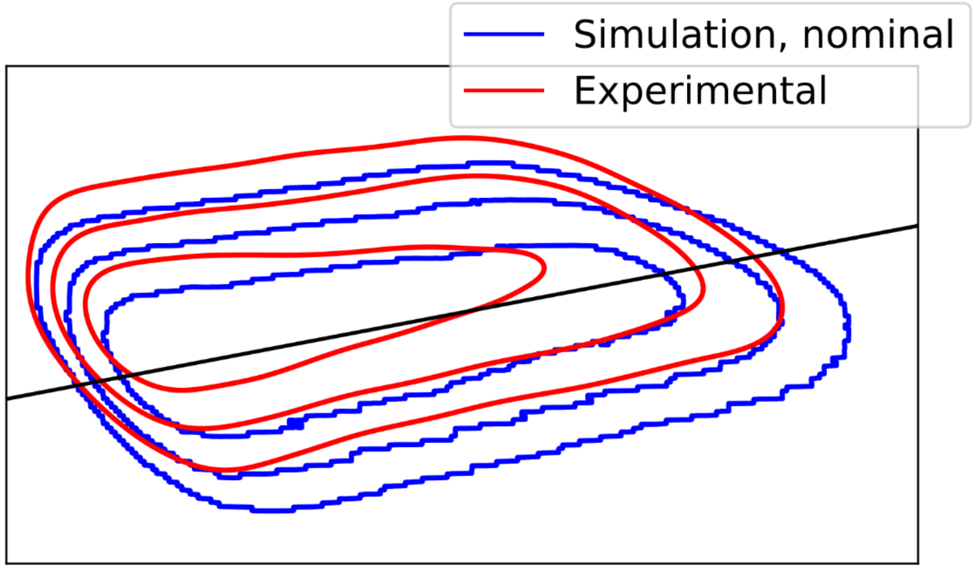

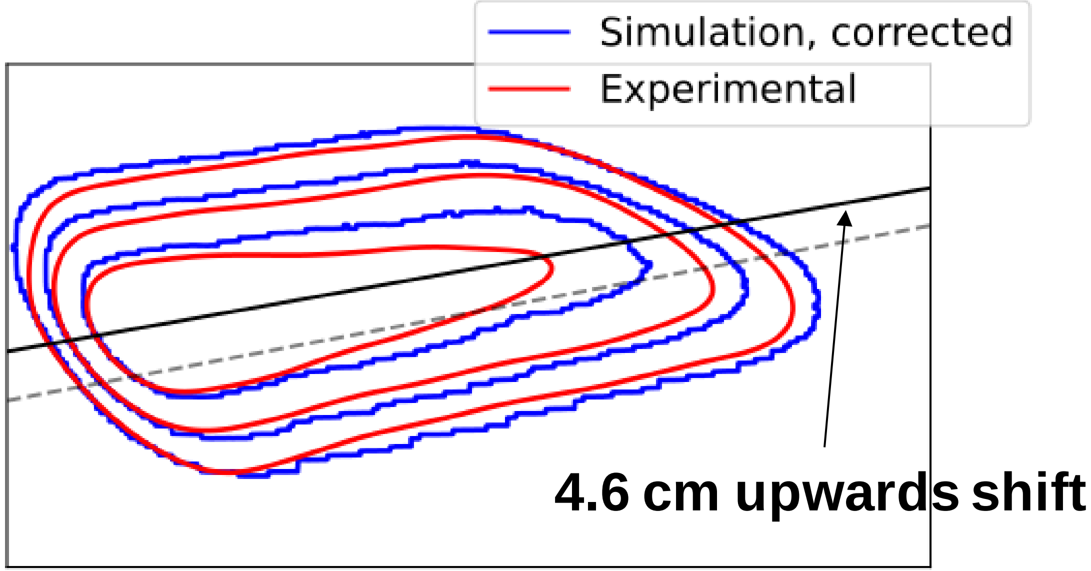

[5] C. Swee et al., PPCF 2022
[6] S. Bannmann et al., JINST 2023
[7] S. Lazerson et al., IAEA FEC 2023

2D Carbon impurity density maps

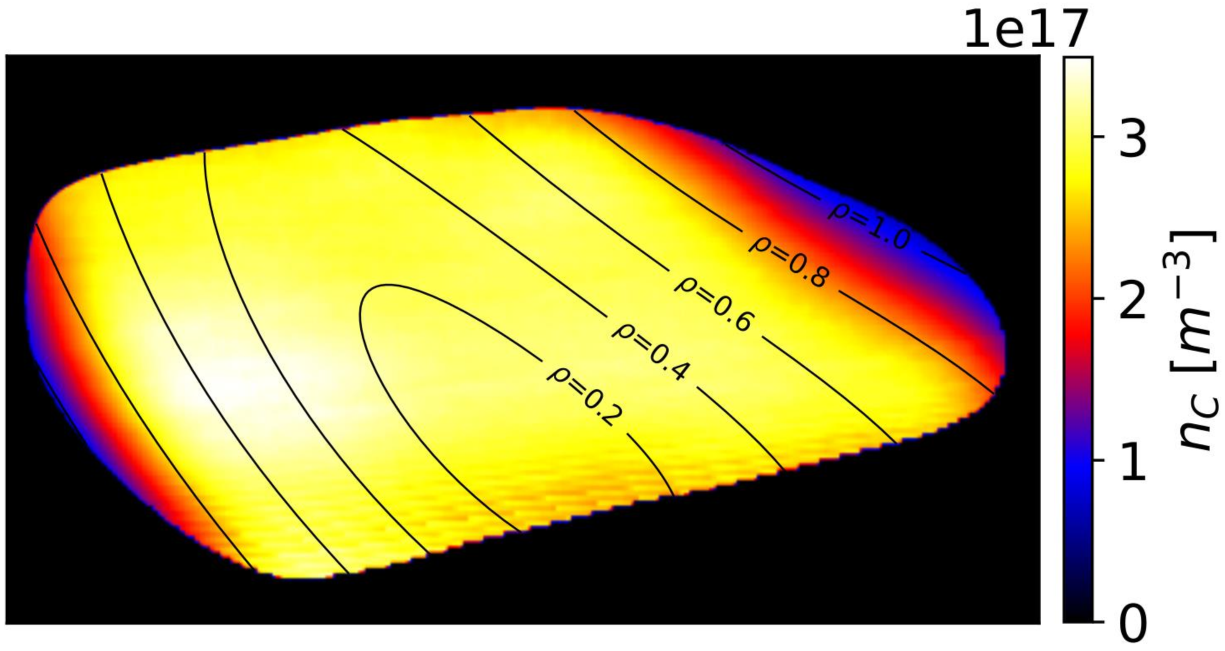

- pyFIDAsim **NBI modelling** to derive $\boldsymbol{n_C}$

$$n_C = \frac{4\pi I_{CX}}{\sum_{E,i} \int_{LOS} n_H^{E,i} \langle \sigma v \rangle_{E,i} \, dl}$$

2D Carbon impurity density maps

- pyFIDAsim **NBI modelling** to derive $\boldsymbol{n_C}$

$$n_C = \frac{4\pi I_{CX}}{\sum_{E,i}\int_{LOS} n_H^{E,i}\langle\sigma v\rangle_{E,i}\,dl}$$

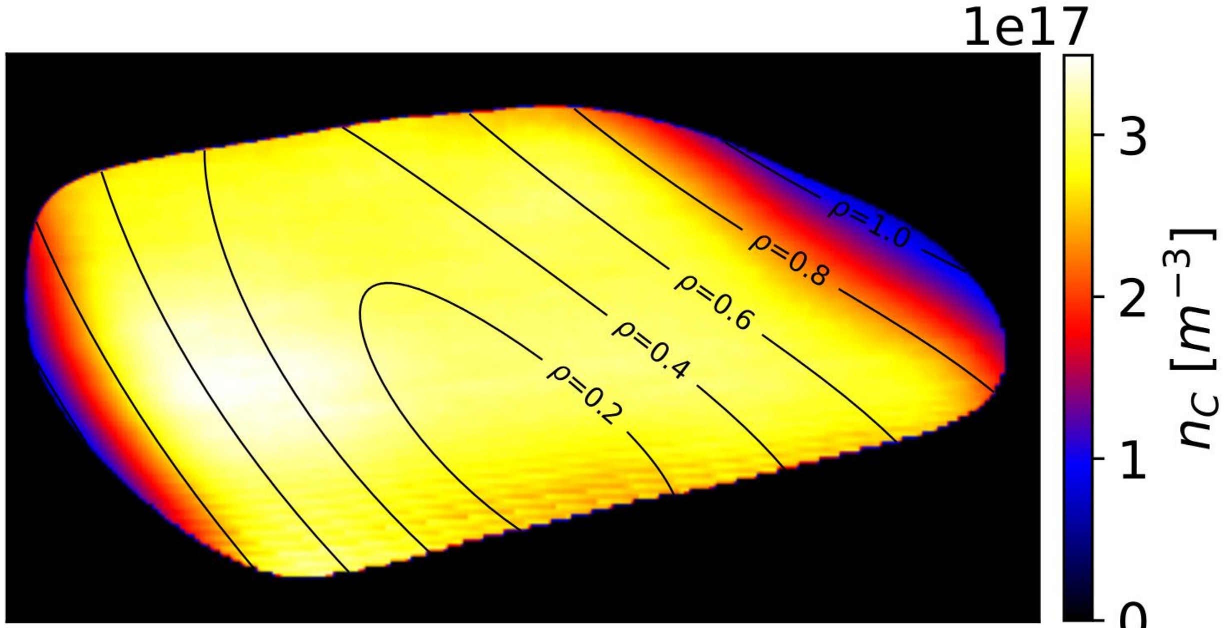

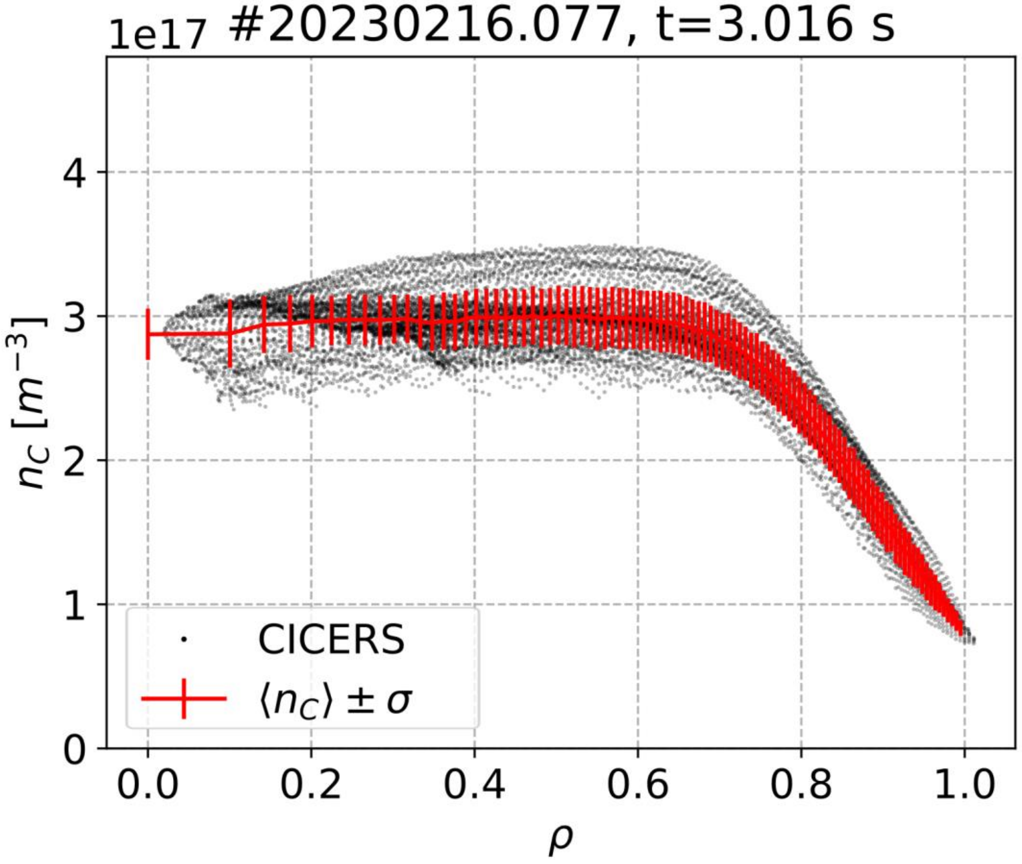

2D Carbon impurity density maps

- pyFIDAsim **NBI modelling** to derive $\boldsymbol{n_C}$

$$n_C = \frac{4\pi I_{CX}}{\sum_{E,i} \int_{LOS} n_H^{E,i} \langle \sigma v \rangle_{E,i} \, dl}$$

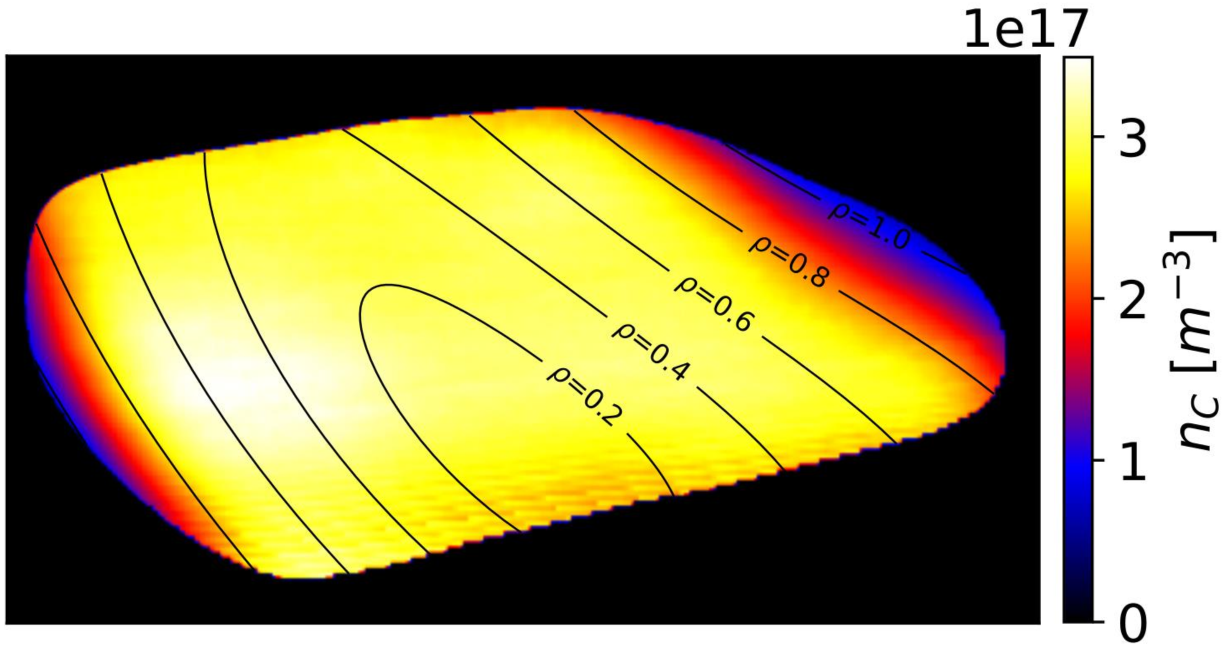

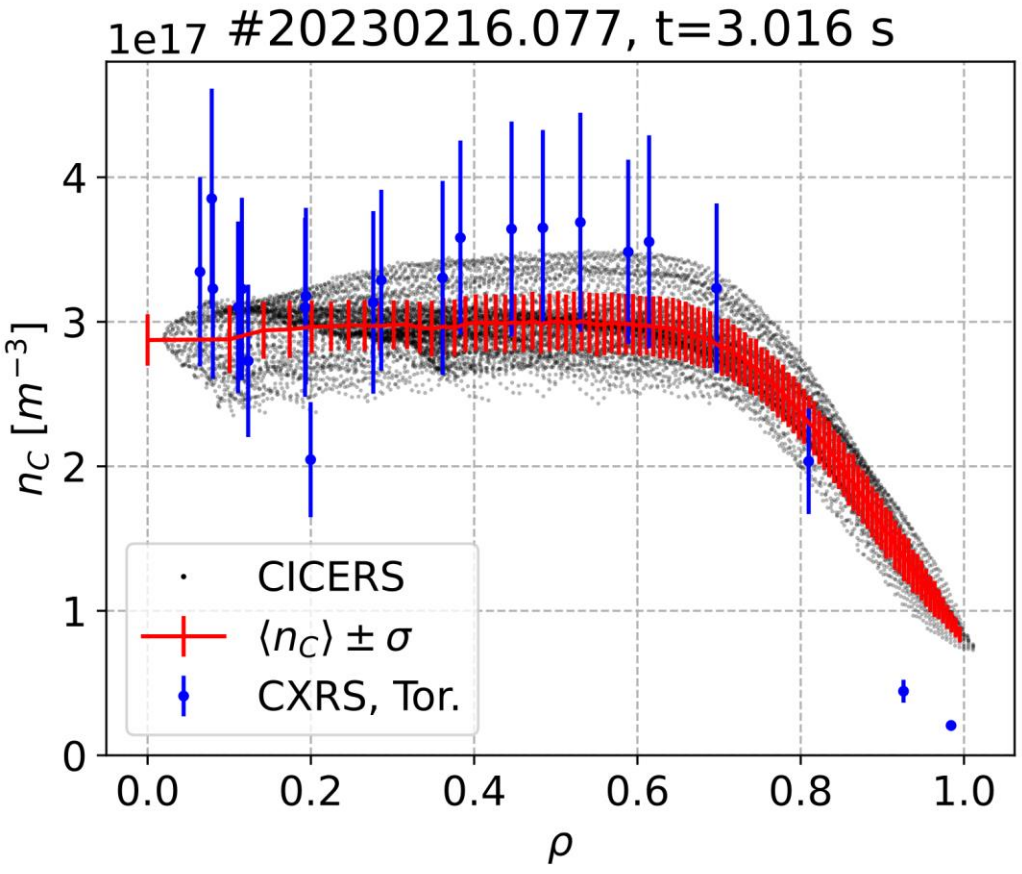

- NBI nominal power (1.8 MW) downscaled $\times$ 0.6 to match CXRS n_C profile.

2D measurements on T_i flattening

- High n_e discharge, no proper background subtraction

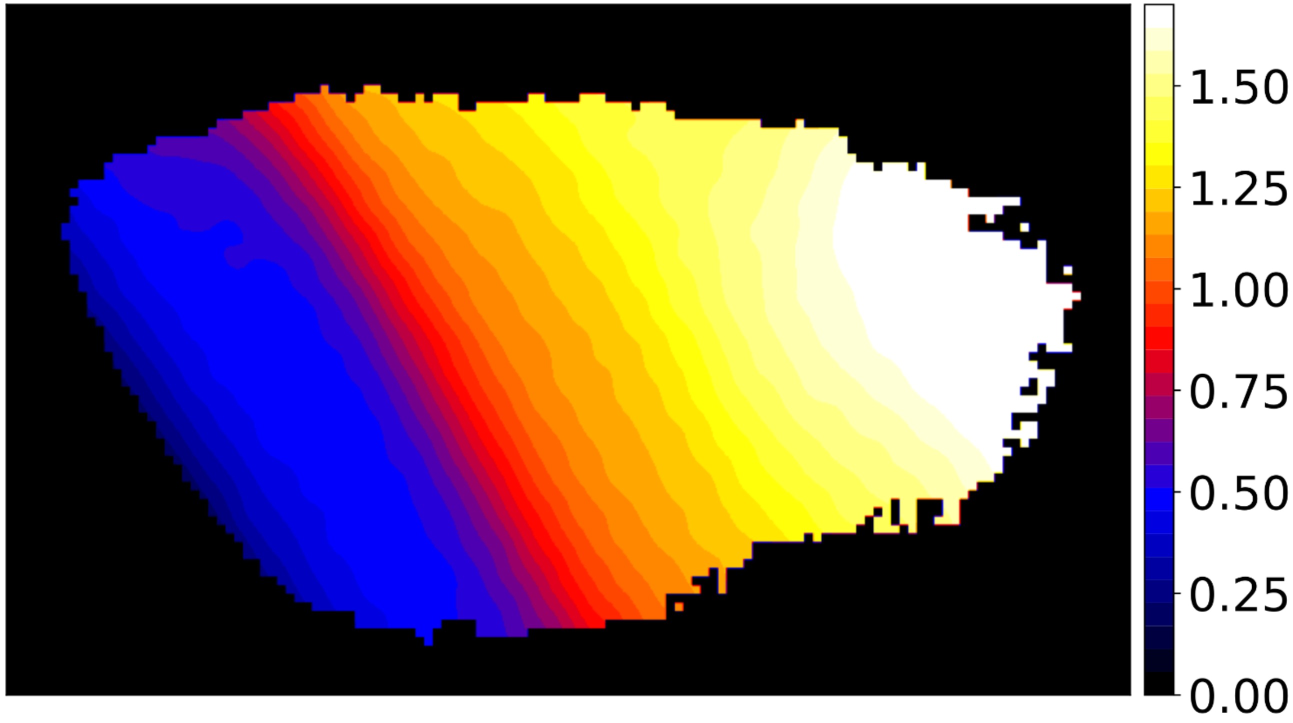

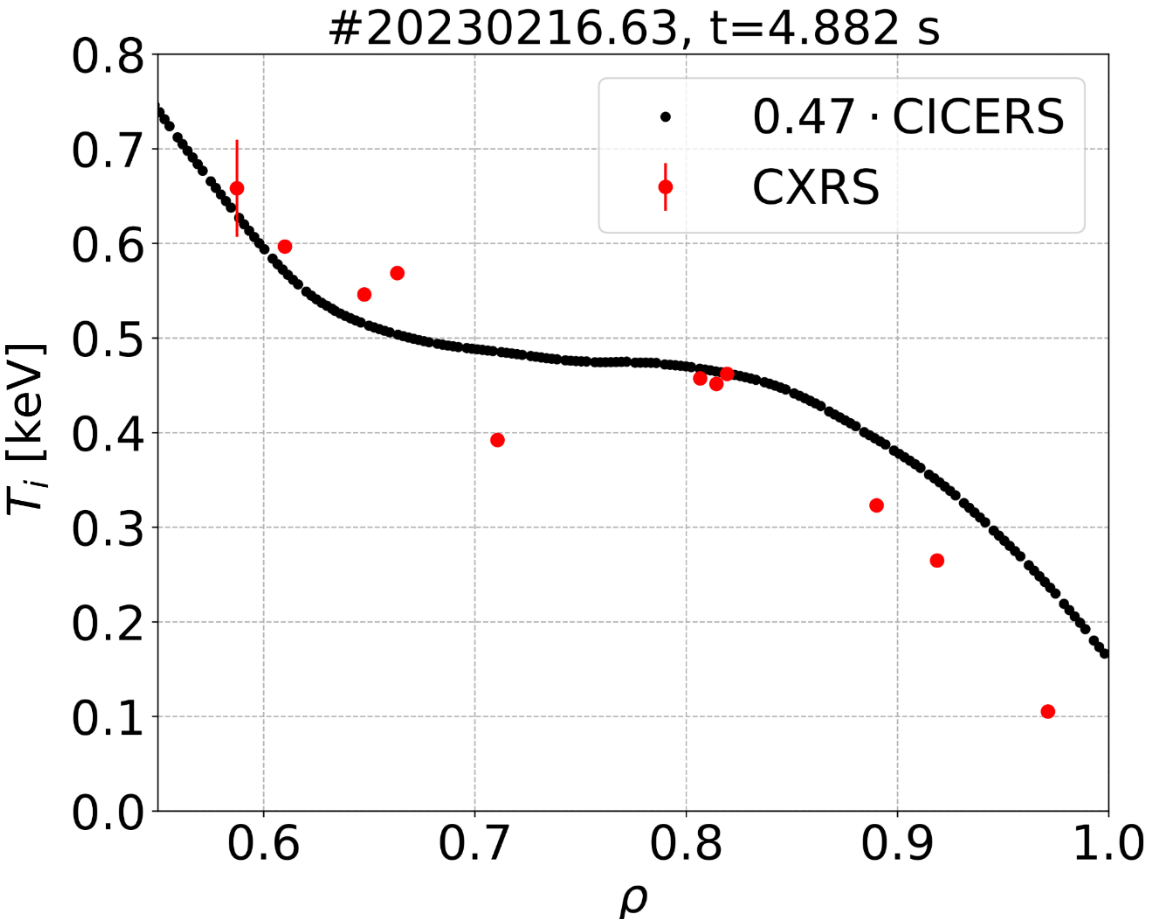

2D measurements on T_i flattening

- High n_e discharge, no proper background subtraction

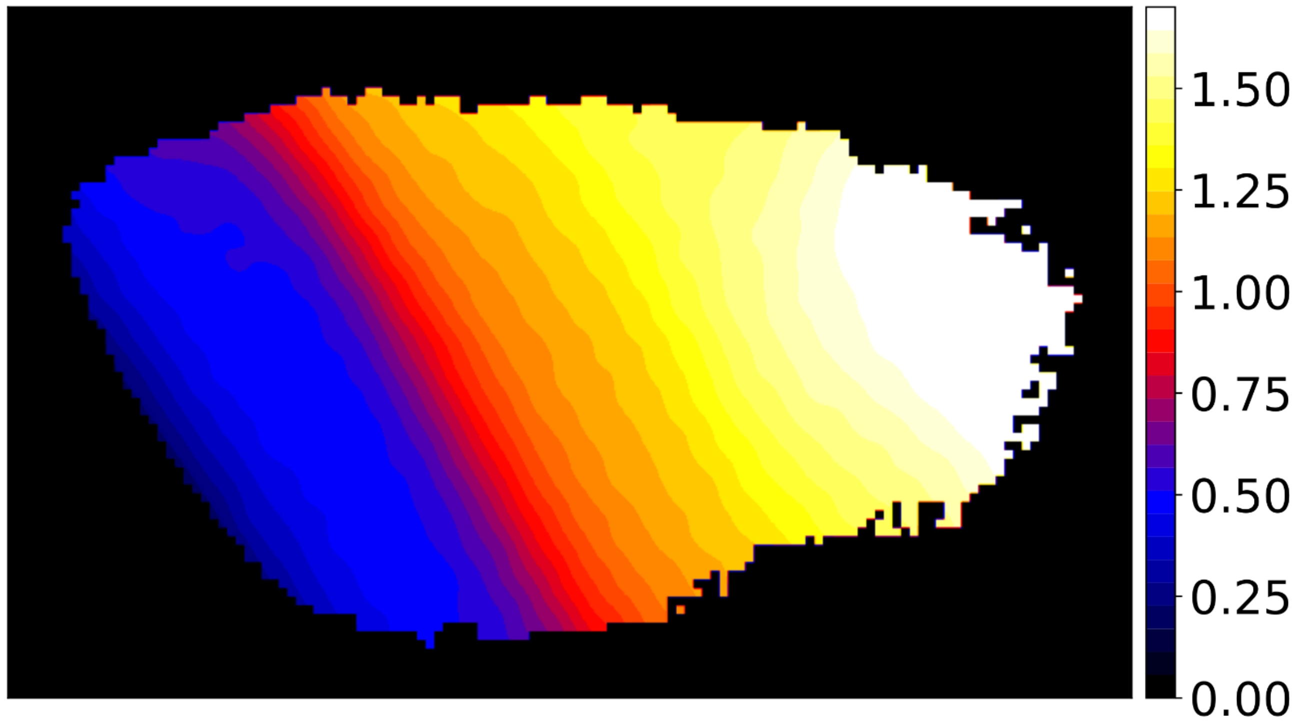

$T_i^{CICERS} \times 0.47$ to match CXRS data

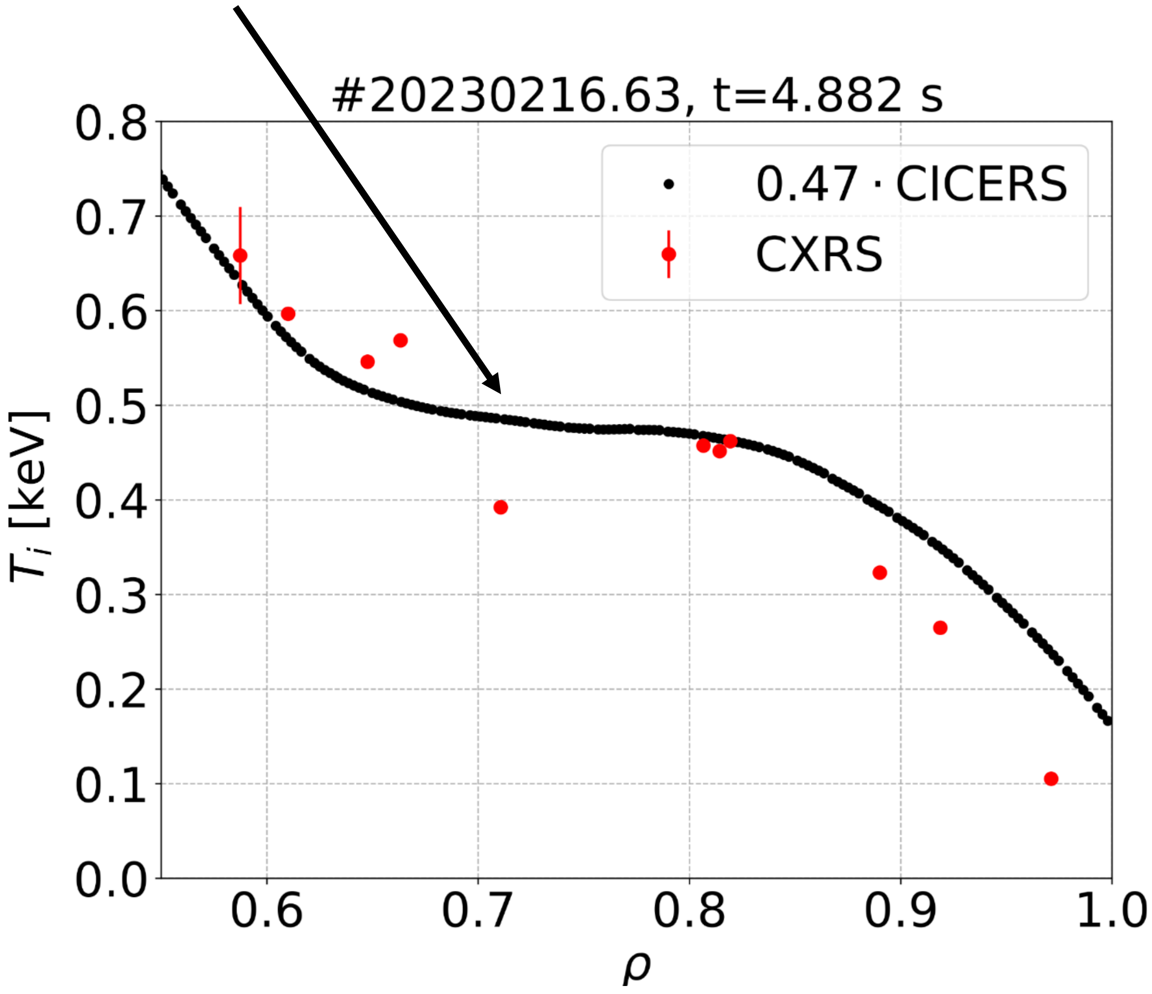

T_i flattening in magnetic core island

- High n_e discharge, no proper background subtraction

$T_i^{CICERS} \times 0.47$ to match CXRS data

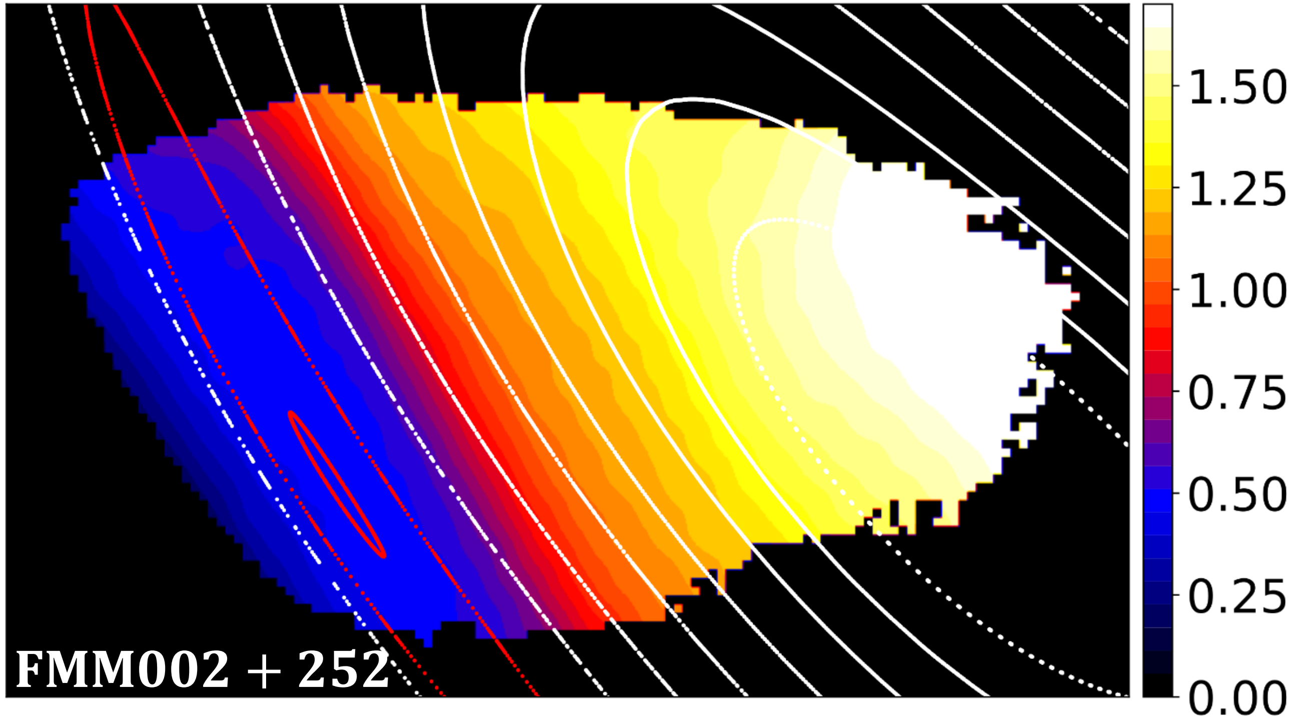

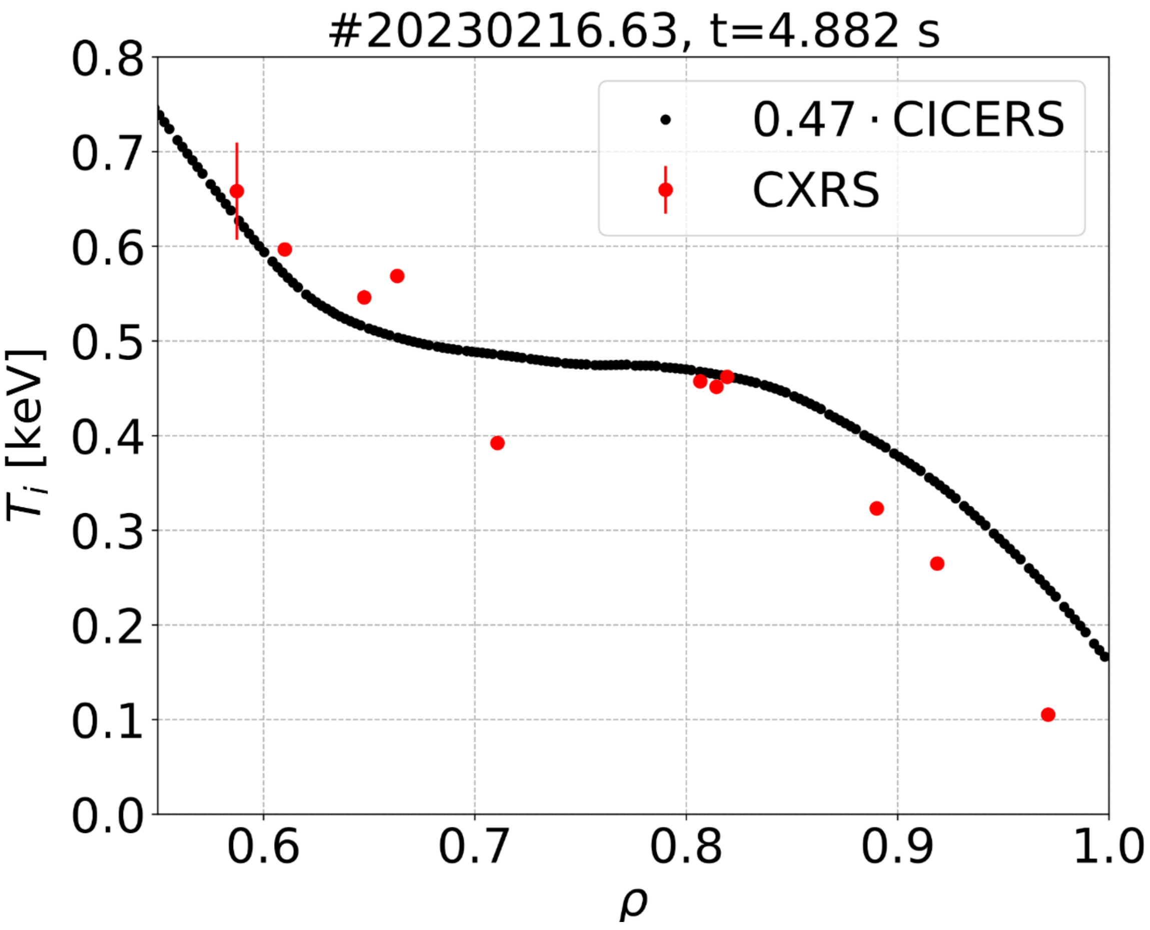

T_i flattening in magnetic core island

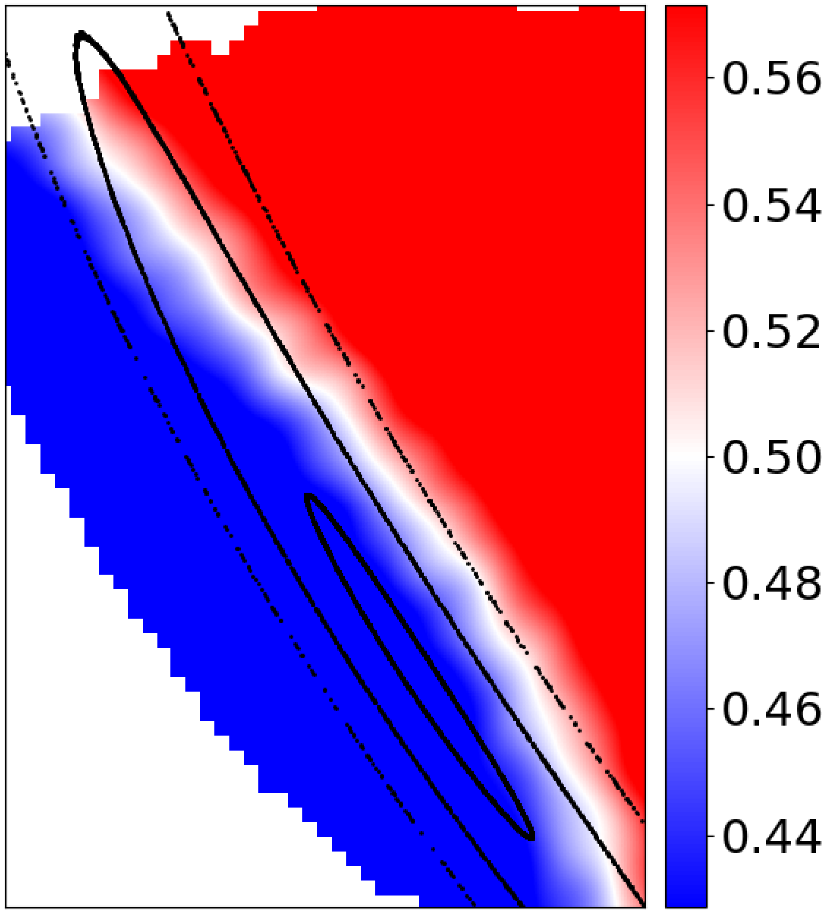

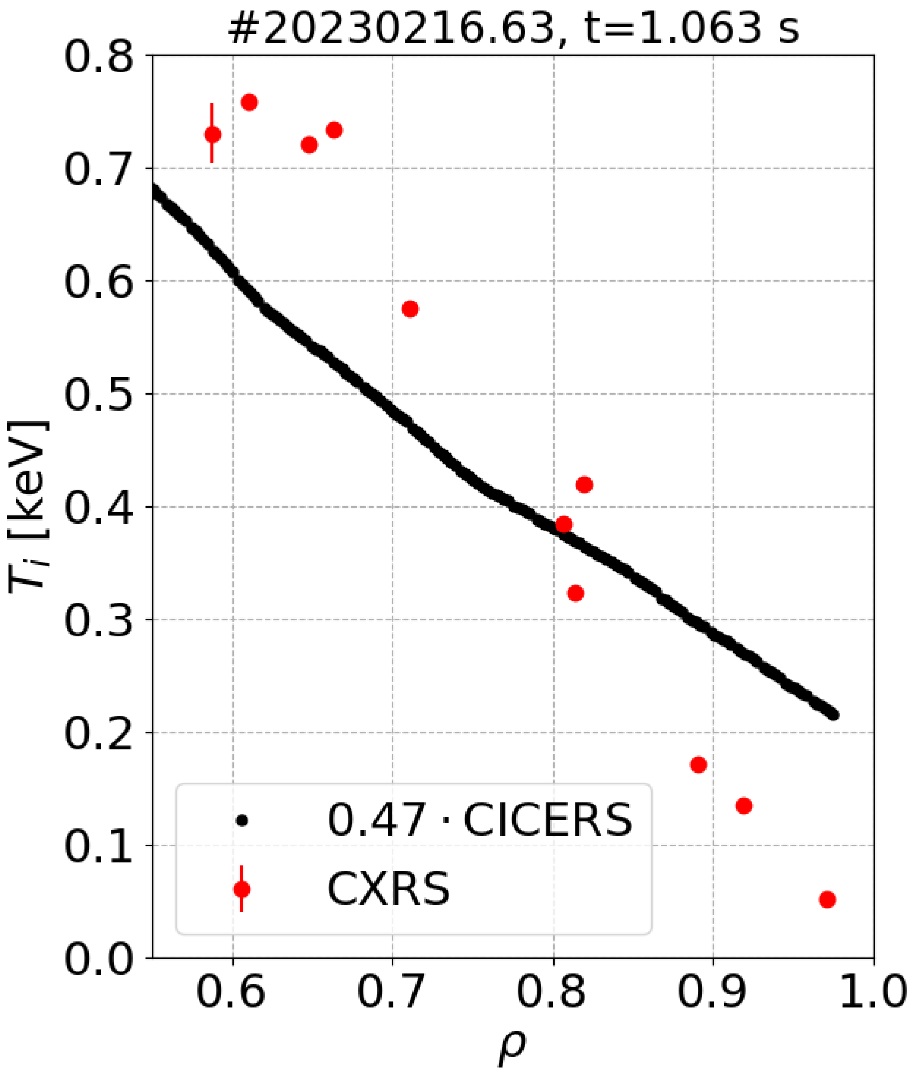

T_i flattening in magnetic core island

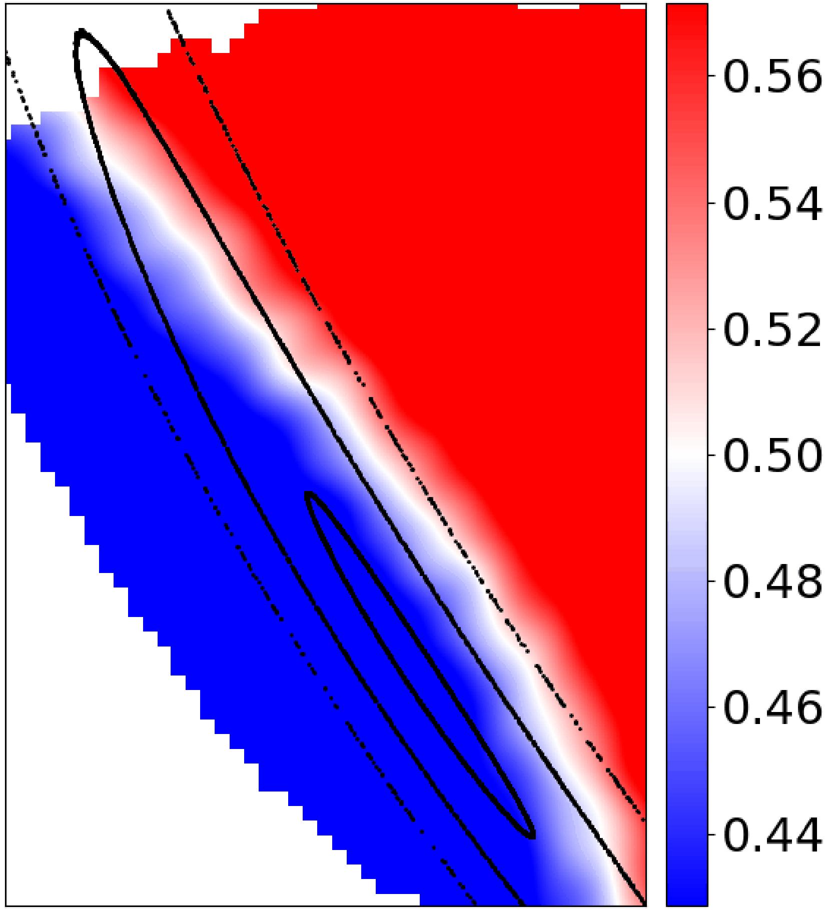

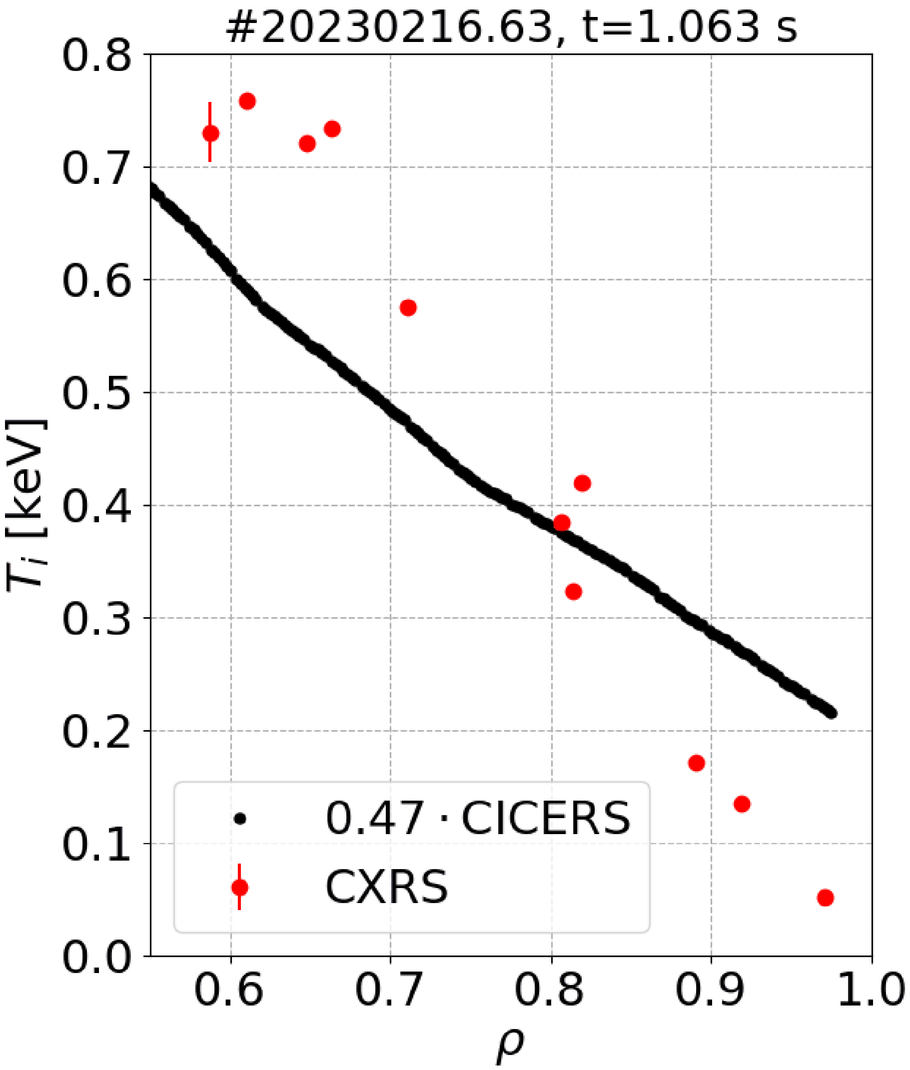

T_i flattening in magnetic core island

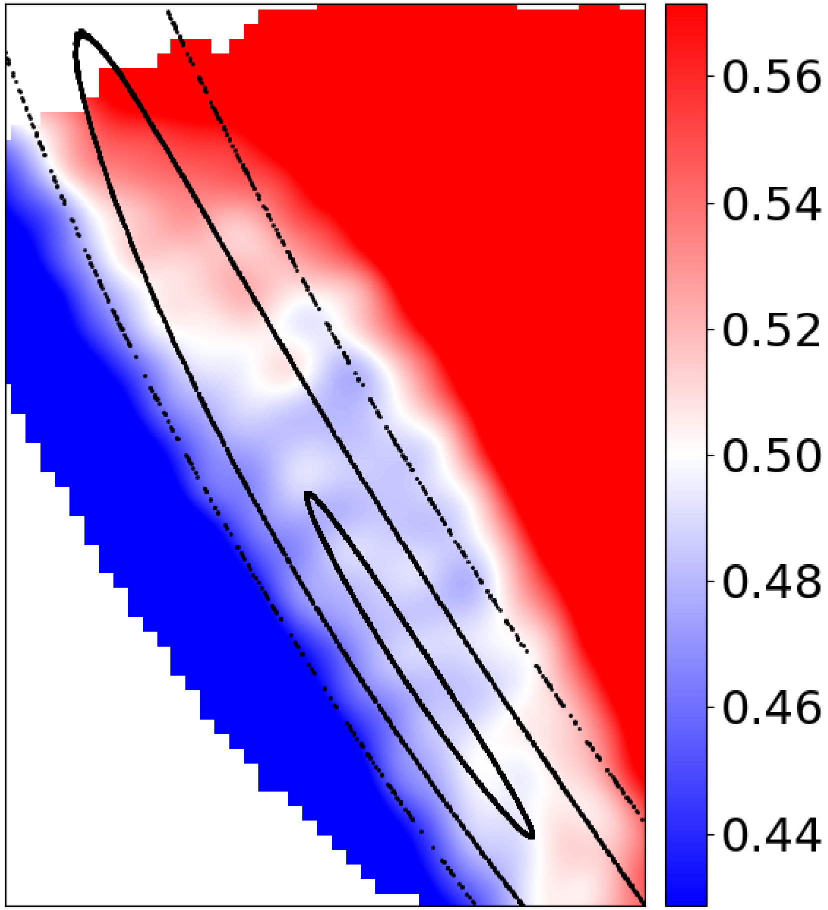

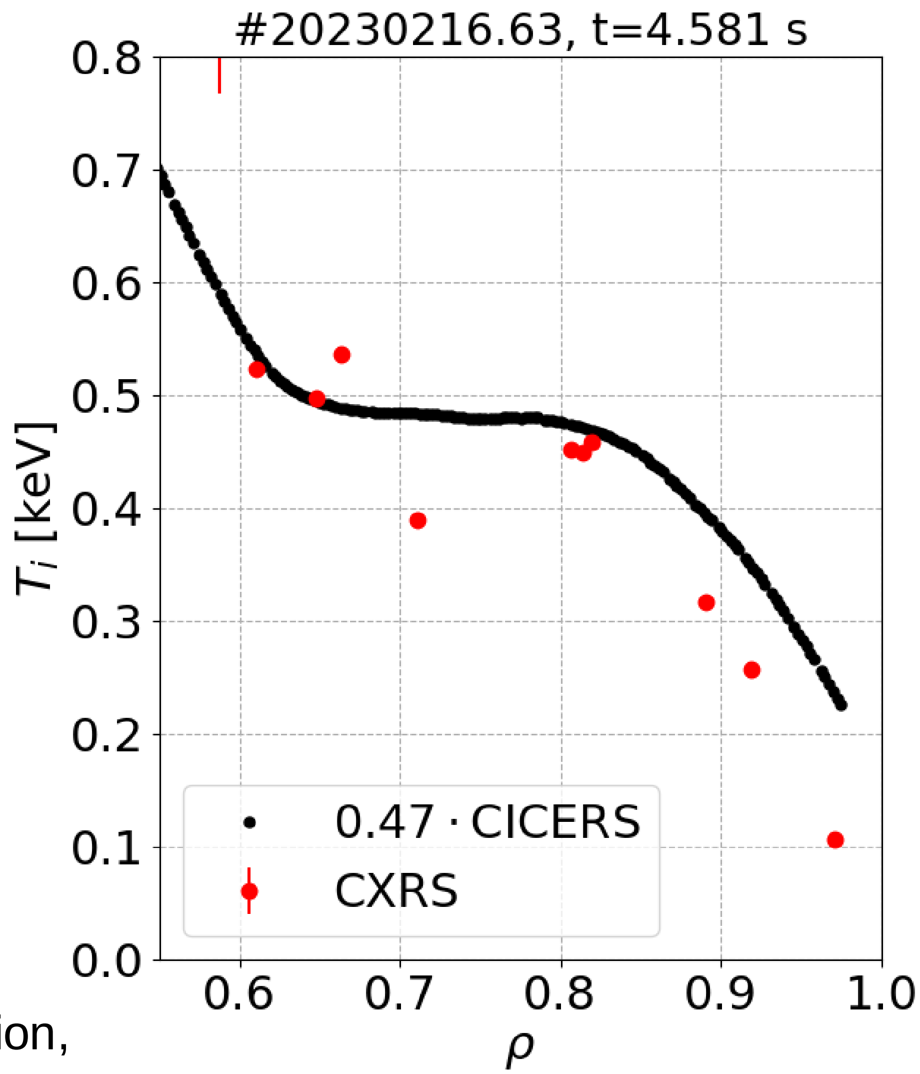

- Even in the absence of proper background subtraction, CICERS signal can be useful for interesting physics!

Conclusions

- **First batch** of experimental results with CICERS from **W7-X OP2.1**
- CICERS extends W7-X **diagnostic capabilities:**
  - **2D T_i** measurements
  - **2D n_C** measurements
- Background radiation:
  - **Modelling approach:** good results at low n_e plasmas for continuous NBI injection.
  - Best: **short NBI blips**

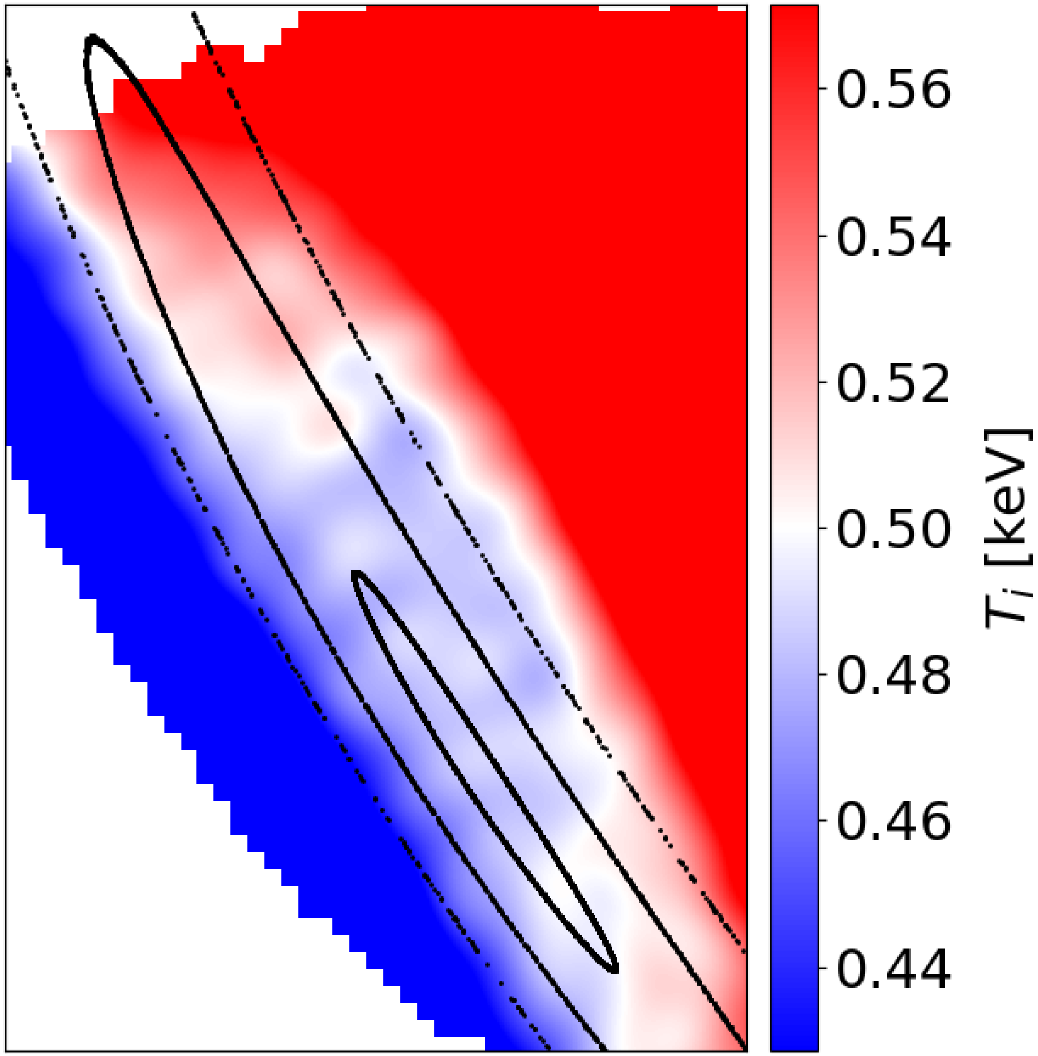

Interferometer cell

[Courtesy of V. Perseo]

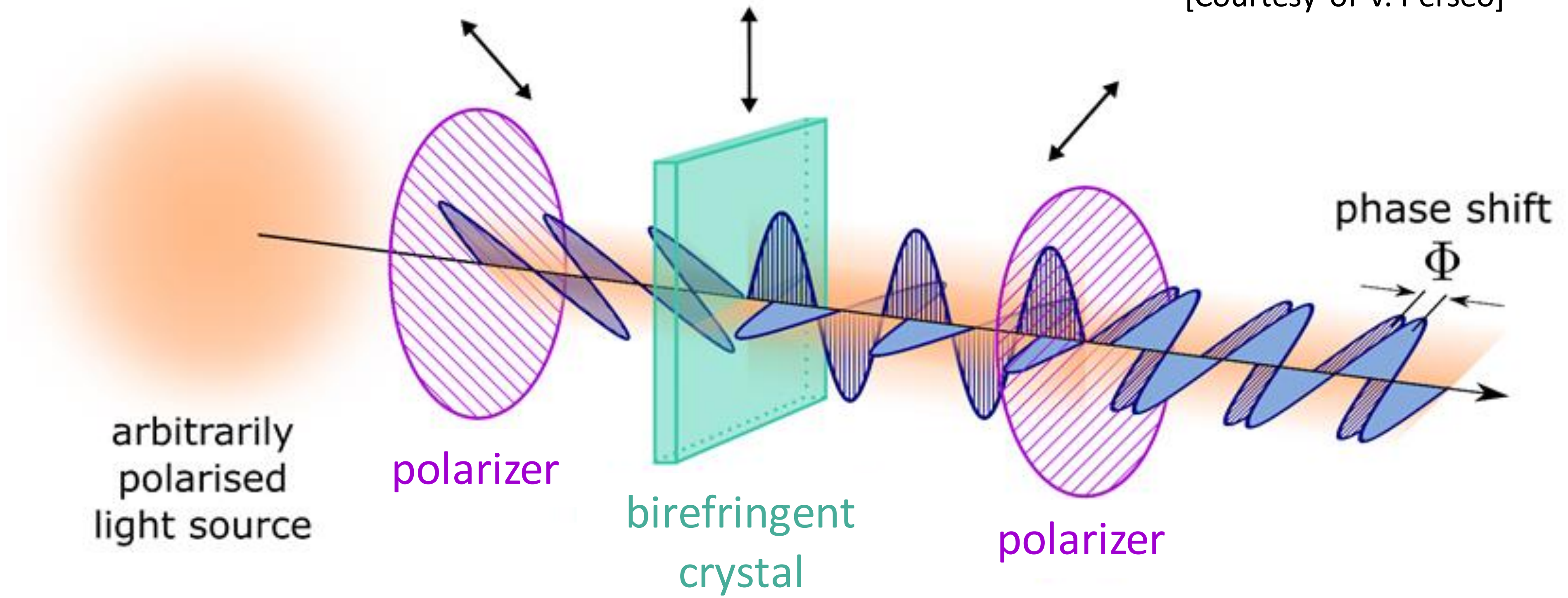

- **Phase shift (Φ)** depends on:
  - Incidence of light w.r.t. crystal → Experimental arrangement.
  - **Wavelength** of light → **Doppler effect** → T_i, v_Z, n_Z

Beam modelling for better insight on signal localization

- **Consistent** spatial localization:
  - **Closest approach** (CA):
    Point of closest approach between **LOS** and **beam axis**.
  - **Center of Mass** (COM)[8]:

$$s_{COM} = \frac{\int_{LOS} s w dl}{\int_{LOS} w \, dl} \qquad w = \sum_{E,i} n_H^{E,i} \langle \sigma v \rangle_{CX}^{E,i}$$

- Assessment of **line-integrated** effects:
  - **FWHM** of weights along **LOS**

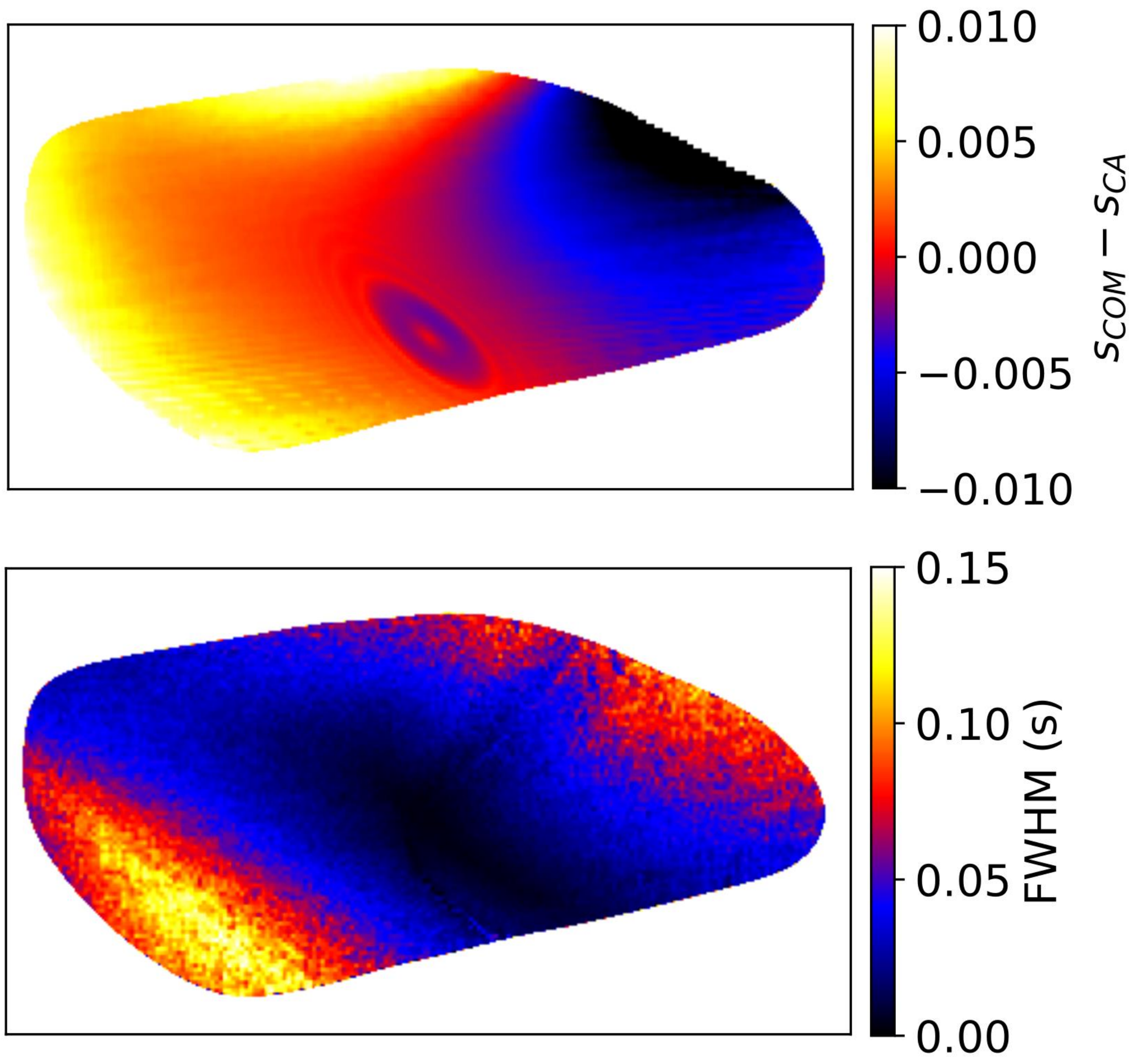

[8] T. Romba et al., PPCF 2023